Universität Rostock
Traditio et Innovatio

From Proteome Center Rostock

Director: Prof. Dr. Michael O. Glocker

Proteome Profiling of Maternal Serum:

A Novel Approach for Intrauterine Growth Restriction Screening During Pregnancy

Dissertation

For the acquirement of the academic degree

Doctor rerum humanarum: "Dr. rer. hum."

Faculty of Medicine, University of Rostock

Submitted by

Charles Ayensu Okai

From Ghana

Rostock, 11.05.2020

Personal declaration

I hereby declare that the herein submitted dissertation is the result of my work and it has not been submitted for any degree or examination in any other university / institution. All sources of information used have been duly acknowledged and references provided in the dissertation.

Charles Ayensu Okai

I dedicate this work to my wife and children.

Acknowledgements

Table of Contents

1. Summary

1.1 Introduction

1.1.1 Pregnancy complications with fetal growth restriction

Definition and types of fetal growth restriction

The fetal growth restriction diseases are divided into two large groups, one termed "intra-uterine growth restriction (IUGR)" and the other "small for gestational age (SGA)" [1]. IUGR is defined as a condition in which the fetus does not reach its genetically given growth potential, resulting in low birth weight. The newborns are below the 10th percentile in weight for their estimated gestational age [2-5]. This is true also for the other group of newly born babies with birth weights below the 10th percentile referred to as SGA. The majority of SGA neonates by genetic constitution grow in utero in accordance with their percentiles [2,3,5,6]. The gestational age of IUGR and SGA pregnancies has been found to range from 24 – 36 and 37 – 41 weeks respectively [7], whiles normal pregnancies on average last 39 – 41 weeks [8].

Depending upon the gestational age (after application of a cut-off of 32 weeks) when growth restriction is diagnosed, IUGR can be classified as early onset or late onset [9]. Early onset IUGR occurs before 32 weeks gestation representing about 20 - 30 % of all IUGR cases. It is distinguished by severe systemic cardiovascular adaption in *utero* due to chronic hypoxia resulting from significant disruption to placental perfusion [10,11]. Fetuses from early onset are prone to be born preterm, hence have a higher risk of morbidity or mortality [12]. Late onset IUGR occurs more frequent (about 80 % of IUGR occurrences) and starts after 32 weeks gestation. This late onset IUGR is usually associated with a milder placental insufficiency and a lower degree of hemodynamic fetal variation. Fetuses within this category are at a greater risk of rapid deterioration, leading to intrauterine fetal death although the dysfunction of the placenta is not considered severe [10,13].

Epidemiology, Prevalence, and Sequelae of IUGR

Low birth weight is defined as newborns with birth weight of less than 2500 g irrespective of the gestational age [14]. This measure includes infants affected by SGA and IUGR. Low birth weight rate affects approximately 16% of all neonates in developing countries, which is about six times higher than in developed countries [15].

IUGR complicates about 5 - 10 % of all pregnancies [16,17]. It is estimated that IUGR affects about 3 - 8 % and 24 % of all neonates in developed [18] and developing [15] countries respectively. However, incidence of IUGR in neonates is about 3 - 7 % of the total population [19].

IUGR is a major cause of perinatal morbidity and mortality [2,20,21], such as birth asphyxia, meconium aspiration, neonatal hypoglycemia, hypothermia and intrauterine fetal death [20,22,23]. Besides its contribution to perinatal morbidity and mortality, several epidemiologic studies have shown that IUGR contributes to neurodevelopmental

delay or functioning [24-26] and also increases the infant's risk of cardiovascular and metabolic diseases [27-33] later in adulthood.

Etiology, Pathogenicity, and Symptoms of IUGR

Pregnant women who abuse drugs, drink alcohol, smoke, or have heart disease, high blood pressure, sickle cell anemia, kidney disease, infections, etc., are most probable to have their fetuses affected by IUGR. However, combination of other factors also contribute to IUGR. Hence, the causes of IUGR can be categorized into maternal, fetal or placental [2,5,34-36]. The maternal causes result from pregnancy-associated hypertensive disease [37,38], autoimmune diseases [2,39,40], substance abuse [38,41-44] and teratogen exposure [45-48]. Fetal causes result from multiple gestations [49], infections [50,51] and genetic and structural disorders [52,53]. Placental dysfunction accounts for the majority of IUGR cases [21,54-57].

The pathogenesis of IUGR unfortunately has not been clearly defined but it is believed that the primary pathophysiological mechanisms underlying the maternal, fetal or placental conditions [2,5,34-36], although different, play decisive roles usually ending in an eventual prevalent result: suboptimal uterine-placental perfusion and restricted fetal nutrition leading to development of IUGR [2,21,58].

The key symptom of IUGR is a small for gestational age fetus which is initially identified by measuring the fundal height after 20 weeks during antenatal care. Normal pregnancies grow at 1 cm / week hence, any fundal height that is 3 cm or more behind weeks of pregnancy suggests IUGR. Further clinical assessments such as ultrasound investigations are required to confirm the diagnosis [59,60]. It is imperative in most countries, that pregnant women attend hospitals / clinics regularly because during antenatal care, close surveillance can best identify pregnancy-related complications. Identification of pregnant women who are at risk and referring them to specialists early will reduce perinatal morbidity and mortality [61,62].

Clinical diagnostic methods for IUGR detection

Currently, ultrasound biometry is the "gold standard" for assessing fetal growth restriction. Biparietal diameter, head circumference, abdominal circumference and femur length are the four biometric measurements most commonly used. The percentiles established for each of these parameters are then combined to generate an estimated fetal weight [2,6,63,64]. When the estimated fetal weight is below the 10th percentile for gestational age, additional ultrasonographic examinations such as amniotic fluid index (oligohydramnios) [2,65-67] and Doppler velocimetry (measurement of absent or reversed end-diastolic flow in the umbilical artery) [2,68,69] are used to monitor fetuses during antenatal in the second or third trimester. The absent or reversed end-diastolic flow in the umbilical artery has been associated with an increased risk of IUGR and perinatal mortality [70,71]. Though antenatal monitoring with

the umbilical artery Doppler velocimetry has led to about 30 % reduction of perinatal mortality in high-risk pregnancies [72], up to about 80 % of IUGR fetuses remained undetected until delivery [23].

Another difficulty is that, SGA fetuses (constitutionally small) may not be distinct during antenatal Doppler velocimetry examinations resulting in a diagnostic challenge of differentiating SGA pregnancies from IUGR pregnancies by clinical means [2,73]. Clinical screening of risk assessments during antenatal using the ultrasound biometry approach is known to have low sensitivity [35] and is unable to predict the pathological conditions of pregnancy before their clinical manifestation [74].

Blood-based diagnostic tests for assaying pregnancy complications and neonatal diseases

Biomarkers which are biomolecules found in serum, plasma or tissues and serve as measurable indicators of specific physiological conditions to determine the presence or absence of a disease state [75,76], have found critical roles in clinical applications such as screening, diagnosis, and prognosis of diseases [75,77,78].

In the clinics, dried blood spots, have been used in risk assessments of neonates by the analysis of phenylalanine for the detection of phenylketonuria in newborns using bacterial inhibition test [79]. Glucose test strips are used to determine the blood glucose levels of pregnant women based on simple blood tests in the diagnosis of gestational diabetes mellitus [80-82] and immunoanalytical assays e.g. enzyme linked immune-sorbent assays (ELISAs), are used in the diagnosis of preeclampsia by the analysis of either placental growth factor (PlGF) concentrations [83,84] and/or the ratio of maternal soluble fms-like tyrosine kinase-1, (sFlt1) to PlGF, (sFlt1/PlGF) [85-87].

Screening assays of pregnant women based on simple blood tests to detect biomarkers indicative of placental insufficiency has become an attractive method for identifying high-risk pregnancies [35]. Maternal PlGF is reported to be associated with placental dysfunction and fetal growth restriction [88,89]. Hence, measurements of maternal PlGF concentrations have been included in pregnancy management when there was suspected cases of fetal growth restriction and showed beneficial outcome when the obstetrician's decision was guided by those results [35,90]. However, low PlGF concentrations which were associated with lower perinatal mortality and birth weight <3rd centile, appeared to lead to earlier delivery with more neonatal respiratory morbidity [91].

The ratio of sFlt1/PlGF has found useful application in the prediction of fetal growth restriction outcome [92-94] and in conjunction with either Doppler ultrasound or ultrasound biometry there is an improvement in the prediction [95,96]. Despite the progress made in the use of these assays in the prediction of fetal growth restriction outcome, the analytical methods employed in these studies are not able to distinguish IUGR fetuses from that of SGA before time of birth [97,98].

Therapy for IUGR

Currently, there is no specific treatment for pregnant women diagnosed with IUGR but the assessment of fetal health and timely delivery are the main concerns for management of IUGR [2,3]. The well-being of an IUGR fetus is monitored by using umbilical artery Doppler velocimetry to examine the fetus' umbilical blood flow and serial ultrasonographic measurements to measure the growth of the fetus [2,3]. Under some rather rare circumstances, medications may be administered to assist the growth of the fetus [2].

At current, there is no specific criteria that determines the optimal timing of delivery of an IUGR fetus. Hence, signs of fetal deterioration, detected from the monitoring process, determines the time of delivery [2,3].

1.1.2 Application of proteomics methods in prenatal screening

Identification / discovery of biomarkers

Several body fluids such as amniotic fluid, cervical vaginal fluid, umbilical cord blood and maternal blood have been used in the process of discovery of biomarkers for pregnancy complications [74,99,100]. Amniotic fluid is closely related to the fetus and could be a suitable source for discovery of biomarkers associated with pregnancy complications but sampling is not easily accessible and depends on an invasive method such as amniocentesis [74,99,100]. Maternal blood is a much preferred source for discovery of biomarkers because of easy accessibility as little invasive methods can be applied for sampling [74,99,100].

In the analyses of multifaceted pregnancy-related pathophysiological disorders, such as hemolysis, elevated liver enzymes, and low platelets (HELLP) syndrome, preeclampsia and IUGR, analytical methods that can deal with the complexity of the biological samples are needed [101]. The emergence of proteomics-based technologies such as two-dimensional gel electrophoresis (2-DE), liquid chromatography multiple-reaction-monitoring mass spectrometry (LC-MRM/MS) and matrix assisted laser desorption/ionization-time of flight mass spectrometry (MALDI-TOF-MS) which are capable of identifying and characterizing biomolecules of various body fluids in normal and diseased states has contributed immensely to the discovery and/or identification of biomarkers associated with pregnancy-related complications [74,76,102,103].

Global Proteomics and Targeted Proteomics Research Approaches

Proteomic approaches make it possible for precise classification of proteins in multifaceted biological organisms, by offering significant information on the state of biological systems [104]. Based on the goal of a research study, proteomic approaches

can be categorized into two main groups: global approaches and targeted approaches [105].

Global proteomics approaches are applied in discovery / identification projects as a profiling tool to identify many undefined sets of modified proteins and the proteome profiles are compare to different physiological or pathological states [104]. This is called the "data-driven" research approach. Global proteomic approaches are grouped into gel based methods, i.e. two-dimensional gel electrophoresis (2-DE) separation of proteins, e.g. from biological fluids, based on their molecular masses and isoelectric points, is followed by mass spectrometry based analytics. Generally, MALDI-ToF-MS and liquid chromatography – electrospray ionization - mass spectrometry (LC-ESI-MS) methods have been developed in combination with gel-based high resolution protein separation methods. The limitations of 2-DE include poor gel-to-gel variability, low reproducibility, substantial time required for the analysis and the difficulty to automate the process. Due to these reasons, the method is usually preferred for the preliminary stage of biomarker discovery and has not been directly transferred into clinical applications [74,76,100]. The LC-ESI-MS based analysis strategy is further divided into two: isotope-labeling and label-free approaches [104]. Most of label-free LC-MS approaches employed in the identification of proteome signatures use the so-called "shotgun" technique, in which the pre-separated proteins are enzymatically digested before the generated peptides are subjected to LC-ESI-MS analysis [106-109].

The targeted proteomics approach is used for quantitation of a smaller number of defined sets of proteins and is applied in "hypothesis-driven" research studies [110]. Liquid chromatography multiple-reaction-monitoring mass spectrometry (LC-MRM-MS) is a mass spectrometry-based method which is used for quantitation of proteins based on selection and fragmentation of a targeted peptide ions with detection of specific fragment ions, compared to added isotopically labelled synthetic peptides which serve as internal standards [111-113]. Even though MRM-MS based quantitation is normally used for clinical validation of potential biomarkers [111,114,115], MRM-MS assays can also be applied in the discovery of biomarkers [111]. The application of MRM-MS for analyses of maternal serum identified a putative proteomic biomarkers for trisomy 21 [116] and a potential biomarker associated with early spontaneous preterm birth (early SPTB) [117]. While MRM-MS has shown to be accurate, specific and reproducible [111], assay of clinical samples require a prolonged LC separation time [118], which will likely prolong the duration of sample analyses in clinical applications. Hence, LC-MRM-MS analyses of clinical samples require the installation of highly specialized laboratories run by trained specialists.

Both, global and targeted proteomics approaches have contributed immensely to the identification of proteome signatures for characterizing complications associated with pregnancies on the molecular level. 2-DE approaches have revealed putative plasma biomarkers of gestational diabetes mellitus when maternal plasma from women with normal pregnancies were compared with those who had developed gestational diabetes mellitus [119]. Proteome studies of umbilical cord blood using 2-DE identified

protein markers potentially responsible for IUGR associated complications [120,121] and also analyses of maternal plasma with 2-DE identified proteome signatures for HELLP-syndrome [122,123].

Affinity proteomics screening / diagnosis of pregnancy complications

MALDI-ToF-MS is a rather simple, rapid and now even automated analytical technique which is suitable for the detection of a broad spectrum of biomolecules, such as peptides and proteins from clinically obtained body fluids [124,125]. The major bottle-neck for analyses of body fluids using MALDI-ToF-MS is a sample preparation procedure that will purify the complex body fluids and additionally enrich the peptides or proteins of interest [126]. To overcome these limitations, magnetic beads with hydrophobic surfaces have been found valuable for purification and enrichment of peptides or proteins of interest prior to MALDI-ToF-MS profiling of body fluids. Serum protein profiling for the analysis of peptides or proteins using magnetic bead fractionation in combination with MALDI-ToF-MS has aided in the identification of potential biomarkers for diseases due to its ease of operation, sensitivity, good reproducibility and robustness [127-129].

Proteome profiles of maternal blood serum obtained by MALDI-ToF-MS identified biomarkers that differentiated pre-eclampsia patients from those of healthy controls [130]. Mass spectrometric proteome profiling of umbilical cord blood serum identified proteome signatures that differentiated neonates that were born after pregnancies had been complicated by IUGR from those who had been small for gestational age and / or normal (control) individuals [131,132]. Proteome profiling of maternal blood serum identified proteome signatures that differentiated pregnancies carrying IUGR fetuses from those carrying normal (control) fetuses [133]. The identification of these proteome signatures using MALDI-ToF-MS will contribute to the understanding of the underlying pathological conditions and the clinical diagnosis of multifactorial pregnancy disorders leading to an improved maternal healthcare.

Translation of affinity proteomics to the clinics

IUGR is a worldwide clinical problem [134] and the use of ultrasound for serial assessment of growth in all pregnancies is not practicable even in developed countries [60]. Blood tests are cost effective and favorable sources implemented even in developing countries for clinical analyses [135,136].

Over the past years, our group has researched into the application of mass spectrometric profiling methods as a possible screening or diagnostic tool for pregnancy complications. A protein profiling method for analysis of plasma samples from HELLP patients and from healthy women prior to and after delivery without fractionation of the plasma samples [123] that used a cryodetector mass spectrometer [137] was developed. Though there was no sample fractionation prior to analyses, the

mass spectrometric profiling analysis displayed high molecular mass proteins with significant differences in ion intensities between post-HELLP (control) samples and HELLP patients which were detected using the cryodetector MS equipment. The most conspicuous difference in the spectra between most of the HELLP cases and those from the same persons after delivery post-HELLP (control) was the presence or absence of an ion signal at 11.8 kDa which was assigned to serum amyloid A (SAA). The cryodetector MS-based screening technique permits a rapid and reliable differentiation of HELLP patients from healthy women. The role of SAA for identification of HELLP and separation from preecclampsia has later been confirmed by ELISA-based investigations [138].

Furthermore, a MALDI-ToF-MS method was developed to analyze serum proteins of pregnant women with severe early-onset preeclampsia and those of control individuals [130]. Here, reversed-phase coated magnetic beads were used for the fractionation of serum proteins. The fractionation produced serum proteins suitable for MALDI-ToF-MS profiling without the need for additional work-up. In order to differentiate between preeclampsia and control groups by accurately assigning protein ion signals to either, a variety of distinctive signatures signals which could be used for the characterization of a sample were examined. Three best group of differentiating singly charged protein ion signals regarded as a "signature for preeclampsia", i.e. transthyretin and its derivatives, were selected because they carried sufficient information to form the rules that enabled accurate sorting of individual spectra. A multiparametric analysis was performed by bringing the ion signal areas within each spectrum into context with each other. The "signature for preeclampsia", i.e. transthyretin and derivatives, differentiated pregnant women with severe early-onset preeclampsia from control individuals.

The probable diagnostic value and clinical practicality of the established affinity-based MALDI-TOF-MS method capable of distinguishing preeclampsia patients from controls [130] was assessed in a multicenter setting [139]. The MALDI-ToF-MS serum profiling with center-wise standardization presents a rapid and robust method to categorize preeclampsia.

Carrying the research studies further, the established affinity MALDI-ToF-MS profiling method previously proven successful in a multiparametric characterization of blood serum samples from preeclampsia pregnant women [130] was utilized in the analysis of umbilical cord blood serum samples belonging to either IUGR or normal (control) neonates by subjecting the umbilical cord blood serum samples to fractionation by affinity chromatography using a bead system with hydrophobic interaction capabilities and the prepared protein mixtures were then analyzed by MALDI-ToF-MS [132]. The best differentiating ion signals were identified as belonging to apolipoprotein C-III protein species, i.e. $apoC\text{-}III_0$, $apoC\text{-}III_1$, and $apoC\text{-}III_2$, which were collectively assigned as "IUGR proteome signature". This proteome signature was used for the multiparametic analysis upon which IUGR neonates were successfully separated from control neonates.

Encouraged by the results obtained from the analyses of umbilical cord blood serum by affinity MALDI-ToF-MS profiling [132], the method was further used to analyze different umbilical cord blood serum samples from IUGR, SGA, and control infants [131]. The established proteome signature (apolipoprotein C-III protein species) was able to differentiated IUGR infants from SGA and control infants at time of birth [131].

In an effort to aid the screening of pregnant women for the early detection of pregnancy-related complications such as IUGR via affinity mass spectrometry, molecular profiling of maternal peripheral blood was anticipated to play a vital in the monitoring the health conditions of fetuses. To develop such a minimally invasive assay, the established affinity MALDI-ToF-MS profiling method for the analyses of blood proteins of pregnant women with preeclampsia [130,139] and umbilical cord blood proteins from IUGR and SGA infants [131,132] was applied to analyze peripheral blood serum samples from pregnant women carrying IUGR fetuses or normal (control) fetuses after affinity fractionation with magnetic beads [133]. The peripheral maternal blood serum used [133] was obtained from respective maternal counterparts of the infants from the previous study of fetal cord blood proteome profiling [132]. The best differentiating protein ion signals from the maternal serum were apolipoprotein C-II and apolipoprotein C-III protein species (previously identified in fetal cord blood proteome profiling). Together they constituted the "maternal IUGR proteome signature" and were used for relative quantitation analysis. The "maternal IUGR proteome signature" differentiated IUGR pregnancies from control with high confidence.

Hence, with the emergence of MALDI-ToF-MS in clinical applications [131-133], in future, the screening and diagnosis of IUGR during pregnancy may be based on blood protein assays using MALDI-ToF-MS in combination with clinical assessments such as determination of fundal height [60] in the absence of ultrasound data. These approaches may have the potential to improve screening and diagnostic accuracy in developed countries as well as developing ones.

1.2 Aim of the study

Currently, differentiating between IUGR fetuses and SGA fetuses in the clinics remains a challenge which shall be overcome by blood-based analyses which are capable of determining the individual´s proteome signature(s). Therefore, the objectives of this thesis were (i) to profile blood samples from pregnant women using the affinity mass spectrometric method to identify proteome signature(s) that can differentiate IUGR pregnancies from SGA and/or normal pregnancies (ii) to broaden the spectrum for the identification and quantification of proteome signature(s) for IUGR using a multiplexing serological assay based on liquid chromatography–multiple-reaction-monitoring mass spectrometry, (LC-MRM-MS) and (iii) to develop a workflow that will circumvent the necessity of the "cold-chain", but still keep proteins intact during transportation of serum samples from the clinics to the mass spectrometry laboratory for in-depth analysis.

First, within this thesis, a targeted multiplexing mass spectrometric method was employed for identification and quantification of protein(s) capable of differentiating pregnancies affected with IUGR from normal pregnancies.

Second and foremost within this thesis, relative protein abundances of maternal blood serum were analyzed using affinity proteomics, i.e. MALDI-ToF-MS profiling of fractionated serum proteins. Changes in serum protein composition in relation to gestational age lead to the development of a "three value regime" for classification of patient cohorts, separating IUGR cases from both, SGA and control individuals.

Third, within this thesis, an analytical procedure was developed where intact proteins from maternal blood serum samples were stored on filter membranes at room temperature ("dried serum spot"). Resolubilization steps for elution were developed and made compatible with analysis by MALDI-ToF-MS. The developed analytical procedure was compared with the conventional procedure which included "freeze-thaw cycles" for storing, shipping, and preparation of serum protein solutions for analysis. In summary, maternal blood serum samples from the clinics could be stored on a "storage discs" and shipped by regular mail or courier to the mass spectrometry laboratory, thereby reducing costs of transportation and storage.

The user friendly linear MALDI-ToF-MS analysis of intact proteins has reached a state of maturation that is ready to be employed in profiling of the relative abundances of serum proteins of interest, termed the IUGR proteome signature. This affinity – mass spectrometry procedure shall in greater length help to improve risk assessment of pregnancy complications not only in the developed world but also developing countries.

1.3 Methods

1.3.1 Quantification of apolipoproteins in maternal serum

In the analyses of clinically obtained biological fluids, pre-analytical factors such as sample collection and sample storage are significant stages because they have the tendency to affect accuracy and reproducibility. Due to the delicate nature of peptides / proteins present in biological fluids, a sample storage system which will avoid freezing temperatures and still preserve peptides / proteins is an ideal one.

Lyophylization is a process of removal of water (drying) from biological samples without the application of heat. It is usually applied to samples that contain proteins and/or peptides that are sensitive to heat. The dried proteins and/or peptides can be stored for a longer period of time without the need for applying freezing temperatures. Lyophylization helps with sample stability and easy handling during transportation from one laboratory to the other.

In this thesis, we developed two different sample work-up protocols from maternal blood serum form pregnant women diagnosed to be carrying IUGR fetuses and those carrying normal fetuses. The sample work-ups were analyzed using liquid chromatography – multiple-reaction-monitoring – mass spectrometry (LC-MRM-MS).

For the first sample work-up, the maternal serum proteins were reduced, alkylated and digested to obtain the native (NAT) peptides. Synthesized stable isotope-labeled (SIS) peptides obtained in the dried form (lyophilized to dryness and shipped to the lab), were re-solubilized and added to the NAT peptides. The peptide mixtures (both NAT and SIS) were desalted and lyophilized to dryness. The dried peptide mixtures (both NAT and SIS) were then re-solubilized and the final solution was labeled as MS1 prior to analysis. For the second sample work-up, the maternal serum proteins were obtained in the dried form (lyophilized to dryness and shipped to the lab). Afterwards, it was re-solubilized, reduced, alkylated and digested to obtain the NAT peptides. SIS peptides, already in solution, were added and the peptide mixtures (both NAT and SIS) were desalted. The final solution was labeled as MS2 prior to analysis.

There was no significant difference between the results obtained for sample work-up MS1 (peptide level) and sample work-up MS2 (intact protein level) indicating that serum proteins samples can be shipped at both the processed peptide level and the intact protein level without loss of quality.

The apolipoprotein B100 levels were found to decrease in pregnant women whose fetuses were complicated by IUGR compared to pregnant women with healthy fetuses. For more information on apolipoprotein B100 levels in maternal serum see Chapter 1.4.1.

1.3.2 Application of three value regimes: below – in between – above cut-offs to maternal blood serum samples

The complexity and abundance of maternal blood protein compositions change in relation to advancing gestational age. For any blood protein-based analytical method to find suitable application in pregnant women, this information plays a critical role.

In this thesis, we investigated peripheral blood serum protein abundance differences from 45 Caucasian pregnant women using our developed affinity - MALDI-ToF-MS serum proteome profiling method. Of the Caucasian pregnant women whose serum samples were used for the study, 15 were clinically diagnosed to carry normal fetuses; referred to as the Control (CTRL) group, another 15 were clinically diagnosed to carry SGA fetuses, and the third group of 15 were clinically diagnosed to carry IUGR fetuses. The CTRL group consisted of women with unsuspicious pregnancies who delivered healthy babies after normal gestational periods, ca. 39.6 (± 0.7) weeks of gestation. The IUGR group delivered after ca. 30.5 (± 1.3) weeks, and the SGA group delivered after ca. 38.1 (± 0.7) weeks of gestation. The CTRL group was chosen to match with the IUGR and the SGA groups only at the gestational age at blood sampling, which took place at ca. 31.0 (± 1.5) weeks. The duration between blood sampling and delivery for the CTRL, SGA and IUGR groups were around 71, 50, and 6 days, respectively. From the results of our training set, "best cut-off" values were determined using the Youden index (Jmax) analysis procedure.

Previously, our group had established cut-off values for CTRL and IUGR cohorts but because in that earlier study [133] the CTRL group consisted of pregnant women who delivered preterm, ca. 32.8 (± 2.6) weeks of gestation for various reasons (premature rupture of the membrane, spontaneous onset of labor, vaginal bleeding), these cut-off values were considered not suitable for this study. To optimize our procedure of assigning a specific mass spectrum to either of the groups, we generated a new set of cut-off values and combined both sets of "cut-off" values to generate a three value regimes (below – in between – above cut-offs). Application of our novel three value regimes cut-off successfully differentiated IUGR from CTRL / SGA with high confidence. For more information on application of three value regimes: below – in between – above cut-offs to maternal blood serum samples see Chapter 1.4.2.

1.3.3 Analysis of intact proteins from "dried serum spot"

Mass spectrometry-based proteome profiling provides a formidable technique to diagnose pregnancy-related diseases like IUGR due to its ability to characterize individual serum samples based on multifaceted proteome signatures from pregnant women. Nonetheless, transferring of biological fluids from the clinic to the mass spectrometry laboratory remains a challenge due to high cost of shipping and storage. In order to advance the use of mass spectrometry in clinical applications,

there is the demand to bridge the distance between the clinic and the mass spectrometry laboratory.

In this thesis, we developed a novel work-up procedure for the resolubilization and elution of intact proteins from maternal sera stored on Noviplex^TM cards (referred to as "dried serum spots") prior to analysis with the mass spectrometer.

Maternal serum samples from pregnant donors diagnosed to carrying normal fetuses referred to as control (CTRL) and patients diagnosed to be carrying IUGR fetuses obtained from the clinics were deposited on the ''serum storage discs'' that were mounted on the base sheets of Noviplex^TM cards. Serum was allowed to dry at ambient temperature in a clean box and "dried serum spots" were stored at room temperature for up to three days. The "dried serum spots" were then shipped by courier at room temperature to the mass spectrometry laboratory. The dried serum proteins were resolubilized and eluted using our novel work-up procedure. Another set of serum samples from the same donors and patients were shipped to mass spectrometry laboratory on dry ice and a conventional work-up procedure was used (freezing of serum at the clinics, shipping of samples in the frozen state, and thawing of serum in the laboratory) prior to analysis.

The eluted intact proteins from the "dried serum spots" using our novel work-up procedure and that from fresh frozen and thawed serum using the conventional work-up procedure were analyzed using our affinity - MALDI-ToF-MS serum proteome profiling method and the obtained mass spectra were compared to each other. The resulting proteome profiles of intact serum proteins from the ''dried serum spots'' using our novel work-up procedures were found to be of comparable quality as the ones which were obtained from the same serum using conventional work-up procedures.

Application of our developed multiparametric analysis to proteins of interest differentiated IUGR serum samples from the control serum samples upon both, the novel work-up and the conventional work-up series. Our novel procedure avoids the conventional freeze / thaw cycle, paving the way for potential mass spectrometric analysis of other diseases using intact proteins eluted from "dried serum". For more information on analysis of intact proteins from "dried serum spot" see Chapter 1.4.3.

1.4 Results

1.4.1 Maternal Apolipoprotein B100 Serum Levels are Diminished in Pregnancies with Intrauterine Growth Restriction and Differentiate from Controls

Purpose: Intrauterine growth restriction, a major cause of fetal morbidity and mortality, is defined as a condition in which the fetus does not reach its genetically given growth potential. Screening for intrauterine growth restriction biomarkers in the mother's blood would be of great help for optimal pregnancy management and timing of delivery as well as for identifying fetuses requiring further surveillance during their infancies.

Experimental Design: A multiplexing serological assay based on liquid chromatography–multiple-reaction-monitoring mass spectrometry is applied for distinguishing serum samples of pregnant women.

Results: Assessment of concentrations of apolipoproteins and of proteins that belong to the lipid transport system is performed with maternal serum samples, consuming only 10 µL of serum per multiplex assay from each patient. Of all investigated proteins the serum concentrations of apolipoprotein B100 shows the greatest power for discriminating intrauterine growth restriction from control samples, reaching areas under curves above 0.85 in receiver-operator-characteristics analyses.

Conclusions: These results indicate the potential of liquid chromatography-multiple-reaction-monitoring mass spectrometry to become of clinical importance in the future for intrauterine growth restriction risk assessment based on maternal apolipoprotein B100 serum levels.

For detailed information on apolipoproteins levels in maternal serum using LC-MRM/MS see Chapter 2.1

1.4.2 Precision Diagnostics by Affinity - Mass Spectrometry: A Novel Approach for Fetal Growth Restriction Screening During Pregnancy

Fetal growth restriction (FGR) affects about 3 to 8% of pregnancies leading to higher perinatal mortality and morbidity. Current strategies for detecting fetal growth impairment are based on ultrasound inspection. However, antenatal detection rates are insufficient and critical in countries with substandard care. To overcome difficulties with detection and to better discriminate between high risk FGR and low risk small for gestational age (SGA) fetuses we here investigated suitability of risk assessment based on analysis of a recently developed proteome profile derived from maternal serum in different study groups. Maternal serum, collected at around 31 weeks of gestation was analyzed in 30 FGR, 15 SGA, and 30 control (CTRL) pregnant women who delivered between 31 and 40 weeks of gestation. From the 75 pregnant women of this study, 2 were excluded because of deficient raw data and 2

patients could not be grouped due to indeterminate results. Consistency between proteome profile and sonography results was obtained for 59 patients (26 true positive and 33 true negative). Of the by proteome profiling 12 contrarious grouped individuals, 3 were false negative and 9 were false positive cases with respect to ultrasound data. Both, true positive and false positive grouping transfer the respective patients to closer surveillance and thorough pregnancy management. Accuracy of the test is considered high with an area-under-curve value of 0.88 in receiver-operator-characteristics analysis. Proteome profiling by affinity – mass spectrometry during pregnancy provides a reliable method for risk assessment of impaired development in fetuses and consumes just minute volumes of maternal peripheral blood. Additive to clinical testing proteome profiling by affinity – mass spectrometry may improve risk assessment, referring pregnant women to specialists early, thereby improving perinatal outcome.

For detailed information on Precision Diagnostics using Affinity - Mass Spectrometry see Chapter 2.2

1.4.3 Comparison of blood serum protein analysis by MALDI-MS from either conventional frozen samples or storage disc-deposited samples: A study with human serum from pregnant donors and from patients with intrauterine growth restriction

Mass spectrometric profiling of intact serum proteins, i.e. determination of relative protein abundance differences, was performed using two different serum sample preparation methods: one with frozen and thawed serum, the other with at room temperature deposited and dried serum. Since in a typical clinical setting freezing of serum is difficult to achieve, sampling at room temperature is preferred and can be met when using the Noviplex^{TM} card system. Once deposited and dried, serum proteins can be stored and shipped at room temperature. After resolubilization of serum proteins from "dried serum spots", mass spectra of high quality have been recorded comparable to those that were obtained using fresh-frozen and subsequently thawed serum samples. Differentiation between patients with intrauterine growth restriction and control individuals was achievable, independent from the sample work-up procedure. Having at hand a reliable and robust method for serum storage and shipment which works at room temperature bridges the gap between the clinics and the protein analysis laboratory. Our novel serum handling protocol reduces costs for both, storage and shipping, and ultimately enables clinical risk assessment based on mass spectrometric determination of intact protein abundance profiles.

For detailed information on comparison of blood serum protein analysis by MALDI-MS from either conventional frozen samples or storage disc-deposited samples see Chapter 2.3.

1.5 Discussion

Screening for biomarkers associated with diseases during pregnancy is a significant phase of clinical diagnosis due to its impact on clinical decision making in improving maternal healthcare [140]. Currently in the clinics, screening of pregnancy-related complication like preeclampsia depends on immunoassays e.g. ELISA, which is based on an antigen-antibody reactions [83-87]. The antibody has the ability to react with other antigens (with similar configurations) present in biological fluids other than the specific antigen to which it was raised, leading to cross-reactivity [141]. Due to interferences, these diagnostic techniques quite often produce false positive and false negative results [124,125,141].

The challenges associated with classical immunoassay diagnostic methods are gradually being overcome by the development of powerful analytical techniques such as MALDI-ToF-MS which directly identifies biomolecules in biological fluids by means of their mass-to-charge (m/z) ratios with high accuracy [124,125,142].

Likewise, in the area of clinical microbiology, conventional techniques employed in the detection microorganisms are costly, complicated and time consuming [143,144]. MALDI-ToF-MS has contributed tremendously to overcoming these limitations by the identification of microorganisms based on their protein profiles with accuracy and consistency [145-148]. Upon this successful application, MALDI-ToF-MS has been approved by the U.S. Food and Drug Administration leading to its acceptance and usage in many clinical microbiology laboratories [149] and in some cases, complements the conventional detection techniques [146].

MALDI-ToF-MS has the tendency to probe multiple biomolecules concurrently, leading to the possibility of uncovering "several protein marker" candidates [75,119,150]. It is believed that differentiating a polygenic disease from a healthy one by means of a single marker proteins may not be suitable but the 'several protein marker' candidates, so-called "proteome signatures" might be more appropriate with the capability of stratification of patients [109] and essentially contribute to the specificity and sensitivity of clinical applications [75,119,150]. Similarly, the "proteome signatures" might contribute to the understanding of disease pathways leading to development therapeutic interventions [109].

Two studies [151,152] have previously utilized proteomics approaches to identify biomarkers for IUGR by profiling maternal plasma but no SGA patients were included as is done in this thesis. In one of the studies [151], an isobaric Tag for Relative and Absolute Quantitation (iTRAQ) approach was used to profile maternal plasma in the identification of protein markers for IUGR. However, the gestational ages of IUGR patients were not harmonized with that of the normal ones and also prior to the determination of the relative protein concentration differences, the plasma samples from individual patients were pooled together. The other study [152] employed 2-DE and image analysis to profile maternal plasma to identify a potential biomarker associated with FGR. The spot volumes of individual patients were pooled and the

mean spot volume was used prior to quantification of differences in spot volumes. The protein markers identified in these studies were antichymotrypsin (SERPINA3) and C reactive protein (CRP) [151], and haptoglobin α2 isoform [152] in contrast to our proteome signatures which constitutes of Apo CII and Apo CIII (in addition to its glycosylated/sialylated isoforms). Typically, 2-DE detect proteins in the mass range of 10 – 200 kDa [100] and our proteome signatures (Apo CII and Apo CIII) had mass range of 8 – 9 kDa hence, 2-DE would not have been able to detected them because of their low molecular masses.

Consequently in both [151,152], individual patient classification was not achievable since information on individual sample was not available hence the sensitivity and specificity of these approaches were not established. This is contrary to our affinity MALDI-ToF-MS proteome profiling method employed in this thesis in that, the proteome signatures obtained for each individual was used in the multiparametric analysis for stratification of each patient enabling us to differentiate IUGR from CTRL / SGA individuals and also to perform biostatistical analysis to determine the sensitivity, specificity and receiver operator characteristics (ROC) / area under curve (AUC). So far, there is no other reported literature on differentiating IUGR from SGA using a proteomic approach.

Recently, a study has been published in which was focused on PIGF, placental protein 13 (PP13), A-disintegrin, and metalloprotease 12 (ADAM12) from maternal serum taken at 11–13 weeks of gestation using antibody-based immunoassays. In this study were identified half of pregnancies with SGA neonates [153] but there was no comparison with pregnancies affected by IUGR. In contrast, in this thesis the gestational age of sampling was ca. 31 weeks for our SGA cohorts and our affinity mass spectrometric method was able to distinguished IUGR pregnancies from those with SGA fetuses.

With advancing gestational age, maternal blood protein compositions change in complexity and abundance [154-156], therefore gestational age can be an essential confounding parameter that needs to be considered in assays involving blood protein of pregnant women. Taking into consideration the variety of pregnant women recruited in our analysis and their respective relative protein abundances present in maternal blood, in this thesis we developed a three value regimes: below – in between – above cut-offs for separating IUGR from CTRL / SGA samples / individuals, instead of a typical two value regimes analysis with samples below a given cut-off which are separated from those above.

It should be noted that the components of the proteome signature identified in this thesis play essential roles in triglyceride metabolism.

ApoC-II is required for the metabolism of triglyceride-rich lipoproteins by the activation of lipoprotein lipase for effective lipolysis of triglyceride-rich lipoproteins [157,158]. Reduction of lipoprotein lipase activity in the presence of either excess or deficient apoC-II has been reported to be associated with hypertriglyceridemia [157].

ApoC-III occurs in three isoforms, designated as $apoC\text{-}III_0$, $apoC\text{-}III_1$, and $apoC\text{-}III_2$ depending on the number of sialic acid molecules attached to the protein [159] with each isoform contributing to 10, 55 and 35 % respectively of the overall apoCIII levels in circulation [160]. It has been suggested that ApoC-III affects lipolysis of triglyceride-rich lipoproteins by lipoprotein lipase based on the amount of sialylation [161]. Kinetics studies of $ApoC\text{-}III_1$ and $ApoC\text{-}III_2$ sialylated isoforms revealed that they inhibit the activity of lipoprotein lipase, thereby contributing to metabolic syndrome, including hypertriglyceridemia. These results give credence to the fact that hypertriglyceridemia in humans is associated with the secretion of ApoC-III into the circulation [162-165].

A study by our group on profiling of umbilical cord blood serum form IUGR, SGA and healthy neonates identified $ApoC\text{-}III_0$, $ApoC\text{-}III_1$, and $ApoC\text{-}III_2$ as prospective proteome signatures [131,132] which correlated with the findings of lipid metabolism disorders in newborns with IUGR [166-168]. A recent study on profiling of plasma from preterm and born term preschool children revealed that ApoC-II and ApoC-III were significantly higher in the preterm children than in those born term, indicating potential effects of prematurity. Further, high levels of apolipoprotein CIII may be an indication of a pro-atherogenic risk factor in early childhood [32]. These outcomes strengthen the indications that IUGR babies may be at higher risk to develop cardiovascular diseases later in life [27,29,33,169]. Further studies of the mechanisms on our proposed proteome signatures, apoC-II and C-III (and its isoforms) during pregnancy may improve one's comprehension of the pathomechanism in IUGR and their lasting effects on neonates.

IUGR is considered to be a multifactorial condition and placental insufficiency is deemed to be one of them [2,21]. The placenta is capable of secreting apo B100 [170] and as observed in our study of quantification of apolipoproteins in maternal blood serum, apo B100 levels were lower in pregnancies affected by IUGR as compared to levels from individuals with normal pregnancies, which may be an indication that low levels of apo B100 may be related to placental insufficiency.

Blood plasma and serum are the most preferred clinical samples used for the identification or discovery of disease biomarkers [171,172]. However, preparation of plasma or serum requires centrifugation of blood followed by freezing or keeping it on dry ice and this advanced procedures can only be accomplished at specialized health care centers [130,131,133]. Unfortunately, these specialized facilities are not immediately available worldwide [173,174]. Moreover, individuals living farther away from mass spectrometry laboratories might not benefit from mass spectrometric analysis of their blood plasma or serum due to the distance between them and the mass spectrometry laboratory [175] because transportation of plasma or serum on dry ice is expensive and requires the services of specialized couriers [176]. These challenges have the propensity to hinder the widespread application of a prospective mass spectrometry based profiling method for clinical use in the area of disease screening / diagnosis.

Currently, blood, plasma, and serum samples can be collected on filter paper cards in the form of dried blood spots (DBS), dried plasma spots (DPS) and dried serum spots (DSS), respectively, which enable them to function as appropriate storage and shipment devices for clinical samples. Mass spectrometry techniques have been used to analyze drug metabolites in dried blood spots [177,178], dried plasma spots [179-181] and dried serum spots [182] and likewise, multiple reaction monitoring mass spectrometry (MRM-MS) was used to quantify proteins from dried blood spots by analysis of peptides [183-185]. But in none of these projects were eluted intact proteins from their "dried state" for mass spectrometric analysis. Our novel procedure, developed in this thesis, for the resolubilizing and elution of intact proteins from dried serum spots followed by analyses of their relative abundances by MALDI-ToF-MS enabled us to differentiate healthy donors from patients.

In conclusion, affinity - MALDI ToF MS allows the identification of proteome signatures for screening of pregnancy complications, such as IUGR, using maternal blood. This makes affinity - MALDI ToF MS a significant analytical tool for clinical research which in future may find valuable application in routine clinical diagnostics in combination with clinical examinations such as ultrasound biometry or fundal height determination to improve antenatal care. Furthermore, the novel procedure to resolubilize and elute intact proteins from dried serum spots will bridge the distance between clinics and mass spectrometry laboratories by circumventing the freeze / thaw stages which in future is foreseen to pave the way for potential mass spectrometric evaluations of pregnancy related complications and other diseases worldwide.

1.6 References

(1) Okai, C. A.; Russ, M.; Wölter, M.; Andersen, K.; Rath, W.; Glocker, M. O.; Pecks, U. *Journal of Clinical Medicine* **2020**, *9*, 1374.

(2) American College of Obstetricians and Gynecologists. *Obstetrics and gynecology* **2019**, *133*, e97-e109.

(3) Figueras, F.; Gardosi, J. *American journal of obstetrics and gynecology* **2011**, *204*, 288-300.

(4) Hay, W. W.; Thureen, P. J.; Anderson, M. S. *NeoReviews* **2001**, *2*, e129-e138.

(5) Wollmann, H. A. *Hormone research* **1998**, *49 Suppl 2*, 1-6.

(6) Lee, P. A.; Chernausek, S. D.; Hokken-Koelega, A. C.; Czernichow, P.; International Small for Gestational Age Advisory, B. *Pediatrics* **2003**, *111*, 1253-1261.

(7) Hershkovitz, R.; Erez, O.; Sheiner, E.; Bashiri, A.; Furman, B.; Shoham-Vardi, I.; Mazor, M. *European journal of obstetrics, gynecology, and reproductive biology* **2001**, *97*, 141-146.

(8) American College of Obstetricians and Gynecologists. *Obstetrics and gynecology* **2013**, *122*, 1139-1140.

(9) Savchev, S.; Figueras, F.; Sanz-Cortes, M.; Cruz-Lemini, M.; Triunfo, S.; Botet, F.; Gratacos, E. *Fetal diagnosis and therapy* **2014**, *36*, 99-105.

(10) Baschat, A. A. *Best practice & research. Clinical obstetrics & gynaecology* **2018**, *49*, 53-65.

(11) Hoellen, F.; Beckmann, A.; Banz-Jansen, C.; Weichert, J.; Rody, A.; Bohlmann, M. K. *In vivo* **2016**, *30*, 123-131.

(12) Malhotra, A.; Allison, B. J.; Castillo-Melendez, M.; Jenkin, G.; Polglase, G. R.; Miller, S. L. *Frontiers in endocrinology* **2019**, *10*, 55.

(13) Figueras, F.; Caradeux, J.; Crispi, F.; Eixarch, E.; Peguero, A.; Gratacos, E. *American journal of obstetrics and gynecology* **2018**, *218*, S790-S802 e791.

(14) Cutland, C. L.; Lackritz, E. M.; Mallett-Moore, T.; Bardaji, A.; Chandrasekaran, R.; Lahariya, C.; Nisar, M. I.; Tapia, M. D.; Pathirana, J.; Kochhar, S.; Munoz, F. M.; Brighton Collaboration Low Birth Weight Working, G. *Vaccine* **2017**, *35*, 6492-6500.

(15) de Onis, M.; Blossner, M.; Villar, J. *European journal of clinical nutrition* **1998**, *52 Suppl 1*, S5-15.

(16) Bamfo, J. E.; Odibo, A. O. *J Pregnancy* **2011**, *2011*, 640715.

(17) Seeds, J. W. *Obstetrics and gynecology* **1984**, *64*, 303-310.

(18) Ernst, S. A.; Brand, T.; Reeske, A.; Spallek, J.; Petersen, K.; Zeeb, H. *BioMed research international* **2017**, *2017*, 1746146.

(19) Romo, A.; Carceller, R.; Tobajas, J. *Pediatric endocrinology reviews : PER* **2009**, *6 Suppl 3*, 332-336.

(20) Kady, S. M.; Gardosi, J. *Best practice & research. Clinical obstetrics & gynaecology* **2004**, *18*, 397-410.

(21) Mandruzzato, G.; Antsaklis, A.; Botet, F.; Chervenak, F. A.; Figueras, F.; Grunebaum, A.; Puerto, B.; Skupski, D.; Stanojevic, M.; Wapm. *Journal of perinatal medicine* **2008**, *36*, 277-281.

(22) Jang, D. G.; Jo, Y. S.; Lee, S. J.; Kim, N.; Lee, G. S. *Archives of gynecology and obstetrics* **2011**, *284*, 73-78.

(23) Monier, I.; Blondel, B.; Ego, A.; Kaminiski, M.; Goffinet, F.; Zeitlin, J. *BJOG : an international journal of obstetrics and gynaecology* **2015**, *122*, 518-527.

(24) Hartkopf, J.; Schleger, F.; Keune, J.; Wiechers, C.; Pauluschke-Froehlich, J.; Weiss, M.; Conzelmann, A.; Brucker, S.; Preissl, H.; Kiefer-Schmidt, I. *Frontiers in physiology* **2018**, *9*, 1278.

(25) Levine, T. A.; Grunau, R. E.; McAuliffe, F. M.; Pinnamaneni, R.; Foran, A.; Alderdice, F. A. *Pediatrics* **2015**, *135*, 126-141.

(26) Miller, S. L.; Huppi, P. S.; Mallard, C. *The Journal of physiology* **2016**, *594*, 807-823.

(27) Barker, D. J.; Bull, A. R.; Osmond, C.; Simmonds, S. J. *Bmj* **1990**, *301*, 259-262.

(28) Barker, D. J.; Osmond, C. *Lancet* **1986**, *1*, 1077-1081.

(29) Cosmi, E.; Fanelli, T.; Visentin, S.; Trevisanuto, D.; Zanardo, V. *Journal of Pregnancy* **2011**, *2011*.

(30) Hales, C. N.; Barker, D. J.; Clark, P. M.; Cox, L. J.; Fall, C.; Osmond, C.; Winter, P. D. *Bmj* **1991**, *303*, 1019-1022.

(31) Phipps, K.; Barker, D. J.; Hales, C. N.; Fall, C. H.; Osmond, C.; Clark, P. M. *Diabetologia* **1993**, *36*, 225-228.

(32) Posod, A.; Pechlaner, R.; Yin, X.; Burnap, S. A.; Kiechl, S. J.; Willeit, J.; Witztum, J. L.; Mayr, M.; Kiechl, S.; Kiechl-Kohlendorfer, U. *Journal of the American Heart Association* **2019**, *8*, e011199.

(33) Skilton, M. R. *Pediatrics* **2008**, *121*, 570-574.

(34) Bernstein, P. S.; Divon, M. Y. *Clinical obstetrics and gynecology* **1997**, *40*, 723-729.

(35) Gaccioli, F.; Aye, I.; Sovio, U.; Charnock-Jones, D. S.; Smith, G. C. S. *American journal of obstetrics and gynecology* **2018**, *218*, S725-S737.

(36) Pollack, R. N.; Divon, M. Y. *Clinical obstetrics and gynecology* **1992**, *35*, 99-107.

(37) Duvekot, J. J.; Cheriex, E. C.; Pieters, F. A.; Menheere, P. P.; Schouten, H. J.; Peeters, L. L. *Obstetrics and gynecology* **1995**, *85*, 361-367.

(38) Ounsted, M.; Moar, V.; Scott, A. *BJOG: An International Journal of Obstetrics & Gynaecology* **1985**, *92*, 226-232.

(39) Lechtig, A.; Yarbrough, C.; Delgado, H.; Martorell, R.; Klein, R. E.; Béhar, M. *American journal of obstetrics and gynecology* **1975**, *123*, 191-201.

(40) Smyth, A.; Oliveira, G. H.; Lahr, B. D.; Bailey, K. R.; Norby, S. M.; Garovic, V. D. *Clinical journal of the American Society of Nephrology : CJASN* **2010**, *5*, 2060-2068.

(41) Bada, H. S.; Das, A.; Bauer, C. R.; Shankaran, S.; Lester, B. M.; Gard, C. C.; Wright, L. L.; Lagasse, L.; Higgins, R. *Journal of perinatology : official journal of the California Perinatal Association* **2005**, *25*, 631-637.

(42) Little, B. B.; Snell, L. M.; Klein, V. R.; Gilstrap, L. C., 3rd. *Obstetrics and gynecology* **1989**, *73*, 157-160.

(43) Mills, J. L.; Graubard, B. I.; Harley, E. E.; Rhoads, G. G.; Berendes, H. W. *Jama* **1984**, *252*, 1875-1879.

(44) Naeye, R. L.; Blanc, W.; Leblanc, W.; Khatamee, M. A. *The Journal of pediatrics* **1973**, *83*, 1055-1061.

(45) Aviles, A.; Diaz-Maqueo, J. C.; Talavera, A.; Guzman, R.; Garcia, E. L. *American journal of hematology* **1991**, *36*, 243-248.

(46) Farmen, A. H.; Grundt, J.; Tomson, T.; Nakken, K. O.; Nakling, J.; Mowinchel, P.; Lossius, M. *Seizure* **2015**, *28*, 76-80.

(47) Hall, J. G.; Pauli, R. M.; Wilson, K. M. *The American journal of medicine* **1980**, *68*, 122-140.

(48) Maulik, D. *Clinical obstetrics and gynecology* **2006**, *49*, 228-235.

(49) Yinon, Y.; Mazkereth, R.; Rosentzweig, N.; Jarus-Hakak, A.; Schiff, E.; Simchen, M. J. *Obstetrics and gynecology* **2005**, *105*, 80-84.

(50) Desai, M.; ter Kuile, F. O.; Nosten, F.; McGready, R.; Asamoa, K.; Brabin, B.; Newman, R. D. *The Lancet. Infectious diseases* **2007**, *7*, 93-104.

(51) Seitz, J.; Morales-Prieto, D. M.; Favaro, R. R.; Schneider, H.; Markert, U. R. *Frontiers in endocrinology* **2019**, *10*, 98.

(52) Gross, S. J. *Clinical obstetrics and gynecology* **1997**, *40*, 730-739.

(53) Rochelson, B.; Kaplan, C.; Guzman, E.; Arato, M.; Hansen, K.; Trunca, C. *Obstetrics and gynecology* **1990**, *75*, 59-63.

(54) Catanzarite, V. A.; Hendricks, S. K.; Maida, C.; Westbrook, C.; Cousins, L.; Schrimmer, D. *Ultrasound in obstetrics & gynecology : the official journal of the International Society of Ultrasound in Obstetrics and Gynecology* **1995**, *5*, 98-105.

(55) Leung, A. K. C.; Robson, W. L. M. *JAMA Pediatrics* **1989**, *143*, 108-111.

(56) Mifsud, W.; Sebire, N. J. *Fetal diagnosis and therapy* **2014**, *36*, 117-128.

(57) Wilkins-Haug, L.; Roberts, D. J.; Morton, C. C. *American journal of obstetrics and gynecology* **1995**, *172*, 44-50.

(58) Sankaran, S.; Kyle, P. M. *Best practice & research. Clinical obstetrics & gynaecology* **2009**, *23*, 765-777.

(59) Engstrom, J. L. *Journal of obstetric, gynecologic, and neonatal nursing : JOGNN* **1988**, *17*, 172-178.

(60) Morse, K.; Williams, A.; Gardosi, J. *Best practice & research. Clinical obstetrics & gynaecology* **2009**, *23*, 809-818.

(61) Chamberlain, G. *BMJ: British Medical Journal* **1991**, *302*, 774.

(62) Konje, E. T.; Magoma, M. T. N.; Hatfield, J.; Kuhn, S.; Sauve, R. S.; Dewey, D. M. *BMC pregnancy and childbirth* **2018**, *18*, 394.

(63) Campbell, S.; Thoms, A. *British journal of obstetrics and gynaecology* **1977**, *84*, 165-174.

(64) Hadlock, F. P.; Harrist, R. B.; Sharman, R. S.; Deter, R. L.; Park, S. K. *American journal of obstetrics and gynecology* **1985**, *151*, 333-337.

(65) Chamberlain, P. F.; Manning, F. A.; Morrison, I.; Harman, C. R.; Lange, I. R. *American journal of obstetrics and gynecology* **1984**, *150*, 245-249.

(66) Philipson, E. H.; Sokol, R. J.; Williams, T. *American journal of obstetrics and gynecology* **1983**, *146*, 271-278.

(67) Varma, T. R.; Bateman, S.; Patel, R. H.; Chamberlain, G. V.; Pillai, U. *International journal of gynaecology and obstetrics: the official organ of the International Federation of Gynaecology and Obstetrics* **1988**, *27*, 185-192.

(68) Aditya, I.; Tat, V.; Sawana, A.; Mohamed, A.; Tuffner, R.; Mondal, T. *J Neonatal Perinatal Med* **2016**, *9*, 117-126.

(69) Trudinger, B. J.; Giles, W. B.; Cook, C. M.; Bombardieri, J.; Collins, L. *British journal of obstetrics and gynaecology* **1985**, *92*, 23-30.

(70) Brar, H. S.; Platt, L. D. *American journal of obstetrics and gynecology* **1988**, *159*, 559-561.

(71) Smith, G. C.; Yu, C. K.; Papageorghiou, A. T.; Cacho, A. M.; Nicolaides, K. H.; Fetal Medicine Foundation Second Trimester Screening, G. *Obstetrics and gynecology* **2007**, *109*, 144-151.

(72) Unterscheider, J.; Daly, S.; Geary, M. P.; Kennelly, M. M.; McAuliffe, F. M.; O'Donoghue, K.; Hunter, A.; Morrison, J. J.; Burke, G.; Dicker, P.; Tully, E. C.; Malone, F. D. *American journal of obstetrics and gynecology* **2013**, *208*, 290 e291-296.

(73) Mazarico, E.; Martinez-Cumplido, R.; Diaz, M.; Sebastiani, G.; Ibanez, L.; Gomez-Roig, M. D. *PloS one* **2016**, *11*, e0150152.

(74) Anagnostopoulos, A. K.; Tsangaris, G. T. *Clinical biochemistry* **2013**, *46*, 487-496.

(75) Rifai, N.; Gillette, M. A.; Carr, S. A. *Nature biotechnology* **2006**, *24*, 971-983.

(76) Zhang, X.; Li, L.; Wei, D.; Yap, Y.; Chen, F. *Trends in biotechnology* **2007**, *25*, 166-173.

(77) Anderson, N. L. *Molecular & cellular proteomics : MCP* **2005**, *4*, 1441-1444.

(78) Wu, C.; Liu, T.; Baker, E. S.; Rodland, K. D.; Smith, R. D. In *General Methods in Biomarker Research and their Applications*, Preedy, V. R.; Patel, V. B., Eds.; Springer Netherlands: Dordrecht, 2015, pp 17-48.

(79) Guthrie, R.; Susi, A. *Pediatrics* **1963**, *32*, 338-343.

(80) American Diabetes, A. *Diabetes care* **2004**, *27 Suppl 1*, S88-90.

(81) Garrison, A. *American family physician* **2015**, *91*, 460-467.

(82) Serlin, D. C.; Lash, R. W. *American family physician* **2009**, *80*, 57-62.

(83) Duckworth, S.; Chappell, L. C.; Seed, P. T.; Mackillop, L.; Shennan, A. H.; Hunter, R. *PloS one* **2016**, *11*, e0164276.

(84) Duhig, K. E.; Myers, J.; Seed, P. T.; Sparkes, J.; Lowe, J.; Hunter, R. M.; Shennan, A. H.; Chappell, L. C.; group, P. t. *Lancet* **2019**, *393*, 1807-1818.

(85) Huhn, E. A.; Kreienbuhl, A.; Hoffmann, I.; Schoetzau, A.; Lange, S.; Martinez de Tejada, B.; Hund, M.; Hoesli, I.; Lapaire, O. *Frontiers in medicine* **2018**, *5*, 325.

(86) Pant, V.; Yadav, B. K.; Sharma, J. *BMC pregnancy and childbirth* **2019**, *19*, 266.

(87) Sovio, U.; Gaccioli, F.; Cook, E.; Hund, M.; Charnock-Jones, D. S.; Smith, G. C. *Hypertension* **2017**, *69*, 731-738.

(88) Benton, S. J.; McCowan, L. M.; Heazell, A. E.; Grynspan, D.; Hutcheon, J. A.; Senger, C.; Burke, O.; Chan, Y.; Harding, J. E.; Yockell-Lelievre, J.; Hu, Y.; Chappell, L. C.; Griffin, M. J.; Shennan, A. H.; Magee, L. A.; Gruslin, A.; von Dadelszen, P. *Placenta* **2016**, *42*, 1-8.

(89) Molvarec, A.; Gullai, N.; Stenczer, B.; Fugedi, G.; Nagy, B.; Rigo, J., Jr. *BMC pregnancy and childbirth* **2013**, *13*, 161.

(90) Ormesher, L.; Johnstone, E. D.; Shawkat, E.; Dempsey, A.; Chmiel, C.; Ingram, E.; Higgins, L. E.; Myers, J. E. *Pregnancy hypertension* **2018**, *14*, 234-239.

(91) Sharp, A.; Chappell, L. C.; Dekker, G.; Pelletier, S.; Garnier, Y.; Zeren, O.; Hillerer, K. M.; Fischer, T.; Seed, P. T.; Turner, M.; Shennan, A. H.; Alfirevic, Z. *Pregnancy hypertension* **2018**, *14*, 228-233.

(92) Birdir, C.; Droste, L.; Fox, L.; Frank, M.; Fryze, J.; Enekwe, A.; Koninger, A.; Kimmig, R.; Schmidt, B.; Gellhaus, A. *Pregnancy hypertension* **2018**, *12*, 124-128.

(93) Herraiz, I.; Dröge, L. A.; Gómez-Montes, E.; Henrich, W.; Galindo, A.; Verlohren, S. *Obstetrics & Gynecology* **2014**, *124*, 265-273.

(94) Schoofs, K.; Grittner, U.; Engels, T.; Pape, J.; Denk, B.; Henrich, W.; Verlohren, S. *Journal of perinatal medicine* **2014**, *42*, 61-68.

(95) Herraiz, I.; Simon, E.; Gomez-Arriaga, P. I.; Quezada, M. S.; Garcia-Burguillo, A.; Lopez-Jimenez, E. A.; Galindo, A. *Pregnancy hypertension* **2018**, *13*, 279-285.

(96) Visan, V.; Scripcariu, I. S.; Socolov, D.; Costescu, A.; Rusu, D.; Socolov, R.; Avasiloaiei, A.; Boiculese, L.; Dimitriu, C. *Medicine* **2019**, *98*, e16069.

(97) Hendrix, M.; Bons, J.; van Haren, A.; van Kuijk, S.; van Doorn, W.; Kimenai, D. M.; Bekers, O.; Spaanderman, M.; Al-Nasiry, S. *Annals of clinical biochemistry* **2019**, 4563219882042.

(98) Ruchob, R.; Rutherford, J. N.; Bell, A. F. *Biological research for nursing* **2018**, *20*, 272-283.

(99) Choolani, M.; Narasimhan, K.; Kolla, V.; Hahn, S. *Expert review of proteomics* **2009**, *6*, 87-101.

(100) Klein, J.; Buffin-Meyer, B.; Mullen, W.; Carty, D. M.; Delles, C.; Vlahou, A.; Mischak, H.; Decramer, S.; Bascands, J. L.; Schanstra, J. P. *Expert review of proteomics* **2014**, *11*, 75-89.

(101) Glocker, M. O.; Röwer, C.; Wölter, M.; Koy, C.; Reimer, T.; Pecks, U. In *Handbook of Spectroscopy*, Gauglitz, G.; Moore, D. S., Eds.; Wiley-VCH Verlag GmbH & Co. KGaA, 2014, pp 407-428.

(102) Peng, J.; Gygi, S. P. *Journal of mass spectrometry : JMS* **2001**, *36*, 1083-1091.

(103) Shankar, R.; Gude, N.; Cullinane, F.; Brennecke, S.; Purcell, A. W.; Moses, E. K. *Reproduction* **2005**, *129*, 685-696.

(104) Shen, X.; Young, R.; Canty, J. M.; Qu, J. *Proteomics. Clinical applications* **2014**, *8*, 488-505.

(105) Mallick, P.; Kuster, B. *Nature biotechnology* **2010**, *28*, 695-709.

(106) Kumar, V. V.; James, B. L.; Russ, M.; Mikkat, S.; Suresh, A.; Kammerer, P. W.; Glocker, M. O. *Oral oncology* **2018**, *78*, 207-215.
(107) Röwer, C.; George, C.; Reimer, T.; Stengel, B.; Radtke, A.; Gerber, B.; Glocker, M. O. *Translational oncology* **2018**, *11*, 1-10.
(108) Röwer, C.; Koy, C.; Hecker, M.; Reimer, T.; Gerber, B.; Thiesen, H. J.; Glocker, M. O. *Journal of the American Society for Mass Spectrometry* **2011**, *22*, 440-456.
(109) Röwer, C.; Vissers, J. P.; Koy, C.; Kipping, M.; Hecker, M.; Reimer, T.; Gerber, B.; Thiesen, H. J.; Glocker, M. O. *Analytical and bioanalytical chemistry* **2009**, *395*, 2443-2456.
(110) Yang, J.; Finke, J. C.; Yang, J.; Percy, A. J.; von Fritschen, U.; Borchers, C. H.; Glocker, M. O. *Medicine* **2016**, *95*, e4808.
(111) Cohen Freue, G. V.; Borchers, C. H. *Circulation. Cardiovascular genetics* **2012**, *5*, 378.
(112) Lange, V.; Picotti, P.; Domon, B.; Aebersold, R. *Molecular systems biology* **2008**, *4*, 222.
(113) Pan, S.; Aebersold, R.; Chen, R.; Rush, J.; Goodlett, D. R.; McIntosh, M. W.; Zhang, J.; Brentnall, T. A. *Journal of proteome research* **2009**, *8*, 787-797.
(114) Shi, T.; Song, E.; Nie, S.; Rodland, K. D.; Liu, T.; Qian, W. J.; Smith, R. D. *Proteomics* **2016**, *16*, 2160-2182.
(115) Shi, T.; Su, D.; Liu, T.; Tang, K.; Camp, D. G., 2nd; Qian, W. J.; Smith, R. D. *Proteomics* **2012**, *12*, 1074-1092.
(116) Lopez, M. F.; Kuppusamy, R.; Sarracino, D. A.; Prakash, A.; Athanas, M.; Krastins, B.; Rezai, T.; Sutton, J. N.; Peterman, S.; Nicolaides, K. *Journal of proteome research* **2011**, *10*, 133-142.
(117) Parry, S.; Zhang, H.; Biggio, J.; Bukowski, R.; Varner, M.; Xu, Y.; Andrews, W. W.; Saade, G. R.; Esplin, M. S.; Leite, R.; Ilekis, J.; Reddy, U. M.; Sadovsky, Y.; Blair, I. A.; Eunice Kennedy Shriver National Institute of Child, H.; Human Development, G.; Proteomic Network for Preterm Birth, R. *American journal of obstetrics and gynecology* **2014**, *211*, 678 e671-612.
(118) Domon, B.; Gallien, S. *Proteomics. Clinical applications* **2015**, *9*, 423-431.
(119) Georgiou, H. M.; López, S. I.; Rice, G. E. *Gestational diabetes* **2011**, 1-20.
(120) Cecconi, D.; Lonardoni, F.; Favretto, D.; Cosmi, E.; Tucci, M.; Visentin, S.; Cecchetto, G.; Fais, P.; Viel, G.; Ferrara, S. D. *Electrophoresis* **2011**, *32*, 3630-3637.
(121) Karamessinis, P. M.; Malamitsi-Puchner, A.; Boutsikou, T.; Makridakis, M.; Vougas, K.; Fountoulakis, M.; Vlahou, A.; Chrousos, G. *Molecular & cellular proteomics : MCP* **2008**, *7*, 591-599.
(122) Heitner, J. C.; Koy, C.; Kreutzer, M.; Gerber, B.; Reimer, T.; Glocker, M. O. *Journal of chromatography. B, Analytical technologies in the biomedical and life sciences* **2006**, *840*, 10-19.
(123) Koy, C.; Heitner, J. C.; Woisch, R.; Kreutzer, M.; Serrano-Fernandez, P.; Gohlke, R.; Reimer, T.; Glocker, M. O. *Proteomics* **2005**, *5*, 3079-3087.
(124) Cho, Y. T.; Su, H.; Huang, T. L.; Chen, H. C.; Wu, W. J.; Wu, P. C.; Wu, D. C.; Shiea, J. *Clinica chimica acta; international journal of clinical chemistry* **2013**, *415*, 266-275.
(125) Cho, Y. T.; Su, H.; Wu, W. J.; Wu, D. C.; Hou, M. F.; Kuo, C. H.; Shiea, J. *Advances in clinical chemistry* **2015**, *69*, 209-254.
(126) Hortin, G. L. *Clinical chemistry* **2006**, *52*, 1223-1237.
(127) Baumann, S.; Ceglarek, U.; Fiedler, G. M.; Lembcke, J.; Leichtle, A.; Thiery, J. *Clinical chemistry* **2005**, *51*, 973-980.
(128) Callesen, A. K.; Madsen, J. S.; Vach, W.; Kruse, T. A.; Mogensen, O.; Jensen, O. N. *Proteomics* **2009**, *9*, 1428-1441.
(129) de Noo, M. E.; Tollenaar, R. A.; Ozalp, A.; Kuppen, P. J.; Bladergroen, M. R.; Eilers, P. H.; Deelder, A. M. *Analytical chemistry* **2005**, *77*, 7232-7241.
(130) Pecks, U.; Seidenspinner, F.; Röwer, C.; Reimer, T.; Rath, W.; Glocker, M. O. *Journal of the American Society for Mass Spectrometry* **2010**, *21*, 1699-1711.
(131) Pecks, U.; Kirschner, I.; Wölter, M.; Schlembach, D.; Koy, C.; Rath, W.; Glocker, M. O. *Translational research : the journal of laboratory and clinical medicine* **2014**, *164*, 57-69.
(132) Wölter, M.; Röwer, C.; Koy, C.; Reimer, T.; Rath, W.; Pecks, U.; Glocker, M. O. *Electrophoresis* **2012**, *33*, 1881-1893.
(133) Wölter, M.; Röwer, C.; Koy, C.; Rath, W.; Pecks, U.; Glocker, M. O. *Journal of proteomics* **2016**, *149*, 44-52.
(134) Sharma, D.; Shastri, S.; Sharma, P. *Clinical medicine insights. Pediatrics* **2016**, *10*, 67-83.
(135) Mabey, D.; Peeling, R. W.; Ustianowski, A.; Perkins, M. D. *Nature reviews. Microbiology* **2004**, *2*, 231-240.
(136) Peeling, R. W.; Mabey, D. *Clinical microbiology and infection : the official publication of the European Society of Clinical Microbiology and Infectious Diseases* **2010**, *16*, 1062-1069.
(137) Christ, P.; Rutzinger, S.; Seidel, W.; Uchaikin, S.; Pröbst, F.; Koy, C.; Glocker, M. O. *European journal of mass spectrometry* **2004**, *10*, 469-476.
(138) Reimer, T.; Rohrmann, H.; Stubert, J.; Pecks, U.; Glocker, M. O.; Richter, D. U.; Gerber, B. *The journal of maternal-fetal & neonatal medicine : the official journal of the European Association of*

Perinatal Medicine, the Federation of Asia and Oceania Perinatal Societies, the International Society of Perinatal Obstet **2013**, *26*, 263-269.

(139) Pecks, U.; Schutt, A.; Rower, C.; Reimer, T.; Schmidt, M.; Preschany, S.; Stepan, H.; Rath, W.; Glocker, M. O. *Hypertension in pregnancy* **2012**, *31*, 278-291.

(140) Mitchell, M. D.; Rice, G. E. *Recent Advances in Research on the Human Placenta* **2012**, 1-11.

(141) Tate, J.; Ward, G. *The Clinical biochemist. Reviews* **2004**, *25*, 105-120.

(142) Pusch, W.; Kostrzewa, M. *Current pharmaceutical design* **2005**, *11*, 2577-2591.

(143) Biswas, S.; Rolain, J. M. *Journal of microbiological methods* **2013**, *92*, 14-24.

(144) Bizzini, A.; Greub, G. *Clinical microbiology and infection : the official publication of the European Society of Clinical Microbiology and Infectious Diseases* **2010**, *16*, 1614-1619.

(145) Clark, A. E.; Kaleta, E. J.; Arora, A.; Wolk, D. M. *Clinical microbiology reviews* **2013**, *26*, 547-603.

(146) Croxatto, A.; Prod'hom, G.; Greub, G. *FEMS microbiology reviews* **2012**, *36*, 380-407.

(147) Dingle, T. C.; Butler-Wu, S. M. *Clinics in laboratory medicine* **2013**, *33*, 589-609.

(148) Nomura, F. *Biochimica et biophysica acta* **2015**, *1854*, 528-537.

(149) Greco, V.; Piras, C.; Pieroni, L.; Ronci, M.; Putignani, L.; Roncada, P.; Urbani, A. *Expert review of proteomics* **2018**, *15*, 683-696.

(150) Anderson, N. L.; Anderson, N. G. *Molecular & cellular proteomics : MCP* **2002**, *1*, 845-867.

(151) Auer, J.; Camoin, L.; Guillonneau, F.; Rigourd, V.; Chelbi, S. T.; Leduc, M.; Laparre, J.; Mignot, T. M.; Vaiman, D. *Journal of proteomics* **2010**, *73*, 1004-1017.

(152) Gupta, M. B.; Seferovic, M. D.; Liu, S.; Gratton, R. J.; Doherty-Kirby, A.; Lajoie, G. A.; Han, V. K. *Clinical Proteomics* **2006**, *2*, 169.

(153) Karagiannis, G.; Akolekar, R.; Sarquis, R.; Wright, D.; Nicolaides, K. H. *Fetal diagnosis and therapy* **2011**, *29*, 148-154.

(154) Abbassi-Ghanavati, M.; Greer, L. G.; Cunningham, F. G. *Obstetrics and gynecology* **2009**, *114*, 1326-1331.

(155) Flood-Nichols, S. K.; Tinnemore, D.; Wingerd, M. A.; Abu-Alya, A. I.; Napolitano, P. G.; Stallings, J. D.; Ippolito, D. L. *Molecular & cellular proteomics : MCP* **2013**, *12*, 55-64.

(156) Winkler, K.; Wetzka, B.; Hoffmann, M. M.; Friedrich, I.; Kinner, M.; Baumstark, M. W.; Wieland, H.; Marz, W.; Zahradnik, H. P. *The Journal of clinical endocrinology and metabolism* **2000**, *85*, 4543-4550.

(157) Kei, A. A.; Filippatos, T. D.; Tsimihodimos, V.; Elisaf, M. S. *Metabolism: clinical and experimental* **2012**, *61*, 906-921.

(158) Wolska, A.; Dunbar, R. L.; Freeman, L. A.; Ueda, M.; Amar, M. J.; Sviridov, D. O.; Remaley, A. T. *Atherosclerosis* **2017**, *267*, 49-60.

(159) Ito, Y.; Breslow, J. L.; Chait, B. T. *Journal of lipid research* **1989**, *30*, 1781-1787.

(160) Wopereis, S.; Grunewald, S.; Morava, E.; Penzien, J. M.; Briones, P.; Garcia-Silva, M. T.; Demacker, P. N.; Huijben, K. M.; Wevers, R. A. *Clinical chemistry* **2003**, *49*, 1839-1845.

(161) Taskinen, M. R.; Packard, C. J.; Boren, J. *Current atherosclerosis reports* **2019**, *21*, 27.

(162) Batal, R.; Tremblay, M.; Barrett, P. H.; Jacques, H.; Fredenrich, A.; Mamer, O.; Davignon, J.; Cohn, J. S. *Journal of lipid research* **2000**, *41*, 706-718.

(163) Cohn, J. S.; Patterson, B. W.; Uffelman, K. D.; Davignon, J.; Steiner, G. *The Journal of clinical endocrinology and metabolism* **2004**, *89*, 3949-3955.

(164) Zheng, C.; Khoo, C.; Furtado, J.; Sacks, F. M. *Circulation* **2010**, *121*, 1722-1734.

(165) Zheng, C.; Khoo, C.; Ikewaki, K.; Sacks, F. M. *Journal of lipid research* **2007**, *48*, 1190-1203.

(166) Pecks, U.; Brieger, M.; Schiessl, B.; Bauerschlag, D. O.; Piroth, D.; Bruno, B.; Fitzner, C.; Orlikowsky, T.; Maass, N.; Rath, W. *Journal of perinatal medicine* **2012**, *40*, 287-296.

(167) Pecks, U.; Caspers, R.; Schiessl, B.; Bauerschlag, D.; Piroth, D.; Maass, N.; Rath, W. *Hypertension in pregnancy* **2012**, *31*, 156-165.

(168) Rodie, V. A.; Caslake, M. J.; Stewart, F.; Sattar, N.; Ramsay, J. E.; Greer, I. A.; Freeman, D. J. *Atherosclerosis* **2004**, *176*, 181-187.

(169) Barker, D. J.; Winter, P. D.; Osmond, C.; Margetts, B.; Simmonds, S. J. *Lancet* **1989**, *2*, 577-580.

(170) Madsen, E. M.; Lindegaard, M. L.; Andersen, C. B.; Damm, P.; Nielsen, L. B. *The Journal of biological chemistry* **2004**, *279*, 55271-55276.

(171) Chutipongtanate, S.; Chatchen, S.; Svasti, J. *Proteomics. Clinical applications* **2017**, *11*.

(172) Ng, E. W.; Wong, M. Y.; Poon, T. C. *Topics in current chemistry* **2014**, *336*, 139-175.

(173) Spooner, N. *Bioanalysis* **2010**, *2*, 1343-1344.

(174) Willyard, C. *Nature medicine* **2007**, *13*, 1131.

(175) Kim, J. H.; Woenker, T.; Adamec, J.; Regnier, F. E. *Analytical chemistry* **2013**, *85*, 11501-11508.

(176) Wollner, G. C. *Laboratory Medicine* **1980**, *11*, 87-92.

(177) Li, Y.; Henion, J.; Abbott, R.; Wang, P. *Bioanalysis* **2011**, *3*, 2501-2514.

(178) Perez, J. W.; Pantazides, B. G.; Watson, C. M.; Thomas, J. D.; Blake, T. A.; Johnson, R. C. *Analytical chemistry* **2015**, *87*, 5723-5729.

(179) Barfield, M.; Wheller, R. *Analytical chemistry* **2011**, *83*, 118-124.

(180) Kolocouri, F.; Dotsikas, Y.; Loukas, Y. L. *Analytical and bioanalytical chemistry* **2010**, *398*, 1339-1347.

(181) Kostic, N.; Dotsikas, Y.; Jovic, N.; Stevanovic, G.; Malenovic, A.; Medenica, M. *Journal of pharmaceutical and biomedical analysis* **2015**, *109*, 79-84.

(182) Osteresch, B.; Viegas, S.; Cramer, B.; Humpf, H. U. *Analytical and bioanalytical chemistry* **2017**, *409*, 3369-3382.

(183) Chambers, A. G.; Percy, A. J.; Yang, J.; Borchers, C. H. *Molecular & cellular proteomics : MCP* **2015**, *14*, 3094-3104.

(184) Lehmann, S.; Picas, A.; Tiers, L.; Vialaret, J.; Hirtz, C. *Critical reviews in clinical laboratory sciences* **2017**, *54*, 173-184.

(185) Ozcan, S.; Cooper, J. D.; Lago, S. G.; Kenny, D.; Rustogi, N.; Stocki, P.; Bahn, S. *Scientific reports* **2017**, *7*, 45178.

1.7 Contribution to Publications

Paper 1: Maternal Apolipoprotein B100 Serum Levels are Diminished in Pregnancies with Intrauterine Growth Restriction and Differentiate from Controls.

C.A.O. performed part of the data analysis and took part in writing the paper.

Paper 2: Precision Diagnostics by Affinity - Mass Spectrometry: A Novel Approach for Fetal Growth Restriction Screening During Pregnancy.

C.A.O. took part in the planning of the experiments, performed the experiments, the data analysis and wrote the draft manuscript.

Paper 3: Comparison of blood serum protein analysis by MALDI-MS from either conventional frozen samples or storage disc-deposited samples: A study with human serum from pregnant donors and from patients with intrauterine growth restriction.

C.A.O. performed part of the experiments, part of the data analysis and took part in writing the paper.

2. Publication Collection

Wolter, M., **Okai, C. A.**, Smith, D. S., Ruß, M., Rath, W., Pecks, U., Borchers, C. H. and Glocker, M. O. Maternal Apolipoprotein B100 Serum Levels are Diminished in Pregnancies with Intrauterine Growth Restriction and Differentiate from Controls. *Proteomics. Clin. Appl*. **2018**, 12 (6), e1800017

Okai, C. A., Russ, M., Wölter, M., Andresen, K., Rath, W., Pecks, U. and Glocker, M. O., Precision Diagnostics by Affinity - Mass Spectrometry: A Novel Approach for Fetal Growth Restriction Screening During Pregnancy. *J. Clin. Med*. **2020**, 9(5), 1374

Wölter, M., Russ, M., **Okai, C. A.**, Rath, W., Pecks, U. and Glocker, M. O. Comparison of blood serum protein analysis by MALDI-MS from either conventional frozen samples or storage disc-deposited samples: A study with human serum from pregnant donors and from patients with intrauterine growth restriction. *Eur. J. Mass Spectrom*. **2019**, 25(4), 381–390

2.1 Maternal Apolipoprotein B100 Serum Levels are Diminished in Pregnancies with Intrauterine Growth Restriction and Differentiate from Controls

Maternal Apolipoprotein B100 Serum Levels are Diminished in Pregnancies with Intrauterine Growth Restriction and Differentiate from Controls

Manja Wölter, Charles A. Okai, Derek S. Smith, Manuela Ruß, Werner Rath, Ulrich Pecks, Christoph H. Borchers, and Michael O. Glocker*

Purpose: Intrauterine growth restriction, a major cause of fetal morbidity and mortality, is defined as a condition in which the fetus does not reach its genetically given growth potential. Screening for intrauterine growth restriction biomarkers in the mother's blood would be of great help for optimal pregnancy management and timing of delivery as well as for identifying fetuses requiring further surveillance during their infancies.
Experimental Design: A multiplexing serological assay based on liquid chromatography–multiple-reaction-monitoring mass spectrometry is applied for distinguishing serum samples of pregnant women.
Results: Assessment of concentrations of apolipoproteins and of proteins that belong to the lipid transport system is performed with maternal serum samples, consuming only 10 μL of serum per multiplex assay from each patient. Of all investigated proteins the serum concentrations of apolipoprotein B100 shows the greatest power for discriminating intrauterine growth restriction from control samples, reaching areas under curves above 0.85 in receiver-operator-characteristics analyses.
Conclusions: These results indicate the potential of liquid chromatography-multiple-reaction-monitoring mass spectrometry to become of clinical importance in the future for intrauterine growth restriction risk assessment based on maternal apolipoprotein B100 serum levels.

1. Introduction

Affecting 3–8% of all pregnancies, intrauterine growth restriction (IUGR) is defined as a condition in which the fetus does not reach its genetically given growth potential. Resulting in low fetal weight, IUGR is a major cause of fetal morbidity and mortality.[1,2] The mother´s metabolic and cardiovascular conditions, such as obesity, diabetes mellitus, and hypertension are known risk factors for IUGR.[3] In accordance, several epidemiologic studies indicate that abnormal intrauterine conditions increase the infant's risk for cardiovascular and metabolic diseases, for example, atherosclerosis, in its later life.[4] One possible mechanism is an accumulation of oxidized low density lipoproteins (oxLDL) leading to fatty streak formation in the fetal vessels[5] which results in an increased intima media thickness which is measurable by ultrasound in the IUGR fetus.[6] Increased intima media thickness has been shown to (i) persist up to at least the age of 18 months after birth

Dr. M. Wölter, C. A. Okai, M. Ruß, Prof. M. O. Glocker
Proteome Center Rostock
Medical Faculty and Natural Science Faculty
University of Rostock
Schillingallee 69, 18057, Rostock, Germany
E-mail: michael.glocker@med.uni-rostock.de
D. S. Smith, Dr. C. H. Borchers
University of Victoria-Genome British Columbia Proteomics Center
Vancouver Island Technology Park
University of Victoria
4464 Markham St #3101, BC V8Z 7X8, Victoria, Canada
Dr. C. H. Borchers
Department of Biochemistry and Microbiology
University of Victoria
Petch Building Room 207, 3800 Finnerty Rd., V8P 5C2, Victoria, BC, Canada

Segal Cancer Proteomics Centre, Lady Davis Institute
Jewish General Hospital
McGill University
3755 Cote-Ste-Catherine Road, H3T 1E2, Montréal, QC, Canada
Gerald Bronfman Department of Oncology, Jewish General Hospital
McGill University
3755 Cote-Ste-Catherine Road, H3T 1E2, Montréal, QC, Canada
Prof. W. Rath, Dr. U. Pecks
Department of Obstetrics and Gynecology
Medical Faculty
RWTH Aachen University
Pauwelsstraße 30, 52074, Aachen, Germany
Dr. U. Pecks
Department of Obstetrics and Gynecology
Medical Faculty
University of Schleswig-Holstein
Campus Kiel
Arnold-Heller-Straße 3, 24105, Kiel, Germany

Clinical Relevance

Risk assessment of development impairment in fetuses is of tremendous importance for (i) optimal pregnancy management, (ii) timing of delivery, and (iii) for identifying preterm babies who require further surveillance during their infancies. Although ultrasound sonography has been accepted as "gold standard" for determining IUGR by clinical means, its application is limited to excellently equipped care centers. Despite clinical settings, successful screening assays with pregnant women will only be practicable when they are either noninvasive or serological, that is, based on simple blood tests. Proteome profiling of maternal serum during pregnancy provides the prerequisites for risk assessment of development impairment in fetuses, because Liquid Chromatography–Multiple Reaction Monitoring Mass Spectrometry enables multiplexing and hence simultaneous determination of biomarker concentrations by consuming just minute volumes of maternal peripheral blood.

and (ii) correlate with higher blood pressure in affected infants.[7]

Recently, we analyzed maternal serum samples from 30 pregnant Caucasian women, of which subsequently 15 delivered healthy babies and 15 gave birth to infants that suffered from IUGR. We identified specific marker proteins that are known to be involved in the pathomechanisms of atherosclerosis by the regulation of triglyceride levels.[8] Particularly pro-apolipoprotein CII and apolipoprotein CIII together with its distinctly differently glycosylated isoforms enabled us to discriminate pregnancies with IUGR from control individuals ahead of birth, and independent from other biometrical data.[9] Incidentally, apolipoproteins have become important screening biomarkers for predicting cardiovascular risk in the general population[10] and are considered better predictors than traditional serum lipid measurements.[11] Hence, since a deranged lipid metabolism has been observed in both the mother and the fetus, IUGR may be considered a metabolic disease.[12] Screening during pregnancy, that is, detecting the presence of IUGR biomarkers in the mother's blood, would be of great help in many aspects. First goals to reach are optimal pregnancy management and timing of delivery.[1] Second, early detection of IUGR fetuses was beneficial for initiating of both, immediate care of affected newborns and further intensive surveillance during their infancies.

In an effort to potentially widen the spectrum of future screening biomarkers for detection of pregnancy complications, such as IUGR, we conducted a retrospective study with the same 30 maternal serum samples that we had investigated previously.[9] With IUGR in focus and our previous study results in mind, we focused our interest to evaluate levels of further apolipoproteins in peripheral blood of pregnant women. Altogether, 15 protiens (apolipoproteins and proteins that belong to the lipid transport system) were quantified in all 30 maternal serum samples by liquid chromatography–multiple-reaction-monitoring mass spectrometry (LC-MRM/MS). Protein abundance

differences were correlated with clinical IUGR assessment and were biostatistically evaluated for their suitability to detect IUGR during pregnancies.

2. Experimental Section

Patient Stratification, Blood Collection, Serum Generation, and Storage: Blood samples were analyzed from 30 pregnant Caucasian women who attended the Department of Obstetrics and Gynecology, University Hospital of the RWTH Aachen, between March 2008 and August 2010 (Table S1, Supporting Information). IUGR was defined in accordance to the American College of Obstetricians and Gynecologists guidelines[13] as described.[14] Additional preeclampsia (PE) in some of the mothers with IUGR babies was defined according to the International Society for the Study of Hypertension in Pregnancy guideline.[15] Sonographic examinations were done antenatally on Logiq 5 and Voluson 730 Expert Ultrasound Systems (GE Healthcare Systems, Solingen, Germany). The regression equation including biparietal diameter, femur length, and head and abdominal circumferences,[16] was used to estimate fetal weight. Neonatal birth weight centile was determined according to the population-based newborn weight charts.[17]

Blood samples (up to 9 mL, each) were taken from each individual antenatally from the right or left cubital vein using monovette syringes (Serum Z/9 mL; Monovette, Sarstedt, Germany). Serum was prepared in the clinic as described.[2,9,18] Altogether, time between blood sample collection and storage of frozen serum aliquots averaged around less than 1 h. Frozen serum aliquots were shipped on dry ice to Proteome Center Rostock (for more information see Experimental Section, Supporting Information).

Preparation of Peptide Mixtures from Serum Samples and Addition of Stable Isotope-Labeled Standard Peptides: Peptide mixtures (native [NAT] peptides) were prepared for multiple reaction monitoring (MRM) analysis according to previously published protocols[19] with the following modifications. Volumes of 90 μL of 37.5 mM ammonium bicarbonate solution and 12.5 μL of sodium deoxycholate solution (10% w/v in 25 mM ammonium bicarbonate) were added to 10 μL of serum from each patient. Proteins in these diluted serum solutions were reduced for 30 min at 60 °C with 50 mM tris(2-carboxyethyl)phosphine (dissolved in 25 mM ammonium bicarbonate; 3.11 μL). Reduced plasma proteins were alkylated for 30 min at 37 °C in the dark with 100 mM iodoacetamide solution (dissolved in 25 mM ammonium bicarbonate; 3.5 μL). Then, a 100 mM dithiothreitol solution (DTT, dissolved in 25 mM ammonium bicarbonate; 3.5 μL) was added and after 30 min a trypsin solution (Promega, Madison, WI, 0.4 μg μL^{-1} dissolved in 25 mM ammonium bicarbonate; 2.5 μL) was added. The mixtures were incubated for 16 h at 37 °C. Peptide mixtures were acidified by adding 5 μL of 30% v/v formic acid to stop digestion. The sodium deoxycholate precipitate was removed by centrifugation (10 min at 12 000 × g). Sample supernatants containing the "NAT peptides" were transferred into fresh tubes.

To 15 μL of the peptide solution (supernatant) were added 10 μL of stable isotope-labeled standard (SIS) peptide solution (each of the SIS peptides was concentrated to 4 pmol μL^{-1};

ADVANCED
SCIENCE NEWS
www.advancedsciencenews.com

Proteomics
Clinical Applications
www.clinical.proteomics-journal.com

cf.[19]) and 775 μL of 0.1% v/v formic acid. The SIS peptide panel was composed of 17 SIS peptides which were quantotypic for 15 plasma proteins. The average post-synthetic purity for the 17 peptides was 92.0%, as was revealed by capillary zone electrophoresis. In this study, an equimolar SIS peptide mixture (at 250 fmol μL^{-1}) was used. This mixture was prepared from the combination of individual peptide stocks (14 μL, each at 100 pmol μL^{-1}) and 30% acetonitrile/0.1% formic acid (4.9 mL). The concentrated stock was stored as lyophilized aliquots at −80 °C until use.

Such prepared peptide mixtures (800 μL each) were desalted and concentrated prior to MS analysis by solid phase extraction using Waters Oasis reversed-phase 10-mg HLB cartridges (Waters, Milford, MA) following the manufacturer's recommended protocol. Peptides were eluted from the C-18 material with 200 μL of 50% v/v acetonitrile, 0.1% v/v formic acid. The eluted peptide mixtures were either frozen at −80 °C and lyophilized to dryness for shipping or immediately subjected to LC-MRM/MS analysis.

LC-MRM/MS Instrumentation and Measurement Conditions: Prior to LC-MRM/MS analysis, peptides from each patient-derived sample were either redissolved in 400 μL 0.1% v/v formic acid/2% v/v acetonitrile, or taken directly from sample work-up. A volume of 10 μL from the peptide mixture solutions was injected for each MRM analysis. Peptide separations and MRM analyses were performed as described previously.[20] RP-UHPLC was performed on a Zorbax Eclipse Plus C18 Rapid Resolution HD column (150 × 2.1 mm, 1.8 μm particles; Agilent Technologies; Palo Alto, CA, USA). The column and autosampler were maintained at 50 °C and 4 °C, respectively. The peptide mixtures were separated using a 43 min ACN gradient from 3 to 90% mobile phase B (composition: 0.1% FA in 90% ACN) at a flow rate of 0.4 mL min^{-1}. The specific gradient employed was as follows (time, % B): 0, 3; 1.5, 7; 16, 15; 18, 15.3; 33, 25; 38, 45; 39, 90; 42.9, 90; and 43, 3. Each analysis was followed by a 4 min column equilibration. To reduce carryover, a blank injection of mobile phase A (composition: 0.1% FA) was run between each type of sample (i.e., buffer vs plasma in interference screening), and between different concentration levels of the standard when determining the calibration curve. The 1290 Infinity LC system was interfaced to a 6490 triple quadrupole mass spectrometer (both Agilent Technologies) via a standard-flow ESI source that was operated in the positive ion mode. The general MS parameters were identical to those previously published.[21]

MRM Data Processing: To generate the "full analysis set" (FAS) MRM data were processed and visualized with MassHunter Quantitative and Qualitative Analysis software (version B.05.00; Agilent Technologies) using the Agilent integrator algorithm for peak integration, as described previously.[21] Peaks were first manually inspected to determine the accuracy of peak selection and integration, before peak (i.e., retention time, peak width, signal response) and quantitative information (including limits of quantitation, and dynamic range) were extracted. The "best" interference-free transition of one "native" (NAT) peptide, that is, the one with the most intense MRM signal, was used for protein quantitation. Interference assessment was performed in serum through signal-intensity ratio measurements on the NAT and SIS peptide transition. For protein quantitation, seven-point standard curves were prepared with a 1/x2 weighting. By

substituting the measured relative response (RR) into the peptide-specific equation and solving for NATconc, the concentration of an endogenous plasma protein (in fmol μL^{-1}) was calculated: NATconc = (SISconc × m)/(RR−b). Protein concentrations in ng mL^{-1} were calculated using the protein's molecular mass (in g mol^{-1}; obtained from ExPASy's "pI/Mw tool" [http://web.expasy.org/compute_pi/]), the peptide's relative response (NAT/SIS), the corrected SIS peptide concentration (i.e., corrected with the purity values as determined by amino acid analysis and CZE), and a conversion factor (of 1000).[22] In cases where multiple peptides were quantified for a given protein, that is, apolipoprotein D, the one that provided the highest protein concentration was used as the quantifier to finally constellate the "per protocol set" (PPS).

Biostatistical Analyses: Sensitivity and specificity as well as receiver operator characteristics (ROC) and Youden indices (J = sensitivity + specificity − 1)[23] were calculated using the IBM statistics software SPSS (version 20.0, SPSS Inc., Chicago, USA) (Table S2, Supporting Information). Linear interpolation[24] between each pair of two neighboring concentration values was used to calculate "test cutoff" values. Then, sensitivity and specificity[25] were calculated for each of the biostatistical estimations at each "test cutoff" point. Logistic regression analysis[26] was performed using the Origin statistics software (version. 8.1 G; Originlab Corporation, Northampton, MA, USA). Power analysis was conducted using the G*Power software (version 3.1, University of Düsseldorf).[27] A type I error (α) of 0.05 and a type II error (β) of 0.20 was chosen to compare the two means. The required power (1−β error probability) was 0.80.

ELISA Assay for Apolipoprotein B100: A commercially available ELISA test kit (Human Apolipoprotein B, MABTECH AB, Nacka Strand, Sweden) was used in order to quantitatively analyze apolipoprotein B100 expression in maternal sera. All measurements were performed in duplicate. First, sera samples were diluted 1:10 000 with dilution buffer. Diluted standard (100 μL), assay background control, and patient samples were added to the well plate and incubated at room temperature for 2 h. After washing, 100 μL of the 1:1000 diluted solution that contained the detection antibody "LDL-11-biotin" were added and incubated at room temperature for 1 h. A subsequent washing step followed by adding 100 μL of 1:1000 diluted "SA-HRP"-containing solution. Incubation was allowed at room temperature for 1 h. Again, wells were washed and color development was started by adding 100 μL of "TMB substrate" solution. After 15 min of incubation in the dark, reaction was stopped by adding 100 μL of "Stop solution." The absorbance was measured at 450 nm, using the anthos 2010 microplate reader (anthos Mikrosysteme GmbH, Friesoythe, Germany).

3. Results

3.1. Patient Cohorts, Sample Work-Up, and Protein Concentration Determinations

The study was approved by the Ethics Committee of the RWTH Aachen (EK 119/08). Written informed consent was obtained from all 30 participating women. Of those, 15 delivered healthy

Table 1. Clinical parameters and patient characteristics.

Parameter	CTRL					IUGR				
	n	Mean	95% CI	Min.	Max.	n	Mean	95% CI	Min.	Max.
Maternal age [year][a]	15	31.7	28.3–33.9	24.2	40.0	15	30.4	26.9–34.0	19.1	41.5
Maternal pre-pregnancy BMI, [kg m^{-2}]	15	23.7	20.8–26.6	17.6	35.7	15	24.2	22.4–26.1	19.9	31.9
Primiparity, [%]	15	27	n.a.	n.a.	n.a.	15	80	n.a.	n.a.	n.a.
Actual smoking status, [%]	15	20	n.a.	n.a.	n.a.	15	27	n.a.	n.a.	n.a.
Systolic blood pressure, [mmHg]	15	116.2	112.4–119.5	106	129	15	130.8	118.8–141.1	83	162
Diastolic blood pressure, [mmHg]	15	64.9	60.9–69.0	53	81	15	77.2	68.7–85.2	52	101
Gestational age at sampling, [weeks]	15	32.4	29.8–35.0	25	39.3	15	32.1	29.7–34.9	24	40.4
Gestational age at delivery, [weeks]	15	32.8	30.2–35.3	25	39.3	15	33.0	30.5–35.5	26.7	40.4
Mode of delivery, sectio caesarea, [%]	15	86.7	n.a.	n.a.	n.a.	15	100	n.a.	n.a.	n.a.
Fetal birth weight, [g]	15	2129	1584–2673	740	3895	15	1383	1005–1761	490	2665
Fetal birth weight percentile	15	50.7	40.8–60.5	25	85	15	4.0	2.5–5.5	1	9
Fetal gender, female, [%]	15	53.3	n.a.	n.a.	n.a.	15	53.3	n.a.	n.a.	n.a.

[a]At the beginning of hospitalization (time point of sample collection); BMI, body mass index; CI, confidence interval; n.a., not applicable.

infants (control [CTRL]) with adequate for gestational age neonatal weight, that is, within the 10th and 90th percentile as compared to the general population. Yet, 11 of them were born preterm for various reasons (premature rupture of the membrane, spontaneous onset of labor, vaginal bleeding). The other 15 women delivered infants that suffered from IUGR; 12 of them needed mandatory preterm delivery. Of note, to obtain a homogeneous study group, the CTRL group was chosen on the basis to match for gestational age at blood sampling and infant gender and to keep the maternal baseline characteristics similar (**Table 1**).

Upon quantification of apolipoproteins and other proteins that belong to the lipid transport system using LC-MRM/MS, the "full analysis set" (FAS) comprised in total 3060 protein concentration data points (i.e., 17 SIS/NAT peptide tandems × 3 relative ratios per peptide × 30 samples × 2 work-ups). After exclusion of data that did not fulfill the quality criteria and upon removal of redundancies, quantitation of 15 proteins was accomplished in all 30 serum samples for both independent work-ups. The final PPS contained 900 protein concentration values (Table S3, Supporting Information).

Of note, despite the two different sample work-up and transport conditions (see Experimental Section, Supporting Information) there were no significant differences in the determined protein concentrations between first measurement (MS-1) and second measurement (MS-2) data. The determined protein concentrations that were quantified by LC-MRM/MS in this sample set spanned over four orders of magnitude. The protein concentration of the most abundant protein was 7206.13 μg mL^{-1} for apolipoprotein B100 (in sample 9, MS-2), while that of the least abundant protein was 4.92 μg mL^{-1} for apolipoprotein a (in sample 14, MS-1). Data sets from each sample work-up (MS-1 and MS-2) were submitted to independent biostatistical data analysis, but in the following results from MS-1 are reported, whereas data from MS-2 are placed in the Supporting Information.
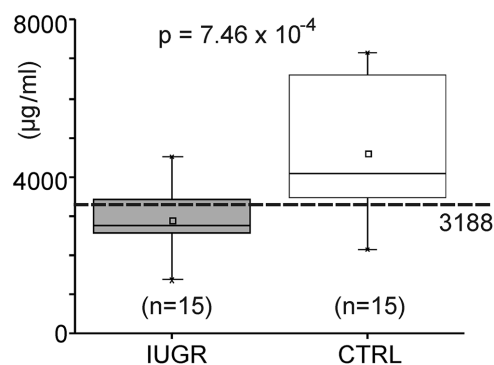
Figure 1. Box-and-whisker plots of apolipoprotein B100 concentrations of LC-MRM/MS measurements (MS-1). The horizontal lines within the boxes represent the medians; the small squares indicate the means. The whiskers specify the 5th and 95th percentiles, and the crosses indicate the 1st and 99th percentiles. IUGR, intrauterine growth restriction; CTRL, control individuals. Sample sizes (n) and the p-value are given. The dashed horizontal line marks the "best cutoff" value.

3.2. Biostatistical Data Analysis and Determination of Apolipoprotein B100 as Best Suitable Marker Protein

Biostatistical evaluation focused on the search for the best discriminating protein, that is, the protein with abundance differences by which one was able to decide whose mother's fetus suffered from IUGR or, alternatively, would fall into the CTRL group. In a first screen, the respective protein concentration distributions of a given protein in each of the two groups (IUGR vs CTRL) were subjected to t-test analysis and were visualized by box-and-whisker plots, as is exemplified with MS-1 data for apolipoprotein B100 (**Figure 1** and Table S3, Supporting Information). While this t-test analysis indicated that only apolipoprotein B100 was capable to differentiate the two groups, that is, distinguish IUGR from CTRL in a sufficient manner, this analysis does not allow to stratify individual patient samples.

ADVANCED
SCIENCE NEWS
www.advancedsciencenews.com

Proteomics
Clinical Applications
www.clinical.proteomics-journal.com

Table 2. Apolipoprotein B100 concentrations in peripheral maternal blood samples and J_{max} determination.

Patient ID[a]	Clinical diagnosis	Conc. [μg mL^{-1}]	Test cutoff	Below cutoff	Above cutoff	TN	FN	FP	TP	Specificity	Sensitivity	J[a]
	Min.	1354.99										
18	IUGR	1355.99	1354.49	0	30	15	15	0	0	1.000	0.000	0.000
21	IUGR	1578.30	1467.14	1	29	15	14	0	1	1.000	0.067	0.067
14	CTRL	2144.52	1861.41	2	28	15	13	0	2	1.000	0.133	0.133
29	IUGR	2379.12	2261.82	3	27	14	13	1	2	0.933	0.133	0.067
27	IUGR	2583.01	2481.06	4	26	14	12	1	3	0.933	0.200	0.133
25	IUGR	2614.94	2598.97	5	25	14	11	1	4	0.933	0.267	0.200
30	IUGR	2653.02	2633.98	6	24	14	10	1	5	0.933	0.333	0.267
16	IUGR	2668.98	2661.00	7	23	14	9	1	6	0.933	0.400	0.333
24	IUGR	2727.94	2698.46	8	22	14	8	1	7	0.933	0.467	0.400
19	IUGR	2937.97	2832.95	9	21	14	7	1	8	0.933	0.533	0.467
28	IUGR	3095.18	3016.58	10	20	14	6	1	9	0.933	0.600	0.533
17	IUGR	3165.19	3130.19	11	19	14	5	1	10	0.933	0.667	0.600
10	CTRL	3210.64	3187.92	12	18	14	4	1	11	0.933	0.733	0.667
6	CTRL	3316.27	3263.45	13	17	13	4	2	11	0.867	0.733	0.600
20	IUGR	3416.99	3366.63	14	16	12	4	3	11	0.800	0.733	0.533
5	CTRL	3480.85	3448.92	15	15	12	3	3	12	0.800	0.800	0.600
23	IUGR	3703.17	3592.01	16	14	11	3	4	12	0.733	0.800	0.533
3	CTRL	3829.68	3766.42	17	13	11	2	4	13	0.733	0.867	0.600
2	CTRL	3876.35	3853.01	18	12	10	2	5	13	0.667	0.867	0.533
26	IUGR	3914.43	3895.39	19	11	9	2	6	13	0.600	0.867	0.467
1	CTRL	4001.63	3958.03	20	10	9	1	6	14	0.600	0.933	0.533
15	CTRL	4074.10	4037.86	21	9	8	1	7	14	0.533	0.933	0.467
7	CTRL	4225.17	4149.64	22	8	7	1	8	14	0.467	0.933	0.400
12	CTRL	4332.03	4278.60	23	7	6	1	9	14	0.400	0.933	0.333
22	IUGR	4510.13	4421.08	24	6	5	1	10	14	0.333	0.933	0.267
11	CTRL	5019.85	4764.99	25	5	5	0	10	15	0.333	1.000	0.333
4	CTRL	6574.81	5797.33	26	4	4	0	11	15	0.267	1.000	0.267
8	CTRL	6644.82	6609.82	27	3	3	0	12	15	0.200	1.000	0.200
13	CTRL	6921.18	6783.00	28	2	2	0	13	15	0.133	1.000	0.133
9	CTRL	7159.46	7040.32	29	1	1	0	14	15	0.067	1.000	0.067
	Max.	7160.46	7159.96	30	0	0	0	15	15	0.000	1.000	0.000

[a] Values from MS-1; [b] Ranking according to apolipoprotein B100 protein concentration after adjoining theoretical min. and max. values; [c] CTRL, control; FN, false negative; FP, false positive; IUGR, intrauterine growth restriction; J, Youden index; TN, true negative; TP, true positive.

To determine which protein concentration from the tested proteins should be used to classify individual patients as either belonging to the IUGR or the CTRL group, a Youden index analysis was performed one by one for all 15 proteins (see Experimental Section, Supporting Information). To select the "best cutoff" value for discriminating IUGR from CTRL samples,[24] all J_{max} values were ranked (**Table 2**). For apolipoprotein B100, a J_{max} value of 0.67 which was obtained with the "best cutoff" value at a concentration of 3187.92 μg mL^{-1} when using the MS-1 data set (**Table 3**).

To evaluate the effectiveness of a discrimination test that is based on maternal apolipoprotein B100 serum concentrations, we performed logistic regression analysis using the individual apolipoprotein serum concentrations. With an apolipoprotein B100 concentration of 3188 μg mL^{-1} as the "best cutoff" value,

25 of the 30 patient samples were mapped to their correct clinical classifications (**Figure 2**). Eleven out of the 15 samples from mothers with fetuses suffering from IUGR were correctly placed into the IUGR group, leaving just four false negative cases (#20, #22, #23, #26). Similarly, 14 out of the 15 control cases were correctly placed in the CTRL group, leaving just one false-positive case (#14).

Biostatistical evaluation of patient stratification based on apolipoprotein B100 serum concentrations (**Table 4**) reached positive predictive values of 0.92 and 0.91, and negative predictive values of 0.78 and 0.74 for MS-1 and MS-2, respectively. At the "best cutoff" value for apolipoprotein B100, the AUC was 0.86 and 0.88 for MS-1 and MS-2, respectively (Table 4 and **Figure 3**). Of all 15 proteins, the concentration of apolipoprotein B100 showed the greatest accuracy in discriminating IUGR from CTRL samples.

Table 3. Best cutoff values and areas under the curves for 15 proteins from 30 peripheral maternal serum samples.

Rank[a]	Protein name	Optimal cutoff [μg mL^{-1}][a]	Sensitivity[a]	1−Specificity[a]	J_{max}[a]	ROC [AUC]
1	Apolipoprotein B 100	3187.92	0.93	0.27	0.67	0.858
2	Apolipoprotein L1	474.94	0.87	0.53	0.33	0.684
3	Apolipoprotein C-I	172.23	0.47	0.67	0.40	0.667
4	Apolipoprotein F	55.08	0.60	0.13	0.47	0.667
5	Apolipoprotein M	214.90	0.60	0.20	0.40	0.651
6	Apolipoprotein IV	367.81	0.93	0.67	0.27	0.613
7	Apolipoprotein C-II	284.95	0.67	0.33	0.33	0.604
8	PON 1	399.84	0.93	0.73	0.20	0.591
9	Beta-2-glycoprotein I (apo H)	1318.86	0.33	0.07	0.27	0.587
10	Apolipoprotein A-II	786.78	0.47	0.13	0.33	0.573
11	Apolipoprotein E	380.71	0.73	0.47	0.27	0.573
12	Apolipoprotein C-III	107.34	0.80	0.53	0.27	0.569
13	LCAT	56.97	0.47	0.27	0.20	0.538
14	Apolipoprotein (a)	667.94	0.20	0.00	0.20	0.473
15	Apolipoprotein D	222.27	0.80	0.67	0.13	0.471

[a] Using data from MS-1; ranking according to ROC; [b] Optimal cutoff concentration at maximum J; [c] Calculated from individual concentrations of all 15 proteins with the SPSS software package; [d] J (Youden's index) defines the maximum potential effectiveness of a biomarker. J = Sensitivity + Specificity − 1.
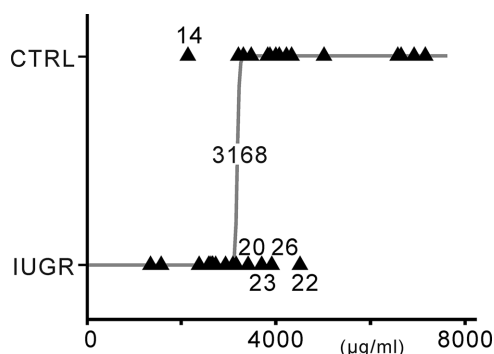
Figure 2. Logistic regression analysis of serum apolipoprotein B100 concentrations of LC-MRM/MS measurements. Individual concentrations are assigned to CTRL (n = 15; *top row*) and IUGR (n = 15; *bottom row*) according to clinical grouping (gold standard). The gray line marks the discriminating threshold at 3168 μg mL^{-1}. False positive and false negative samples are labeled with numbers (numbering as in Table 1).

3.3. Safeguarding of Apolipoprotein B100 as Risk Prognosis Marker

Power analysis indicated that the minimally required total sample size with all the apolipoprotein B100 protein concentrations was 16 for the first measurement series (MS-1) and 14 for the second (MS-2), which both were smaller than the actual number of 30 serum samples. Additionally, the calculated actual power of 0.80 suggested that the test was confidently representing statistical significance in discriminating IUGR cases from controls. To exclude confounding results, that is, to verify that apolipoprotein B100 concentrations were not influenced by potential biases that were associated with other clinical parameters, we performed statistical comparisons, that is, linear regression analyses. No significant correlations were found between apolipoprotein B100 serum concentrations and patient age (R^2 = 0.002), BMI before pregnancy (R^2 = 0.015), parity (R^2 = 0.053), systolic (R^2 = 0.069) and diastolic blood pressure (R^2 = 0.062), proteinuria (R^2 = 0.117) smoking status (R^2 = 0.054), gestational age at delivery (R^2 = 0.039), and birth weight (R^2 = 0.153).

In ELISA analyses with the same 30 maternal serum samples, the apolipoprotein B100 concentrations varied approximately by a factor of six between individuals, ranging from 432.42 μg mL^{-1} to 2616.58 μg mL^{-1} (Table S4, Supporting Information). Box-and-whisker plots indicate that apolipoprotein B100 levels are distinctly different between IUGR samples and controls (p < 0.01) (**Figure 4**) and confirm the LC-MRM/MS data which revealed that apolipoprotein B100 levels are decreased in pregnancies which are complicated by IUGR as compared to those of pregnant women with healthy fetuses.

Table 4. Biostatistical evaluation of patient stratification.

Measurement	True positive	False positive	True negative	False negative	Sensitivity	Specificity	False pos. rate	False neg. rate	Pos. pred. value	Neg. pred. value	ROC [AUC][a]
MS-1	11	1	14	4	0.73	0.93	0.07	0.27	0.92	0.78	0.86
MS-2	10	1	15	5	0.67	0.93	0.07	0.33	0.91	0.74	0.88

[a] Based on apolipoprotein B100 serum concentrations; AUC, area under curve; ROC, receiver operator characteristics.

**ADVANCED
SCIENCE NEWS**
www.advancedsciencenews.com

**Proteomics
Clinical Applications**
www.clinical.proteomics-journal.com

Figure 3. Receiver operator characteristic (ROC) analysis of serum apolipoprotein B100 concentrations from MS-1. Calculated area under curve (AUC) is 0.86. The vertical solid line indicates the maximum Youden's index (J_{max}), the hatched diagonal indicates the 0.5 value.
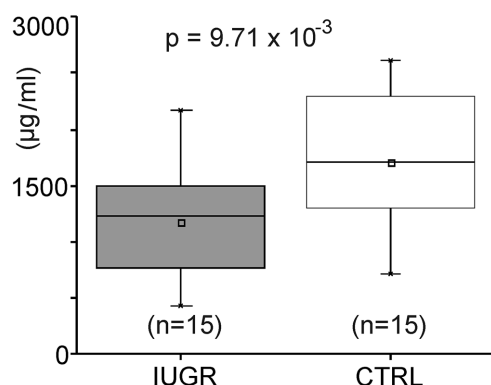
Figure 4. Box-and-whisker plots of apolipoprotein B100 concentrations of ELISA measurements. The horizontal lines within the boxes represent the medians; the small squares indicate the means. The whiskers specify the 5th and 95th percentiles, and the crosses indicate the 1st and 99th percentiles. IUGR, intrauterine growth restriction; CTRL, control individuals. Sample sizes (n) and the p-value are given.

4. Discussion

IUGR is clinically diagnosed by a deceleration (crossing centiles) of fetal growth velocity in serial antenatal sonographic measurements of fetal biometry data[28] or by an estimated low fetal weight in addition to signs of compromised fetal well-being (pathological fetal cardiogram or resistance indices in Doppler sonographic measurements, asymmetry, and/ or reduced amniotic fluid index in ultrasonographic examinations) in the second or third trimester.[13] While sonography has been accepted as "gold standard" for determining IUGR by clinical means, its application is limited to excellently equipped care centers,[1,29] asking for alternative and 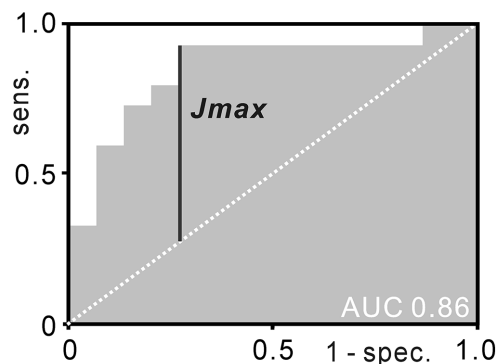easy to apply methods by which pregnant women who are at risk for developing IUGR may be detected. Moreover, up to 80% of IUGR fetuses remain undetected until delivery.[30] Equally important, determination of the optimal time of delivery to avoid still birth on the one hand but to not increase infant prematurity-associated complications on the other hand, is still challenging. Recently, two seminal studies reported inclusion of maternal placental growth factor (PlGF) measurements into pregnancy management when IUGR was suspected and

showed beneficial outcome when the obstetrician's decision was guided by those results.[31] In another study, low PlGF concentrations were associated with lower perinatal mortality and birth weight <3rd centile but appeared to lead to earlier delivery with more neonatal respiratory morbidity.[32] These studies underline the need for biomarkers to better predict adverse pregnancy outcome as well as to optimize determination of the best time point for delivery.

The study cohort described here encompassed serum samples from pregnant women that previously were investigated in both our primary study on fetal cord blood proteome profiling[2] and our recently published study of maternal peripheral blood apolipoprotein CII and CIII proteoform abundances.[9] In both studies, differentiation of serum samples into IUGR and CTRL was achieved with great confidence for which reason this well-studied cohort represented an excellent sample set for the assessment of novel discriminatory methods performed here that provide great potential for future clinical application.

MRM tandem-mass spectrometry (MS/MS) enables reliable and fast quantitation of specific proteins in a given sample by analyzing precursor ions and their fragment ions in a very accurate way. Instrumentation and software have advanced such that ample transitions (pairs of primary and secondary peptide/fragment ions) can be measured by well-designed scheduling and selection of respective m/z windows. Software packages have been developed for the most important analysis components, such as project management, assay development, assay validation, data export, peak integration, quality assessment, and biostatistical analysis that enable researchers to combine these tools for a comprehensive targeted proteomics workflow.[33]

Apolipoprotein B100, which has been identified as best discriminating protein between IUGR and CTRL in this study, is the main structural protein in atherogenic particles and represents the total amount of potentially atherogenic circulating lipoproteins, including LDL, intermediate density lipoprotein, very low-density lipoprotein and lipoprotein (a).[34–37] The apolipoprotein B100 containing chylomicrons can contain large amounts of cholesterol and triglycerides and also serve as carrier of essential lipids such as lipophilic vitamins and glycolipids.[38] The importance of apolipoprotein B containing lipoprotein secretion is evident in the liver and intestine, where both apo B and microsomal triglyceride transfer protein are needed to export large amounts of lipids for usage in peripheral tissues.[39,40] Two main isoforms of apo B exist: apolipoproteins B100 and B48. Apolipoprotein B100 is synthesized in the liver and represents the circulating apo B particles.[37,41] Furthermore, the placenta is capable of secreting apo B particles.[40] Indeed, low apo B levels, as seen in our study in the majority of IUGR cases, may reflect insufficient placental function. This means that apo B levels could be directly related to placental pathology and may be involved in the estimation of individual pathophysiology.

The potential of apolipoprotein B, together with apolipoprotein A1, to function as marker of lipoprotein metabolism has been discussed.[42] Apo A1, the major structural protein component of high-density lipoprotein (HDL) particles, exhibits pleiotropic biological functions and also provides anti-inflammatory properties. These functions include the inhibition of LDL oxidation and scavenging toxic phospholipids.[37] The apo B100/apo A1

ratio—in most cases determined by immuno-analytical assays—has been proposed as a reliable parameter to reflect lipid disturbances and was attributed to correlate with the potential to develop atherosclerosis.[34] Moreover, the apo B100/apo A1 ratio was suggested to predict cardiovascular risk better than any cholesterol index.[36] In our study, we neither investigated apo A1 values nor determined apo B100/apo A1 ratios, because apo A1 was not part of our SIS peptide panel. Nevertheless, our results indicate that apolipoprotein B100 abundance by itself is good enough to distinguish between pregnant women whose fetuses suffer from IUGR and those that are not affected by pregnancy complications (CTRL).

We previously had outlined the fact that (apo B-containing) LDL particles reflected by LDL-cholesterol measurements were not altered in PE, unless there was substantial placental dysfunction, the latter of which was reflected by the presence of IUGR.[14,43] This finding is in agreement with a recent study in which apo B levels in PE were found to be unchanged but apo A1 levels were low.[37] As a result, apo B/apo A1 ratios were increased in PE. Yet, other studies, however, showed contradicting results when they focused on cases in which most fetuses born to mothers with PE were small for gestational age, and hence, with great certainty suffered from IUGR.[44] While this has not been taken into account by the authors, the need of excellent clinical characterization of the study collective and sufficient subgroup analyses in heterogeneous diseases is obvious. A recent meta-analysis of 74 studies found that PE was additionally associated with elevated total cholesterol and non-HDL-cholesterol in the third trimester, suggesting that pure PE is rather associated with increased apo B-containing LDL-particles.[45] Noteworthy, plasma cholesterol concentrations in the newborns from our cohorts (IUGR and CTRL) are markedly reduced compared to those of the mothers (Table S5, Supporting Information), which is in agreement with previously reviewed results.[46]

The results described here from MS-1 and MS-2 are nearly the same and they also demonstrate that sample shipment of serum proteins can be done on both the processed peptide level (results from MS-1) and the intact protein level (results from MS-2). Since serum protein compositions may artificially be altered depending on sample handling and storage conditions,[47] this is not a trivial result. Yet, due to its gentleness on protein integrity, lyophylization has been assumed as a useful method to prepare long lasting samples[48] that do not require freezing temperatures and expensive maintenance of an uninterrupted cold chain.

We found in this study that apolipoprotein B100 is decreased in women whose pregnancies are complicated by IUGR as compared to pregnant women with healthy fetuses. Other studies[14,43,44,49] confirmed that there are lower maternal serum LDL-C and TC concentrations in IUGR pregnancies. These data contribute to the hypothesis of a decreased cholesterol supply to the fetus in IUGR. One possible explanation for a diminished apolipoprotein B100 level in maternal serum is that the reduced maternal LDL cholesterol concentration in IUGR pregnancies is attributed to increased accumulation of oxidized LDL particles within the placenta.[50] With this causal connection of maternal apolipoprotein B100 serum levels to IUGR, the assessment performed here underlines the potential of LC-MRM/MS to become of clinical importance in the future.

Conflict of Interest

The authors declare no conflict of interest.

[1] American College of Obstetricians and Gynecologists. *Obstet. Gynecol.* **2013**, *121*, 1122.
[2] M. Wolter, C. Rower, C. Koy, T. Reimer, W. Rath, U. Pecks, M. O. Glocker, *Electrophoresis* **2012**, *33*, 1881.
[3] M. Kaijser, A. K. Bonamy, O. Akre, S. Cnattingius, F. Granath, M. Norman, A. Ekbom, *Circulation* **2008**, *117*, 405.
[4] D. J. Barker, P. D. Winter, C. Osmond, B. Margetts, S. J. Simmonds, *Lancet* **1989**, *2*, 577.
[5] C. Napoli, F. P. D'Armiento, F. P. Mancini, A. Postiglione, J. L. Witztum, G. Palumbo, W. Palinski, *J. Clin. Invest.* **1997**, *100*, 2680.
[6] M. R. Skilton, N. Evans, K. A. Griffiths, J. A. Harmer, D. S. Celermajer, *Lancet* **2005**, *365*, 1484.
[7] V. Zanardo, S. Visentin, D. Trevisanuto, M. Bertin, F. Cavallin, E. Cosmi, *Hypertens. Res.* **2013**, *36*, 440.
[8] C. Zheng, C. Khoo, J. Furtado, F. M. Sacks, *Circulation* **2010**, *121*, 1722.
[9] M. Wolter, C. Rower, C. Koy, W. Rath, U. Pecks, M. O. Glocker, *J. Proteomics* **2016**, *149*, 44.
[10] J. H. Contois, J. P. McConnell, A. A. Sethi, G. Csako, S. Devaraj, D. M. Hoefner, G. R. Warnick, *Clin. Chem.* **2009**, *55*, 407.
[11] I. Holme, A. H. Aastveit, N. Hammar, I. Jungner, G. Walldius, *Eur. J. Heart Fail.* **2009**, *11*, 1036.

**ADVANCED
SCIENCE NEWS**

www.advancedsciencenews.com

**Proteomics
Clinical Applications**

www.clinical.proteomics-journal.com

[12] U. Pecks, M. Brieger, B. Schiessl, D. O. Bauerschlag, D. Piroth, B. Bruno, C. Fitzner, T. Orlikowsky, N. Maass, W. Rath, *J. Perinat. Med.* **2012**, *40*, 287.

[13] Intrauterine growth restriction. Clinical management guidelines for obstetrician-gynecologists. American College of Obstetricians and Gynecologists. Committee on Practice Bulletins—Gynecology, American College of Obstetricians and Gynecologists, Washington, DC, USA. *Int. J. Gynaecol. Obstet.* **2001**, *72*, 85.

[14] U. Pecks, R. Caspers, B. Schiessl, D. Bauerschlag, D. Piroth, N. Maass, W. Rath, *Hypertens. Pregnancy* **2012**, *31*, 156.

[15] Report of the National High Blood Pressure Education Program Working Group on High Blood Pressure in Pregnancy. *Am. J. Obstet. Gynecol.* **2000**, *183*, S1.

[16] F. P. Hadlock, R. B. Harrist, R. S. Sharman, R. L. Deter, S. K. Park, *Am. J. Obstet. Gynecol.* **1985**, *151*, 333.

[17] M. Voigt, K. T. Schneider, K. Jahrig, *Geburtshilfe Frauenheilkd.* **1996**, *56*, 550.

[18] U. Pecks, I. Kirschner, M. Wolter, D. Schlembach, C. Koy, W. Rath, M. O. Glocker, *Transl. Res.* **2014**, *164*, 57.

[19] M. A. Kuzyk, D. Smith, J. Yang, T. J. Cross, A. M. Jackson, D. B. Hardie, N. L. Anderson, C. H. Borchers, *Mol. Cell. Proteomics* **2009**, *8*, 1860.

[20] A. J. Percy, A. G. Chambers, J. Yang, D. B. Hardie, C. H. Borchers, *Biochim. Biophys. Acta* **2014**, *1844*, 917.

[21] A. J. Percy, A. G. Chambers, J. Yang, D. Domanski, C. H. Borchers, *Anal. Bioanal. Chem.* **2012**, *404*, 1089.

[22] A. G. Chambers, A. J. Percy, J. Yang, A. G. Camenzind, C. H. Borchers, *Mol. Cell. Proteomics* **2013**, *12*, 781.

[23] M. Greiner, D. Pfeiffer, R. D. Smith, *Prev. Vet. Med.* **2000**, *45*, 23.

[24] P. J. Davis, *Interpolation and Approximation*, Courier Corporation, **1975**.

[25] C. E. Metz, *Semin. Nucl. Med.* **1978**, *8*, 283.

[26] C.-Y. J. Peng, K. L. Lee, G. M. Ingersoll, *J. Educ. Res.* **2002**, *96*, 3.

[27] F. Faul, E. Erdfelder, A. G. Lang, A. Buchner, *Behav. Res. Methods* **2007**, *39*, 175.

[28] a) J. Villar, G. Carroli, D. Wojdyla, E. Abalos, D. Giordano, H. Ba'aqeel, U. Farnot, P. Bergsjo, L. Bakketeig, P. Lumbiganon, L. Campodonico, Y. Al-Mazrou, M. Lindheimer, M. Kramer, *Am. J. Obstet. Gynecol.* **2006**, *194*, 921; b) American College of Obstetricians and Gynecologists. *Int. J. Gynaecol. Obstet.* **2000**, *68*, 175.

[29] P. A. Lee, S. D. Chernausek, A. C. Hokken-Koelega, P. Czernichow, *Pediatrics* **2003**, *111*, 1253.

[30] I. Monier, B. Blondel, A. Ego, M. Kaminiski, F. Goffinet, J. Zeitlin, *Bjog* **2015**, *122*, 518.

[31] L. Ormesher, E. D. Johnstone, E. Shawkat, A. Dempsey, C. Chmiel, E. Ingram, L. E. Higgins, J. E. Myers, *Pregnancy Hypertens.* **2018**.

[32] A. Sharp, L. C. Chappell, G. Dekker, S. Pelletier, Y. Garnier, O. Zeren, K. M. Hillerer, T. Fischer, P. T. Seed, M. Turner, A. H. Shennan, Z. Alfirevic, *Pregnancy Hypertens.* **2018**.

[33] C. M. Colangelo, L. Chung, C. Bruce, K.-H. Cheung, *Methods* **2013**, *61*, 287.

[34] P. J. Kappelle, R. T. Gansevoort, J. L. Hillege, B. H. Wolffenbuttel, R. P. Dullaart, *J. Intern. Med.* **2011**, *269*, 232.

[35] Y. H. Lee, S. H. Choi, K. W. Lee, D. J. Kim, *Clin. Endocrinol.* **2011**, *74*, 579.

[36] J. Sierra-Johnson, R. M. Fisher, A. Romero-Corral, V. K. Somers, F. Lopez-Jimenez, J. Ohrvik, G. Walldius, M. L. Hellenius, A. Hamsten, *Eur. Heart J.* **2009**, *30*, 710.

[37] H. Timur, H. K. Daglar, O. Kara, A. Kirbas, H. A. Inal, G. G. Turkmen, Z. Yilmaz, B. Elmas, D. Uygur, *Pregnancy Hypertens.* **2016**, *6*, 121.

[38] a) J. T. Clarke, *Can. J. Biochem.* **1981**, *59*, 412; H. J. Kayden, M. G. Traber, *J. Lipid Res.* **1993**, *34*, 343.

[39] J. R. Wetterau, M. C. Lin, H. Jamil, *Biochim. Biophys. Acta* **1997**, *1345*, 136.

[40] E. M. Madsen, M. L. Lindegaard, C. B. Andersen, P. Damm, L. B. Nielsen, *J. Biol. Chem.* **2004**, *279*, 55271.

[41] S. K. Reaves, J. C. Fanzo, J. Y. Wu, Y. R. Wang, Y. W. Wu, L. Zhu, K. Y. Lei, *J. Nutr.* **1999**, *129*, 1855.

[42] Y. M. Zhu, S. Verma, M. Fung, M. J. McQueen, T. J. Anderson, E. M. Lonn, *Can. J. Cardiol.* **2017**, *33*, 1305.

[43] U. Pecks, W. Rath, N. Kleine-Eggebrecht, N. Maass, F. Voigt, T. W. Goecke, M. G. Mohaupt, G. Escher, *Geburtshilfe Frauenheilkd.* **2016**, *76*, 799.

[44] K. Winkler, B. Wetzka, M. M. Hoffmann, I. Friedrich, M. Kinner, M. W. Baumstark, H. P. Zahradnik, H. Wieland, W. Marz, *J. Clin. Endocrinol. Metab.* **2003**, *88*, 1162.

[45] C. N. Spracklen, C. J. Smith, A. F. Saftlas, J. G. Robinson, K. K. Ryckman, *Am. J. Epidemiol.* **2014**, *180*, 346.

[46] L. Woollett, J. E. Heubi, in *Endotext* (Eds: L. J. De Groot, G. Chrousos, K. Dungan, K. R. Feingold, A. Grossman, J. M. Hershman, C. Koch, M. Korbonits, R. McLachlan, M. New, J. Purnell, R. Rebar, F. Singer, A. Vinik), MDText.com, Inc., South Dartmouth, MA **2000**.

[47] R. E. Gislefoss, T. K. Grimsrud, L. Morkrid, *Clin. Chem. Lab. Med.* **2009**, *47*, 596.

[48] T. W. Randolph, *J. Pharm. Sci.*, *86*, 1198.

[49] N. Sattar, I. A. Greer, P. J. Galloway, C. J. Packard, J. Shepherd, T. Kelly, A. Mathers, *J. Clin. Endocrinol. Metab.* **1999**, *84*, 128.

[50] U. Pecks, W. Rath, R. Caspers, K. Sosnowsky, B. Ziems, H. J. Thiesen, N. Maass, B. Huppertz, *Placenta* **2013**, *34*, 1142.

Supplemental data

Supplemental Table 1: Demographic data. Individual clinical and laboratory parameters for all patients and control individuals.

				mothers					fetus/ infants			
patient/ individual	age[a] [yr]	BMI before pregnancy [kg/m^2]	parity[a]	gestational age at sampling [w+d]	median blood pressure[a,b] [mmHg]	protein-uria[a,c,d] [mg/l]	actual smoking status[e]	gestational age at delivery[f] [w+d]	mode of delivery	birth weight [g]	birth weight percentile	sex
1	24	20	2	27+0	109 / 53	0[f]	20	27+4	sectio caesarea	1355	85	m
2	37	23	2	27+1	108 / 65	0[t]	0	27+4	sectio caesarea	1095	40	m
3	30	22	0	25+0	114 / 61	0[f]	0	25+0	vaginal	740	30	m
4	30	20	1	31+2	124 / 69	0[f]	0	33+6	sectio caesarea	1960	25	f
5	29	21	0	32+0	114 / 71	150	0	32+1	sectio caesarea	1920	50	m
6	24	35	0	31+6	129 /73	0[f]	10	31+6	vaginal	1750	50	f
7	32	22	0	37+4	126 / 63	0[f]	0	37+4	sectio caesarea	3130	50	f
8	31	25	1	37+5	121 / 75	0[t]	0	37+5	sectio caesarea	3465	70	m
9	35	21	1	33+6	122 / 58	0[f]	0	34+6	sectio caesarea	2420	40	f
10	37	19	1	38+6	120 / 60	0[f]	0	39+0	sectio caesarea	3150	30	f
11	39	20	1	36+0	110 / 60	0[f]	0	36+0	sectio caesarea	2920	60	m
12	32	25	2	32+3	110 / 70	0[t]	0	32+3	sectio caesarea	1850	50	f
13	29	24	1	27+5	106 / 61	0[f]	0	28+4	sectio caesarea	1250	60	f
14	24	17	1	28+0	110 / 54	0[t]	5	28+0	sectio caesarea	1030	40	f
15	24	35	1	39+2	120 / 81	0[f]	0	39+2	sectio caesarea	3895	80	m
16	31	22	0	31+0	129 / 76	90	0	32+1	sectio caesarea	1255	9	f
17	23	23	0	30+5	125 / 71	101	10	30+5	sectio caesarea	940	4	f
18	33	31	0	24+0	155 / 100	2324	10	26+5	sectio caesarea	650	4	m
19	25	26	0	37+3	83 / 52	0[f]	0	37+5	sectio caesarea	2550	5	m
20	39	27	0	28+2	148 / 92	300	0	28+2	sectio caesarea	850	8	m
21	34	19	0	32+0	136 / 71	0[t]	0	32+1	sectio caesarea	1310	8	m
22	23	21	0	35+5	162 / 100	500	0	35+5	sectio caesarea	1330	1	f
23	27	22	0	32+6	130 / 68	150	0	33+2	sectio caesarea	1405	6	f
24	19	23	0	35+5	116 / 64	0[t]	10	36+1	sectio caesarea	1870	2	m
25	27	28	3	27+0	112 / 55	0[f]	0	27+0	sectio caesarea	580	3	f
26	31	20	1	38+6	100 / 60	0[f]	0	39+0	sectio caesarea	1970	1	f
27	34	23	2	26+4	140 / 90	1725	0	26+6	sectio caesarea	490	1	m
28	25	22	0	33+6	122 / 79	0[f]	3	36+4	sectio caesarea	1905	3	f
29	37	22	0	40+3	150 / 80	0[f]	0	40+3	sectio caesarea	2665	2	m
30	41	28	0	30+2	155 /101	200	0	32+0	sectio caesarea	975	3	f

a) at beginning of hospitalization (time point of sample collection)   b) systolic/diastolic blood pressure
c) immunoturbidimetric assay (Tina-quant albumin; Roche Diagnostics. Mannheim. Germany); proteinuria is defined as urinary protein excretion >300 mg/L.
d) dip stick assay; significant proteinuria is present with readings of more than +1 (max: +3).   e) cigarettes per day   f) gestational weeks at time point of delivery.

Supplemental Table 2: Best cutoff values and areas under the curves for 15 proteins from 30 peripheral maternal serum samples of second measurement [a].

rank	protein name	optimal cutoff (µg/mL) [b]	sensitivity [c]	1-specificity [c]	J max. [d]	ROC (AUC)
1	apolipoprotein B 100	3256.09	0.93	0.20	0.73	0.876
2	apolipoprotein L1	533.83	0.60	0.13	0.47	0.702
3	apolipoprotein C-I	177.71	0.40	0.07	0.33	0.622
4	apolipoprotein F	37.48	0.80	0.53	0.27	0.658
5	apolipoprotein M	195.36	0.73	0.27	0.47	0.662
6	apolipoprotein IV	418.12	0.87	0.60	0.27	0.629
7	apolipoprotein C-II	324.41	0.40	0.13	0.27	0.604
8	PON 1	552.07	0.60	0.33	0.27	0.591
9	beta-2-glycoprotein I (Apo H)	1134.54	0.53	0.20	0.33	0.604
10	apolipoprotein A-II	817.01	0.40	0.20	0.20	0.556
11	apolipoprotein E	386.98	0.67	0.40	0.27	0.604
12	apolipoprotein C-III	102.67	0.80	0.60	0.20	0.547
13	LCAT	66.43	0.20	0.13	0.07	0.447
14	apolipoprotein (a)	362.26	0.27	0.13	0.13	0.440
15	apolipoprotein D	185.71	0.87	0.73	0.13	0.460

a) ranking according to ROC.
b) optimal cut-off concentration at maximum *J.*
c) calculated from individual concentrations of all 15 proteins with the SPSS software package.
d) *J* (Youden's index) defines the maximum potential effectiveness of a biomarker. *J* = Sensitivity + Specificity - 1.

Supplemental Table 3: Per Protocol Set: Concentrations of 15 protein

protein	UniProt Acc. No.	protein MW (Da)
apolipoprotein (a)	P08519	498944.46
apolipoprotein AII	P02652	8706.91
apolipoprotein AIV	P06727	43376.26
apolipoprotein B100	P04114	512834.66
apolipoprotein CI	P02654	6630.58
apolipoprotein CII	P02655	8914.93
apolipoprotein CIII	P02656	8764.68
apolipoprotein D	P05090	19298.08
apolipoprotein E	P02649	34235.72
apolipoprotein F [b)]	Q13790	31495.72
apolipoprotein L1	O14791	41128.72
apolipoprotein M	O95445	21247.32
LCAT	P04180	47077.93
PON 1	P27169	39597.14
beta-2-glycoprotein I (apo H)	P02749	36232.58

a)   Vertical line indicates position of bond breakage
b)   Values mentioned belong to apolipoprotein with propeptide
c)   Numbering according to Supplemental Table 1.

s in 30 maternal serum samples determined by LC-MRM/MS analysis.

selected peptide [a)]	transition [m/z] (precursor -> fragment)	run	controls avg. (µg/ml)
LFLE₁PTQADIALLK	(2+) 786.46 -> 1069.63 (y10)	MS-1	195.75
		MS-2	190.34
S₁PELQAEAK	(2+) 486.75 -> 443.24 (y8)	MS-1	735.81
		MS-2	738.76
SLA₁PYAQDTQEK	(2+) 675.83 -> 540.25 (y9)	MS-1	516.46
		MS-2	509.46
FP₁EVDVLTK	(2+) 524.29 -> 803.45 (y7)	MS-1	4587.42
		MS-2	4643.1
T₁PDVSSALDK	(2+) 516.76 -> 466.24 (y9)	MS-1	158.69
		MS-2	157.51
TA₁AQNLYEK	(2+) 519.27 -> 865.44 (y7)	MS-1	326.55
		MS-2	329.05
GWV₁TDGFSSLK	(2+) 598.80 -> 854.43 (y8)	MS-1	131.05
		MS-2	130.45
VL₁NQELR	(2+) 436.25 -> 659.35 (y5)	MS-1	275.94
		MS-2	276.01
LG₁PLVEQGR	(2+) 484.78 -> 399.73 (y7)	MS-1	423.68
		MS-2	437.37
SGVQQL₁IQYYQDQK	(3+) 566.62 -> 613.33 (b6)	MS-1	108.2
		MS-2	98.51
VTE₁PISAESGEQVER	(2+) 815.90 -> 651.32 (y12)	MS-1	582.95
		MS-2	582.15
AF₁LLTPR	(2+) 409.25 -> 599.39 (y5)	MS-1	216.81
		MS-2	216.03
SSGLVSNA₁PGVQIR	(2+) 692.88 -> 669.40 (y6)	MS-1	53.23
		MS-2	50.99
IQ₁NILTEEPK	(2+) 592.83 -> 943.51 (y8)	MS-1	534.34
		MS-2	533.44
ATV₁VYQGER	(2+) 511.77 -> 751.37 (y6)	MS-1	1145.62
		MS-2	1135.36

(n=15)	IUGR (n=15)		t-test		
std. dev.	avg. (µg/ml)	std. dev.	p value	1	2
181.33	485.64	908.53	0.24	54.12	257.09
172.55	618.9	1423.86	0.26	40.59	281.69
180.55	681.52	161.57	0.39	798.15	835.75
184.19	673.11	175.1	0.33	793.49	908.05
180.28	592.79	168.78	0.24	677.70	585.71
176.26	598.57	178.63	0.18	731.90	502.55
1535.71	2886.96	818.06	<0,01	4001.63	3876.35
1544.14	2863.86	795.69	<0,01	4133.05	4050.76
46.89	134.77	37.23	0.13	159.27	196.79
46.08	137.5	35	0.19	151.34	200.66
165.96	277.72	70.36	0.30	206.59	416.28
172.14	276.56	72.78	0.29	224.53	371.86
39.33	124.04	50.68	0.68	112.60	156.96
38.04	124.51	50.65	0.72	119.66	153.11
87.88	284.46	101.77	0.81	286.23	372.97
91.16	284.3	106.49	0.82	289.12	381.97
129.5	393.83	127.77	0.53	261.52	426.98
129.39	392.73	133.28	0.48	259.34	466.94
43.31	85.17	22.28	0.08	134.81	176.81
39.46	78.88	25.36	0.12	105.31	149.35
141.24	491.78	99.05	0.05	531.50	441.08
123.26	484.18	101.85	0.02	466.10	413.96
54.91	190.74	35.69	0.13	147.97	228.72
58.17	189.29	36.13	0.14	145.51	231.67
10	52.49	12.12	0.86	57.01	49.67
12.51	55.43	14.45	0.38	38.93	73.26
153.15	596.58	197.02	0.34	558.72	525.31
156.8	591.86	194.3	0.37	545.15	542.29
250.96	1078.65	355.99	0.56	1225.66	1151.52
200.91	1081.62	338.55	0.60	1138.29	1098.37

3	4	5	6	7	8	9
98.41	239.87	541.24	95.95	632.26	243.56	11.07
107.02	239.87	532.63	95.95	579.37	220.19	19.68
885.20	843.84	533.18	731.61	564.68	849.20	1129.18
898.40	840.04	536.24	631.73	584.73	917.02	1131.47
367.65	563.67	454.00	711.24	472.21	499.25	336.88
329.22	513.31	442.50	774.49	405.98	544.61	333.37
3829.68	6574.81	3480.85	3316.27	4225.17	6644.82	7159.46
3824.76	6319.33	3364.17	3302.76	4300.10	6961.71	7206.13
177.63	179.51	119.86	176.62	148.15	198.14	268.83
184.58	183.47	122.89	181.17	138.21	205.57	261.72
299.76	305.94	162.10	289.26	334.96	448.54	810.59
320.83	278.57	157.80	303.44	346.82	465.54	836.25
117.75	178.47	85.87	191.59	110.63	149.81	161.48
127.91	175.58	84.93	196.09	111.30	144.90	161.92
322.47	176.62	217.34	374.52	98.84	391.41	314.07
326.91	161.45	211.99	353.71	107.20	386.15	298.47
430.70	396.55	186.64	582.21	416.18	554.65	623.85
440.58	359.04	184.95	599.95	425.23	562.51	603.66
206.52	116.01	117.39	99.92	52.15	132.81	80.90
169.62	122.19	112.20	78.27	47.64	160.34	74.18
479.11	746.45	614.07	684.86	542.66	743.39	801.54
493.96	641.92	644.62	743.51	558.12	769.52	697.01
217.21	254.47	139.13	223.18	143.55	268.22	356.55
212.23	258.54	134.78	221.07	135.69	258.33	363.28
62.89	51.69	47.00	53.06	31.86	66.56	61.69
50.68	50.59	39.11	49.76	37.64	63.90	69.68
809.74	396.38	493.75	621.94	318.58	855.15	604.03
852.94	383.55	467.17	617.04	333.62	829.40	620.46
1475.41	1220.74	798.50	1419.32	827.36	1168.11	1016.96
1254.79	1015.58	819.59	1427.62	943.59	1191.27	1135.87

						(µg/ml)
10	11	12	13	14	15	16
199.27	105.79	201.73	210.34	4.92	40.59	36.90
174.67	98.41	206.65	221.42	8.61	28.29	27.06
591.90	651.99	473.11	920.27	686.45	542.62	744.68
573.73	616.86	466.69	855.86	709.38	617.67	793.98
829.75	597.53	211.03	350.08	764.37	325.81	636.50
744.57	585.82	210.39	374.79	747.02	408.75	616.27
3210.64	5019.85	4332.03	6921.18	2144.52	4074.10	2668.98
3393.65	4926.50	4386.07	7037.86	2146.98	4292.73	2715.66
130.42	101.01	79.32	144.72	117.33	182.79	156.25
125.89	99.96	85.54	135.54	123.97	162.14	156.22
329.52	356.68	117.23	267.85	151.72	401.24	259.52
320.81	371.26	111.84	262.17	149.04	414.96	266.16
122.83	127.91	61.73	174.21	68.78	145.14	177.70
120.96	125.74	64.16	169.01	70.08	131.47	170.48
335.91	337.51	195.88	161.36	264.13	289.85	358.19
361.12	365.95	184.20	163.17	247.41	301.36	361.38
436.94	510.76	568.75	386.32	261.38	311.72	502.14
415.76	498.56	581.23	390.03	263.06	359.74	447.45
52.74	114.54	81.11	113.00	71.50	72.80	97.58
41.45	95.82	84.29	108.65	60.59	67.78	83.83
767.68	478.50	487.45	478.50	326.11	621.31	416.66
735.17	468.07	534.32	474.08	428.07	663.76	396.29
231.03	225.56	184.52	200.16	197.15	234.68	170.35
239.52	231.88	174.00	197.29	197.78	238.82	176.24
58.48	43.15	48.20	66.56	40.76	59.86	38.01
66.47	38.65	39.02	58.11	39.94	49.12	47.65
556.41	373.49	456.28	383.00	448.16	614.18	592.96
529.46	388.63	443.45	377.65	436.44	634.40	613.08
1424.16	818.98	894.42	1487.85	1330.05	925.19	665.24
1500.56	935.82	959.58	1248.13	1391.84	969.52	737.06

17	18	19	20	21	22	23
98.41	113.17	121.78	24.60	78.73	2231.38	45.51
78.73	5350.87	97.18	27.06	81.19	2210.46	51.66
840.64	411.87	345.19	654.15	775.41	677.04	972.05
879.63	400.45	338.53	619.49	738.79	634.52	954.52
596.14	788.22	442.93	367.97	690.48	490.63	717.21
597.85	786.52	427.49	396.19	657.15	484.88	744.57
3165.19	1355.99	2937.97	3416.99	1578.30	4510.13	3703.17
3209.41	1470.21	2939.20	3209.41	1456.70	4271.85	3563.15
222.28	77.58	103.61	128.21	151.25	165.84	167.84
217.04	81.01	106.90	134.13	132.56	174.25	163.59
336.18	280.64	275.03	272.82	245.56	413.70	258.04
337.99	285.08	258.11	318.07	275.54	336.16	290.36
236.62	126.44	104.04	129.50	99.08	156.09	177.53
234.81	141.56	114.79	123.84	94.03	151.40	183.29
269.73	285.46	182.18	278.69	269.39	330.91	566.69
260.47	298.47	187.22	269.13	273.44	328.89	593.41
541.19	375.10	356.59	331.77	354.06	339.62	437.29
593.43	360.86	341.44	330.44	372.29	341.58	424.11
75.35	135.31	85.67	99.21	114.04	93.11	66.32
67.61	119.06	84.87	102.26	107.86	93.48	44.51
568.80	560.58	447.58	529.54	491.01	471.38	490.89
533.34	524.26	474.94	488.80	477.64	399.97	484.39
267.59	235.03	187.11	178.13	184.59	155.47	124.32
275.73	239.45	183.89	173.92	183.75	152.18	124.81
56.92	71.98	32.87	62.34	40.03	44.16	54.07
59.86	56.74	44.99	77.85	38.93	58.30	46.55
594.80	671.03	403.30	918.74	555.21	420.93	500.02
565.27	688.75	396.75	894.00	558.99	416.50	502.98
1307.67	2080.68	975.05	1284.51	524.90	1037.53	1078.92
1141.75	2052.16	847.41	1118.42	559.38	1073.22	1108.48

24	25	26	27	28	29	30
17.22	3051.84	703.61	46.74	455.13	216.50	43.05
20.91	9.84	578.14	47.97	442.83	223.88	35.67
708.00	761.42	755.91	495.34	769.32	657.35	654.38
727.38	859.99	736.38	448.37	605.85	659.06	699.73
954.75	578.90	514.05	312.93	449.11	672.70	679.30
1037.16	569.31	495.00	344.12	459.01	656.52	706.56
2727.94	2614.94	3914.43	2583.01	3095.18	2379.12	2653.02
2600.20	2602.66	4147.79	2686.18	3079.22	2304.19	2702.15
103.38	137.23	94.27	122.82	137.07	97.25	156.72
102.53	141.52	112.53	130.54	145.92	98.47	165.35
196.68	205.61	136.97	315.85	353.05	257.80	358.33
180.93	198.95	127.40	268.66	410.86	233.60	360.48
46.64	92.65	66.76	75.69	141.89	80.50	149.50
48.20	85.31	69.09	76.10	150.65	77.52	146.51
165.93	227.20	246.98	344.79	237.24	351.94	151.63
153.09	220.39	261.24	321.09	238.62	340.91	156.75
208.44	189.09	437.50	405.67	524.08	251.28	653.58
212.23	191.76	415.90	383.93	549.11	255.98	670.48
80.19	95.86	77.73	46.59	78.65	54.24	77.73
66.70	119.56	68.45	38.57	59.30	59.47	67.70
459.11	642.53	347.46	497.15	704.13	385.25	364.64
496.90	655.91	304.64	521.07	703.02	425.00	376.54
176.24	234.75	178.06	162.28	212.58	197.15	197.43
177.64	223.18	180.52	163.89	205.22	193.43	185.50
43.98	76.47	51.78	52.70	60.04	47.28	54.81
57.10	87.68	38.47	64.45	48.01	38.56	66.38
611.78	1025.52	455.54	292.93	487.84	605.60	812.51
602.83	1016.29	464.86	292.65	466.98	588.44	809.56
1058.53	1233.44	942.73	714.07	1169.49	1047.64	1059.31
1133.20	1422.09	967.96	827.54	1122.74	980.32	1132.59

Supplemental Table 4: Apolipoprotein B100 concentrations from ELISA measurements.

patient / individual	mothers		
	mean [μg/mL] [a]	std. dev. [μg/mL] [a]	CV%
1	1304.50	5.30	0.41
2	1224.08	18.86	1.54
3	1147.42	60.10	5.24
4	1980.33	19.45	0.98
5	2292.00	10.02	0.44
6	1292.83	7.66	0.59
7	1308.67	18.27	1.40
8	2051.17	77.19	3.76
9	2616.58	4.71	0.18
10	1306.58	45.96	3.52
11	1702.00	8.84	0.52
12	1885.33	66.59	3.53
13	2349.92	4.71	0.20
14	715.75	30.64	4.28
15	2365.75	2.36	0.10
16	1404.92	60.10	4.28
17	1224.08	10.61	0.87
18	819.50	46.55	5.68
19	1501.58	68.35	4.55
20	1555.75	57.75	3.71
21	614.92	31.82	5.17
22	1909.92	27.11	1.42
23	1230.33	35.94	2.92
24	953.67	71.30	7.48
25	2164.08	3.02	0.14
26	764.08	2.76	0.36
27	1347.83	8.84	0.66
28	922.00	37.12	4.03
29	668.67	44.19	6.61
30	432.42	15.32	3.54

a) duplicate measurements
b) n.d.: not determined

Supplemental Table 5: Triglyceride, cholesterol, LDL, and HDL levels for all patients and control individuals [a].

patient / individual	mothers				fetus / infants			
	LDL-C (mg/dl)	HDL-C (mg/dl)	cholesterol (mg/dl)	triglyceride (mg/dl)	LDL-C (mg/dl)	HDL-C (mg/dl)	cholesterol (mg/dl)	triglyceride (mg/dl)
1	122	55	222	180	40	29	91	30
2	141	95	261	144	56	50	113	25
3	124	85	252	175	30	33	70	26
4	171	64	294	419	17	21	47	14
5	150	74	248	100	29	26	63	1
6	131	86	233	126	44	33	81	9
7	169	80	293	296	27	39	75	19
8	232	95	397	298	18	30	59	10
9	206	88	375	433	26	41	78	21
10	130	83	254	128	17	47	77	14
11	178	67	292	275	21	29	59	15
12	162	56	254	235	21	43	60	15
13	162	44	249	296	26	29	62	12
14	65	57	151	120	60	26	95	24
15	157	63	257	193	14	19	41	15
16	91	108	236	157	29	11	62	49
17	89	108	231	302	37	26	68	24
18	70	49	151	271	8	27	37	7
19	155	51	248	191	13	11	36	45
20	112	77	272	144	2	4	19	49
21	50	90	154	107	20	23	53	26
22	198	65	330	223	7	9	42	70
23	119	56	214	245	7	7	62	192
24	84	77	175	107	19	9	38	29
25	110	109	245	148	38	13	62	48
26	102	56	203	256	20	23	54	17
27	142	74	236	112	36	12	72	64
28	111	54	211	278	20	17	52	44
29	105	71	231	187	10	13	45	149
30	82	67	216	262	18	13	39	34

a) Blinded analysis of serum triglycerides, cholesterol, LDL-C and HDL-C was performed by colorimetric enzymatic methods using an automated photometric measuring unit (Roche/Hitachi Modular P800, Roche Diagnostics, Basel, Switzerland; triglycerides GPO-PAP reagent, cholesterol CHOD-PAP reagent, LDL-C plus 2nd generation reagent, HDL-C plus 3rd generation reagent, Cobas®, Roche/Hitachi, Mannheim, Germany). Measurement ranges were: TG=4–1000 mg/dL, cholesterol=3–800 mg/dL, LDL-C=3–550 mg/dL, and HDL-C=3–120 mg/dL.

Supplemental Materials and Methods

Patient cohorts and sample work-up
In addition to an estimated fetal weight below the 10th percentile, one of the following criteria had to be fulfilled to be classified IUGR: (1) deceleration of fetal growth velocity during the last 4 weeks, (2) elevated resistance index in umbilical artery Doppler sonography above the 95th percentile or absent or reversed end-diastolic blood flow, (3) fetal asymmetry (head to abdominal circumference ratio above the 95th percentile), or (4) oligohydramnions (Amniotic Fluid Index < 5 cm). Gestational age was established on the basis of the last menstrual period and was confirmed by ultrasonic examination between the 10th and the 14th week of gestation. Patients with one of the following criteria were excluded from the trial: multiple gestation, fetal anomalies, abnormal fetal karyotype, patients with clinical or biochemical sighs of infection, positive TORCH screening results, maternal diabetes mellitus/gestational diabetes, or other severe maternal metabolic disorders, and patient's withdrawal from the study. Peripheral blood was antenatally collected on average 3.7 days ahead of birth (Supplemental Table 1). It needs to be mentioned that the first serum sample work-up for MRM analysis was done at the Proteome Center Rostock, Germany. SIS peptide mixtures were prepared at the UVic Genome BC Proteomics Centre, Canada, and sent by post to the Proteome Center Rostock, Germany. The lyophilized peptide mixtures (containing NAT and SIS peptides) were transported at room temperature to the UVic Genome BC Proteomics Centre, Canada, for re-solubilization and subsequent LC-MRM/MS analysis (MS-1). By contrast, the second serum sample work-up was performed at the UVic Genome BC Proteomics Centre, Canada. For this, 10 μl of each serum sample were lyophilized at the Proteome Center Rostock, Germany, and dried proteins were transported at room temperature to the UVic Genome BC Proteomics Centre, Canada, where they were then re-solubilized and worked-up on site, and immediately subjected to LC-MRM/MS analysis (MS-2).

Youden Index Analysis
The procedure is explained using apolipoprotein B100 as example. First, all 30 patient samples were ranked according to their experimentally determined apolipoprotein B100 concentrations (Table 2). Then two theoretical concentration values were added. The first theoretical concentration was determined by subtracting the value "1" from the lowest concentration and the second by adding the value "1" to the highest concentration. These two additional concentration values were added at the top and at the bottom of the protein concentration list, respectively. Then, "test cut-off" values were determined and with each "test cut-off" value it was assessed how many of the samples had protein concentration values below this "test cut-off" value and how many had protein concentration values above that value. Next, it was determined which of the samples were true positives (TP) and which were false positives (FP) by labeling the samples according to clinical assessment data (the "gold standard"). At each "test cut-off" value the Youden index was determined. The highest J value (J max) in the list of samples determined the best discrimination threshold concentration, i.e., the "best cut-off" value within the samples within this data set. This procedure was repeated for all 15 proteins for both, MS-1 and MS-2 data. Ultimately, this process generated 30 tables, in each of which the J max value for the respective protein was indicated (Table 3, Supplemental Table 2).

2.2 Precision Diagnostics by Affinity - Mass Spectrometry: A Novel Approach for Fetal Growth Restriction Screening During Pregnancy

Article

Precision Diagnostics by Affinity—Mass Spectrometry: A Novel Approach for Fetal Growth Restriction Screening During Pregnancy

Charles A. Okai [1], **Manuela Russ** [1], **Manja Wölter** [1,2], **Kristin Andresen** [3], **Werner Rath** [3,4], **Michael O. Glocker** [1,*], **and Ulrich Pecks** [3,*]

1   Proteome Center Rostock, University Medicine and Natural Science Faculty, University of Rostock, 18051 Rostock, Germany; charles.okai@uni-rostock.de (C.A.O.); manuela.russ@med.uni-rostock.de (M.R.); manja.woelter@googlemail.com (M.W.)
2   Department of Obstetrics and Gynecology, Medical Faculty, University of Rostock, Clinic Südstadt, 18059 Rostock, Germany
3   Department of Obstetrics and Gynecology, Medical Faculty, University of Schleswig-Holstein, Campus Kiel, 24105 Kiel, Germany; wrath@ukaachen.de (W.R.); Kristin.Andresen@uksh.de (K.A.)
4   Department of Obstetrics and Gynecology, Medical Faculty, RWTH Aachen University, 52062 Aachen, Germany
*   Correspondence: ulrich.pecks@uksh.de (U.P.); michael.glocker@med.uni-rostock.de (M.O.G.); Tel: +49–431–500–21421 (U.P.); +49–381–494–4930 (M.O.G.); Fax: +49–431–500–21403 (U.P.); +49–381–494–4932 (M.O.G.)

Abstract: Fetal growth restriction (FGR) affects about 3% to 8% of pregnancies, leading to higher perinatal mortality and morbidity. Current strategies for detecting fetal growth impairment are based on ultrasound inspections. However, antenatal detection rates are insufficient and critical in countries with substandard care. To overcome difficulties with detection and to better discriminate between high risk FGR and low risk small for gestational age (SGA) fetuses, we investigated the suitability of risk assessment based on the analysis of a recently developed proteome profile derived from maternal serum in different study groups. Maternal serum, collected at around 31 weeks of gestation, was analyzed in 30 FGR, 15 SGA, and 30 control (CTRL) pregnant women who delivered between 31 and 40 weeks of gestation. From the 75 pregnant women of this study, 2 were excluded because of deficient raw data and 2 patients could not be grouped due to indeterminate results. Consistency between proteome profile and sonography results was obtained for 59 patients (26 true positive and 33 true negative). Of the proteome profiling 12 contrarious grouped individuals, 3 were false negative and 9 were false positive cases with respect to ultrasound data. Both true positive and false positive grouping transfer the respective patients to closer surveillance and thorough pregnancy management. Accuracy of the test is considered high with an area-under-curve value of 0.88 in receiver-operator-characteristics analysis. Proteome profiling by affinity—mass spectrometry during pregnancy provides a reliable method for risk assessment of impaired development in fetuses and consumes just minute volumes of maternal peripheral blood. In addition to clinical testing proteome profiling by affinity-mass spectrometry may improve risk assessment, referring pregnant women to specialists early, thereby improving perinatal outcomes.

Keywords: FGR; SGA; Proteome profiling; Affinity-MS; Pregnancy complications; Apolipoproteins

1. Introduction

Fetal Growth Restriction (FGR) is a pregnancy condition in which the fetus does not reach its genetically given growth potential. It is a major cause of fetal and neonatal morbidity and mortality, affecting about 3% to 8% of all pregnancies [1–3]. Clinically, FGR needs to be distinguished from constitutionally small for gestational age (SGA) fetuses, which represent "physiological smallness" and hence, are not of the same clinical concern. The current standard of detection of FGR and differentiation from SGA is based on ultrasound examinations [1,3,4]. Once identified, FGR pregnancies need intense observation and should be transferred to perinatal specialists to enhance surveillance and if necessary, induce labor to avoid intra-uterine death while balancing against the risk of prematurity.

Antenatal diagnosis has proven to reduce adverse perinatal outcomes and allows for proper and timely referral of the neonate to intensive care [5–7]. However, antenatal detection rates still are sparse and range at about 20–50%, even in high-income countries [8,9]. FGR diagnosis is often made by observation of fetal growth velocity, which can only be confirmed with significant delay in serial ultrasound measurements which are usually timed at least two weeks apart. Most important, the need for ultrasound equipment and highly trained ultrasound specialists limits routine screening for FGR/SGA in pregnant women in many countries, especially in low-income countries [2]. In recent studies, maternal serological biomarkers have been suggested to improve FGR detection rates. Among other biomarkers, soluble Fms-like thyrosinkinase-1 (sFlt-1) and placental growth factor (PlGF) were applied in concert with ultrasound biometry and maternal risk factor estimations to predict FGR outcome [10], indicating that molecular diagnosis improved clinical screening results.

In our recently published proteome profiling studies, using affinity—mass spectrometry with serum from cord blood as well as from maternal peripheral venous blood, we identified apolipoprotein C-II and apolipoprotein CIII protein species as potential candidates from neonates and from pregnant women to differentiate between FGR and CTRL. By use of five candidate proteins, we developed a proteome-based scoring system for the detection of FGR with high confidence [7,11]. However, owing to the aim of our former study to analyze changes in maternal and fetal blood in parallel, the control (CTRL) cohort contained individuals who gave birth prematurely for other reasons than FGR to match the FGR cohort for gestational age. This cohort matching limited interpretation and generalization of the data.

In the present study, we aim at validating in different clinical scenarios the FGR-specific affinity—mass spectrometry-based serum proteome profiling procedure, which we developed [7,11–14]. For this purpose, we challenged the FGR proteome profile by supplementation of our previous cohorts (FGR II and CTRL II) with three further cohorts: 15 patients with severe early onset FGR requiring early delivery before 34 weeks of gestation (FGR I), 15 individuals with uncomplicated pregnancies who gave birth near term (CTRL I) but blood was sampled at similar gestational ages as with cohort FGR I, and 15 donors with otherwise uncomplicated pregnancies, i.e., without features of FGR, classified as SGA by antenatal sonography (SGA I).

2. Materials and Methods

2.1. Patient and Control Individual Cohorts

The study was approved by the Ethics Committee of the Rheinisch-Westfälisch Technische Hochschule (RWTH) Aachen, Germany (EK 138/06, EK 119/08, EK 154/11). Written informed consent was obtained from all participating women. At time of inclusion in the study, sonographic examinations were done to classify patients into study cohorts using Logiq 5 or Voluson 730 Expert Ultrasound Systems (GE Healthcare Systems, Solingen, Germany). The regression equation including biparietal diameter, femur length, as well as head and abdominal circumferences, proposed by Hadlock et al. [15], was used to estimate fetal weight. Fetal and neonatal birth weight percentiles were determined according to the population-based newborn weight charts, as described previously [16]. FGR was defined in accordance with national and international guidelines [3], as described earlier [7,11–13,16]. In addition to having an estimated fetal weight below the 10th

percentile, one of the following criteria had to be fulfilled: (i) deceleration of fetal growth velocity during the last 4 weeks, (ii) elevated resistance index in umbilical artery Doppler sonography above the 95th percentile or absent or reversed end-diastolic blood flow (ARED), (iii) fetal asymmetry (head to abdominal circumference ratio above the 95th percentile), or (iv) oligohydramnios (amniotic fluid index <5 cm). Neonatal weight was assessed post-partum to verify the diagnosis (<10th percentile). Healthy pregnant women with estimated antenatal fetal weight below the 10th percentile and confirmed fetal growth along their percentiles for more than 4 weeks and otherwise normal sonographic findings were classified into the SGA group. Patients with one of the following criteria were excluded from the trial: multiple gestation, fetal anomalies, abnormal fetal karyotype, patients with clinical or biochemical signs of infection, positive TORCH (Toxoplasmosis, Other (syphilis, varicella-zoster, parvovirus B19), Rubella, Cytomegalovirus, and Herpes) screening results, maternal diabetes mellitus/gestational diabetes, other severe maternal metabolic disorders, and patients' withdrawal from the study, as was done previously [7,11–13,17]. The CTRL groups were chosen to best match to the FGR groups for clinical parameters, such as gestational age at blood sampling, BMI, parity, smoking status, and fetal sex. A part of the CTRL group, cohort CTRL II (patient numbers 151–165), *n* = 15, and a part of the FGR group, cohort FGR II (patient numbers 351–365), *n* = 15), have already been analyzed previously [7] and were included again for further developing the method. Then, 45 serum samples from other individuals were added to validate the established FGR proteome profile. Of those, 15 were from individuals with uncomplicated pregnancies with an estimated fetal weight adequate for gestational age; these were referred to as the CTRL I cohort (patient numbers 101–115). Another 15 blood samples were from patients with otherwise uncomplicated pregnancies carrying SGA fetuses; these were referred to as the SGA I cohort (patient numbers 201–215). The third group of 15 individuals with pregnancies with confirmed FGR fetus are referred to as the FGR I cohort (patient numbers 301–315) (Table 1 and Supplemental Table S1).

Table 1. Summarized or averaged demographic data as well as clinical and laboratory parameters for all patients and control individuals.

Parameter	CTRL I (101–115)[i]					CTRL II (151–165)[j]					FGR I (301–315)[i]					FGR II (351–365)[j]					SGA I (201–215)[i]				
	n	Mean	95% CI	Min.	Max.	n	Mean	95% CI	Min.	Max.	n	Mean	95% CI	Min.	Max.	n	Mean	95% CI	Min.	Max.	n	Mean	95% CI	Min.	Max.
Mat. Age (years)[a]	15	29.4	26.5–32.3	21.5	39.2	15	30.5	27.7–33.3	24.2	39.0	15	28.1	25.1-31.1	22.0	41.8	15	30.4	26.8-34.0	19.1	41.5	15	28.9	24.9–32.8	17.6	40.2
Mat. BMI (kg/m²)[b]	15	22.8	21.7–23.9	19.5	26.9	15	23.3	20.4–26.2	17.6	35.7	15	22.2	20.6–23.9	18.0	28.9	15	24.2	22.4–26.1	19.9	31.9	15	22.4	20.6–24.3	16.2	28.1
Primiparity, (%)	15	100.0	n.a.	n.a.	n.a.	15	80.0	n.a.	n.a.	n.a.	15	93.3	n.a.	n.a.	n.a.	15	86.7	n.a.	n.a.	n.a.	15	86.7	n.a.	n.a.	n.a.
Smoking Status, (%)	15	20.0	n.a.	n.a.	n.a.	15	20.0	n.a.	n.a.	n.a.	15	46.7	n.a.	n.a.	n.a.	15	26.7	n.a.	n.a.	n.a.	15	26.7	n.a.	n.a.	n.a.
Systolic bp, (mmHg)[c]	15	115.6	109.2–122.0	99	135	15	116.2	121.1–120.3	106	129	15	120.4	113.6–127.2	96	139	15	130.9	118.6–143.1	83	162	15	117.5	108.9–126.2	84	146
Diastolic bp, (mmHg)[c]	15	68.9	63.1–74.6	54	87	15	64.9	60.5–69.4	53	81	15	69.1	63.6–74.5	52	82	15	77.3	68.2–86.3	52	101	15	66.3	60.2–72.3	45	84
ga at sample, (weeks)[d]	15	29.4	28.3–30.5	25.7	32.6	15	32.4	29.8–35.0	25	39.3	15	29.6	28.3–30.9	25.4	33.9	15	32.3	29.7–34.9	24	40.4	15	31.0	29.3–32.7	22.9	34.6
ga at delivery, (weeks)[d]	15	39.6	38.9–40.3	37.4	41.6	15	32.8	30.2–35.3	25	39.3	15	30.5	29.2–31.8	25.9	34.1	15	33.0	30.5–35.5	26.7	40.4	15	38.1	37.4–38.8	36.1	40.7
Δt (days)[e]	15	71.3	62.7–79.8	50	105	15	2.7	0.01–5.3	0	18	15	6.3	2.1–10.6	0	31	15	4.7	0.95–8.4	0	19	15	49.9	37.1–62.8	22	105
C-section, (%)[f]	15	20.0	n.a.	n.a.	n.a.	15	86.7	n.a.	n.a.	n.a.	15	100.0	n.a.	n.a.	n.a.	15	100.0	n.a.	n.a.	n.a.	15	66.7	n.a.	n.a.	n.a.
Fetal Birth Weight, (g)	15	3399	3232–3565	2960	3765	15	2129	1584–2673	740	3895	15	1015	845–1185	495	1525	15	1383	1005–1761	490	2665	15	2465	2299–2630	1950	2780
fbw Percentile[g]	15	47.1	37.5–56.8	14	70	15	50.7	40.8–60.5	25	85	15	5.2	3.8–6.6	2	9	15	4.0	2.5–5.5	1	9	15	4.5	3.2–5.7	1	9
Female, (%)[h]	15	60.0	n.a.	n.a.	n.a.	15	53.3	n.a.	n.a.	n.a.	15	40.0	n.a.	n.a.	n.a.	15	53.3	n.a.	n.a.	n.a.	15	46.7	n.a.	n.a.	n.a.

(a) mat: maternal age in years determined at the beginning of hospitalization (time point of blood sampling); n.a.: not applicable; (b) pre pregnancy BMI; (c) blood pressure; (d) gestational age; (e) time interval between sample collection and delivery; (f) c: caesarea, mode of delivery; (g) fbw: fetal birth weight; (h) fetal gender; (i) this study; (j) from [7].

*2.2. Blood Collection, Generation, and Storage of Peripheral Blood Serum*

Blood was taken at admission to Hospital without considering special fasting status. Gestational age was calculated from the time point of the last menstrual period and was verified by first trimester ultrasound scan documentation, which is offered routinely in the German Health System between the 10th and the 14th week of gestation (Table 1). Blood samples (up to 9 mL each) were taken antenatally from each individual from the right or left cubital vein using monovette syringes (Serum Z/9 mL; Monovette®, Sarstedt, Germany). After incubation at room temperature for 15–30 min, samples were subjected to sedimentation of blood cells by centrifugation (Labofuge 400R, Fa. Heraeus Instruments, Waltham, MA, USA) at 2000 × g and at room temperature for 15 min [7,11–14,17]. Serum was aspirated, divided into aliquots (100 µL each), and stored at −80 °C. Altogether, time between blood sample collection and storage of frozen serum aliquots averaged around less than 1 h. Frozen serum aliquots were shipped on dry ice to the Proteome Center Rostock.

2.3. Protein Extract Preparation from Peripheral Blood Serum

Serum protein solutions were prepared from frozen serum samples according to established protocols [7,11–14]. In brief, from each thawed serum aliquot, 5 µL were incubated with 10 µL MB-HIC8 "binding buffer" and 5 µL of MB-HIC8 bead slurry for 1 min (Profiling Kit 100 MB-HIC8; Bruker Daltonik, Bremen, Germany). After washing the beads three times with 100 µL of "wash buffer" each, proteins were eluted with 10 µL of "elution buffer", consisting of a 50% ACN solution. The magnetic MB-HIC8 beads with their hydrophobic surfaces enriched apolipoproteins and depleted the most abundant serum proteins, albumin and IgG [7,11–13].

2.4. MALDI-ToF MS Profiling of Serum Proteins and Internal Calibration of Mass Spectra

After extraction from the beads, serum protein-containing solutions (0.5 µL each) were spotted directly onto stainless steel MTP 384 target plates (Bruker Daltonik, Bremen, Germany) together with 0.5 µL ferulic acid solution (10 mg ferulic acid, SigmaAldrich, München, Germany) dissolved in 330 µL ACN/0.1% aqueous TFA (33/67, v/v) as matrix. After drying, 0.5 µL ferulic acid solution was added to each sample spot again and was allowed to dry, as was done previously [7,11–13]. Protein solutions were spotted in duplicate for each patient/donor for recording the first independent set of measurement series MS1 and the second independent set of measurement series MS2 of the same protein extract preparation (Supplemental Table S2). Protein mixtures embedded in the crystallized matrix were analyzed with a Reflex III MALDI TOF mass spectrometer (Bruker Daltonik, Bremen, Germany), which was equipped with a SCOUT source for delayed extraction and was operated in linear positive ion mode using an acceleration voltage of 20 kV. Spectra were recorded in a mass range from 4 to 20 kDa, respectively, accumulating 900 shots per spectrum. Spectra were externally calibrated using a commercially available Protein Calibration Standard (Bruker Daltonik, Bremen, Germany). All mass spectra were internally recalibrated using average masses of ion signals at m/z 6631.6 (singly charged and unmodified apolipoprotein C-I, Uniprot accession number P02654) and m/z 13762.4 (singly charged and unmodified transthyretin, Uniprot accession number P02766). Ion signal areas were determined with the ClinProTools™ 3.0 software (Bruker Daltronik, Bremen, Germany) using the parameters as described previously [7,11–14,18]. Independent measurement series MS1 and MS2 were recorded for protein samples from individuals belonging to cohorts CTRL I, SGA I, and FGR I (in total, 90 mass spectra (Supplemental Table S2)). From individuals belonging to cohorts CTRL II and FGR II, we recorded four measurement series, MS1, MS2, MS3, and MS4, as described previously [7]. In total, from 75 individuals, 210 mass spectra were recorded, to which is referred to as the "full analysis set (FAS)" (Scheme 1 and Supplemental Scheme S1).
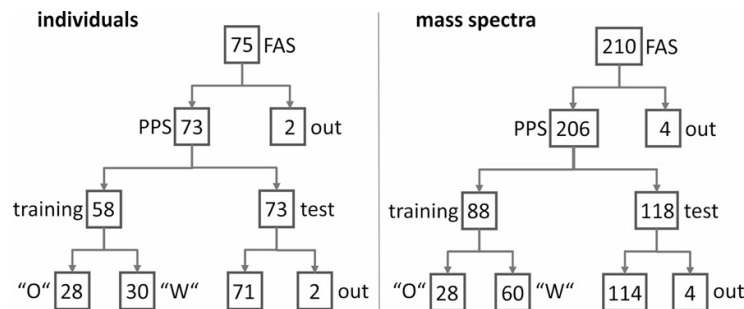
Scheme 1. The use of individual samples and respective mass spectra. Mass spectra which were applied for training sets were not applied in test set analyses. FAS: full analysis set, PPS: per protocol set, "O": training set "O", "W": training set "W", out: individuals or mass spectra that were excluded, test: test set.

The mass spectra of the serum proteins from patient 115 contained very strong ion signals at m/z 11527.0 and m/z 11683.5, corresponding to the protein serum amyloid A1 minus the N-terminal arginyl residue and to full-length serum amyloid A1, respectively [19–21]. These ion signals were absent in all other mass spectra, indicating that this individual's blood protein composition was different from all the others, which was the reason for exclusion. On the other hand, the mass spectra of the serum proteins from patient 315 could not be mass calibrated by the analysis software, although they resembled those of the other patients quite well with respect to ion signal abundances and rough locations of ion signal groups (data not shown). Nevertheless, the mass spectra were excluded as well (Scheme 1 and Supplemental Scheme 1), leaving a "per protocol set (PPS)" of 73 individuals (206 mass spectra).

2.5. Raw Data Processing and Formation of Quotients from Ion Signal Areas

After having determined the areas under each ion signal for each mass spectrum, we applied our established multi-parametric analysis procedure [7,11,18] in which the signal areas of five ion signals, those at m/z 8205, m/z 8766, m/z 8916, m/z 9422, and m/z 9713 (Supplemental Table S2), within each spectrum were brought into context to each other by forming quotients of ion signal areas. The signal area of the ion at m/z 8916 was divided by the signal area of the ion at m/z 8205 from one and the same spectrum to produce a value for spectra assessment (quotient A) as the first assessment value. The signal area of the ion at m/z 8766 over the sum of the signal areas of the ions at m/z 9422 plus m/z 9713 were determined (quotient B) as the second assessment value. The signal area of the ion at m/z 8916 over the sum of the signal areas of the ions at m/z 8766 plus m/z 9422 plus m/z 9713 were determined (quotient C) as the third assessment value. This data processing procedure was applied individually for each of the spectra.

2.6. Youden Index Analyses for Determining Cut-Off Values

To determine "best cut-off" values for quotients A, B, and C (see Raw Data Processing) that can be used to classify an individual spectrum (patient) as either belonging to the FGR I or the CTRL I group, a Youden index analysis was performed [17,22,23]. The first independent measurement series MS1 from both the per protocol set (PPS) for CTRL I ($n = 14$) and FGR I ($n = 14$) were chosen as training set "O" (Scheme 1 and Supplemental Scheme S1). The procedure is explained with quotient A as an example. First, all 28 patient spectra from the PPS were ranked according to their quotient values (Supplemental Table S3). Then, two theoretical quotient A values were added. The first theoretical quotient A value was determined by subtracting the value "1" from the lowest quotient A value and the second by adding the value "1" to the highest quotient A value. These two additional quotient A values were added at the top and the bottom of the quotient A list, respectively. Next, linear interpolation [24] between each pair of two neighboring concentration values was used to determine the "test cut-off" values and with each "test cut-off" value, it was assessed how many of the samples had quotient A values below this "test cut-off"

value and how many had quotient A values above that value. Next, it was determined which of the samples were true positives (TP) and which were false positives (FP) by labeling spectra according to ultrasound assessment data (the "gold standard"). The sensitivity and specificity [25] were calculated for each "test cut-off" point. In addition, at each "test cut-off" value, the Youden index (J = sensitivity + specificity − 1) was determined [17,22,23]. The highest J value (Jmax) in the list of samples determined the best discrimination threshold for the quotient A values, i.e., the "best cut-off" value within the samples within this data set. This procedure was repeated for quotient B and quotient C values accordingly using data from the training set "O" (Supplemental Tables S4 and S5).

2.7. Cumulative Score Assignment

The "cut-off" values of 4.2, 5.0, and 4.0 for quotients A, B, and C, respectively, obtained from training set "O" were combined with the "cut-off" values of 3.4, 7.0, and 5.1 for quotients A, B, and C, respectively, from our previous study (training set "W") [7]. These combined "cut-off" values were then applied to the "validation" test set, which consisted of a second independent measurement series MS2 of the same CTRL I and FGR I sera plus the third and fourth measurement series, MS3 and MS4, of CTRL II and FGR II sera [7]. The following scoring rules were applied: when the quotient value of a specific spectrum (sample) was below or equal to the lower of the two "cut-off" values, a score of "0.0" was assigned. When the quotient value was above the lower of the two "cut-off" values but below or equal to the upper of the two "cut-off" values, a score of "0.5" was assigned. When the quotient value was above the upper of the two "cut-off" values, a score of "1.0" was assigned. This weighting procedure was applied independently to each of the three ion signal ratios A, B, and C for test set "development". Then, the score values of each spectrum from all three ion signal ratios were summed up so that each spectrum (each sample) reached a cumulative score between "0.0" and "3.0".

2.8. Bioinformatic and Biostatistical Analysis

Clinical and biometric data analysis was carried out using the "statistical analysis software, SAS", version 9.1 (SAS Institute, Cary, NC, USA). Clinical data were evaluated by two-way ANOVA analysis of variance and expressed as mean and 95% confidence interval. Differences of serum parameters were tested for significance using the Mann-Whitney *U* test association analyses and Spearman's rank correlation (rho). Graphical representations, such as box-and-whisker plots [26], sensitivity, specificity, and area under the curve from the receiver operator characteristic (ROC) analysis, [27,28] were done using the Origin software (version. 8.1 G; OriginLab Corporation, Northampton, MA; USA). Quotient values A, B, and C of protein ion signal areas were graphically represented in heat maps. Hierarchical clustering was performed based on the complete linkage method and Spearman's correlation coefficient as a measure of similarity. Signal intensities were centered and scaled row-wise for visualization purposes [7,13,29]. Unsupervised principle components analysis (PCA) was performed with quotient values A, B, and C of protein ion signal areas using MATLAB ver. 9.5.0 (R2018b), The MathWorks®, Inc., Natick, MA, USA [29,30]. The first two PCs were selected to project the data into a subspace, which is useful for visualization using the Origin software, and as input for a support vector machine algorithm (SVM). SVM was used to calculate the separation line for the classifier based on PCA projection.

2.9. Power Analysis

A power analysis was carried out [7,12–14] to evaluate the minimally required sample sizes that are needed to discriminate FGR from the CTRL and/or SGA individuals on the basis of the obtained data with the help of the G*Power statistical software (version 3.1.9.2, University of Düsseldorf) [31]. A type I error (α) of 0.05 and a type II error (β) of 0.20 were chosen in a comparison of two means. The minimally required power (1-β error probability) was 0.80.

3. Results

3.1. Patient Cohorts and MALDI Mass Spectrometric Profiling

The University Hospital Aachen is a tertiary care center with a high percentage of high-risk pregnancies. Between August 2006 and November 2011, women with singleton pregnancies attending the Department of Obstetrics and Gynecology for any reason between 24 and 40 weeks of gestation were asked to participate in a prospective observational study for biomarker development for the detection of FGR and preeclampsia. No specific situation was considered, however most of the patients were admitted to the outpatient clinic for routine checks or planning of birth or because of suspected preterm birth, suspected FGR, or suspected preeclampsia. Of the approximately 5000 women who delivered at the University Hospital Aachen during the recruitment period, ca. 10% (531 individuals) agreed to participate in the study. Of those, 167 patients fell into the group of suspected pregnancies with fetal weight below the 10th percentile. In 95 patients, gestational age was 34 weeks and below. Finally, peripheral venous blood samples from 75 Caucasian singleton pregnancies were chosen from the biobank to be subjected to blood serum proteome analysis by affinity—mass spectrometry.

Women with normal pregnancies (cohort CTRL I) delivered healthy infants with adequate for gestational age neonatal weight, i.e., within the 10th and 90th percentile at the expected gestational age of ca. 40 weeks, and hence, represented the general population. The mean time difference between blood sampling and delivery was 71 days. Eleven of the 15 women from cohort CTRL II delivered preterm for various reasons (premature rupture of the membrane, spontaneous onset of labor, vaginal bleeding). The mean time difference between blood sampling and delivery was 3 days. From the FGR I cohort all 15 women and from the FGR II cohort, 13 out of 15 women needed mandatory preterm delivery for non-reassuring fetal well-being. The mean time difference between blood sampling and delivery was 5 and 6 days, respectively. The mean days SGA babies (cohort SGA I) were born after blood sampling was 50 days. Maternal age, BMI, and blood pressure did not differ significantly between groups, as indicated by the overlap of 95% CI. Most of the women in all groups were primiparous. Women within the newly added FGR I cohort were more likely to smoke. As per definition, birth-weight percentiles differed significantly between the FGR/SGA and CTRL groups, as indicated by the non-overlap of the 95% confidence interval (Table 1 and Supplemental Table S1).

Following our standardized protocol for producing protein solutions out of blood samples, on average, about 60 protein ion signals were reproducibly recorded in each mass spectrum within a mass range of m/z 4000 to m/z 20000 (Figure 1). The most prominent ion signals were observed in the mass range between m/z 8000 and m/z 10000 (Figure 1, insert), correlating to singly charged (protonated) ion signals of small proteins. The ion signals of which their areas were used for bio-statistical analysis were, as in our previous study [7,11], from apolipoprotein CII (m/z 8205), pro-apolipoprotein CII (m/z 8916), apolipoprotein $CIII_0$ (m/z 8766), apolipoprotein $CIII_1$ (m/z 9422), and apolipoprotein $CIII_2$ (m/z 9713).
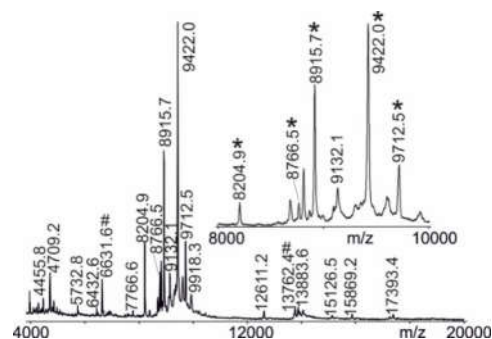

Figure 1. Affinity—MALDI-ToF mass spectrum of intact protein ions. Proteins are from maternal peripheral venous blood serum upon work-up with ClinProt® beads. Ion signals that are selected for

multi-parametric analysis are labeled with "*****" (see insert). Ion signals that are used for internal re-calibration are marked with "#". Ferulic acid is used as the matrix.

The MALDI-ToF mass spectra from proteins of FGR, CTRL, and SGA serum samples displayed high similarities to each other, indicating that relative quantitative differential analysis of ion signal intensities, and of quotients thereof, was feasible. Exceptions were mass spectra from patients 115 and 315, respectively. These were excluded from further analysis to leave a PPS with 206 mass spectra from 73 individuals (Scheme 1).

3.2. Determination of "Best Cut-Off" Values for Quotients A, B, and C to Separate FGR from CTRL

Areas of the five selected ion signals were determined and brought into context with each other following the previously introduced rules, thereby generating quotients A, B, and C. Then, "best cut-off" values for quotients A, B, and C were to be applied in our assay to assign a given mass spectrum (patient sample) to one of the clinical groups, i.e., FGR, SGA, or CTRL. However, because the serum protein composition of the CTRL I cohort was not yet investigated, we decided not to use the "best cut-off" values from our previous study [7], although quotients A, B, and C were determined in the same way as before, using the areas of the same ion signals as was done previously. Instead, we generated a training set "O", which contained 14 mass spectra for CTRL I (series MS1) and 14 mass spectra for FGR I (series MS1) (Supplemental Table S2 and Supplemental Scheme S1). Jmax values indicated the "best cut-off" values of 4.2, 5.0, and 4.0 for quotients A, B, and C, respectively (Supplemental Tables 3–5). Next, the cumulative score for each mass spectrum was calculated according to previously established rules: a score of "1" was assigned to this respective spectrum (sample) when the quotient value of this specific spectrum (sample) was higher than the respective "best cut-off" value. In the contrary case, the score for this spectrum (sample) was set to "0". These assessments were again independently carried out for each of the three ion signal ratios and for each spectrum. In sum, each sample reached a cumulative score between "0" and "3", as was the case in our previous study [7].

Of note, the cumulative score discriminator was kept at 1.0, meaning a cumulative score below or equal to 1.0 assigned a given mass spectrum to the CTRL group and a cumulative score above 1.0 to the FGR group. For training set "O", the distribution of cumulative scores (Figure 2) revealed that one of the 14 FGR spectra were wrongly assigned to the CTRL group and one of the 14 CTRL spectra were wrongly placed in the FGR group.
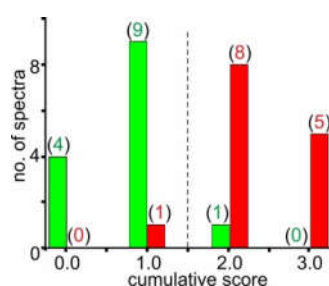

Figure 2. Distribution pattern of cumulative scores with training set "O". Cumulative score values range between "0.0" and "3.0". Spectra of training set "O" (first measurement series, MS1, of CTRL I and FGR I serum samples; *n* = 28) are represented. Green bars represent spectra of CTRL I (patients 101–114) and red bars represent spectra of FGR I (patients 301–314, see Supplemental Table S2). Numbers in parentheses indicate numbers of spectra with the respective cumulative score. The vertical dashed line marks the cumulative score cut-off value which sorts the spectra, which is the respective samples, into either the FGR group (right) or the CTRL group (left).

Accordingly, excellent bio-statistical results were obtained, i.e., sensitivity was 0.93 and specificity was 0.93. Hence, an area under curve (AUC) in the receiver-operator characteristics (ROC) analysis of 0.95 was reached (Table 2). The cumulative score distribution was applied for

power analysis investigations, which showed that the required minimal sample size was 3 FGR and 3 CTRL mass spectra to reach a statistically meaningful separation of the two groups (Supplemental Table S6).

Table 2. Summary of biostatistic evaluation of individual patients [a].

No	Type of Data Set/Cohort	TP	FP	TN	FN	Sens	Spec	FPR	FNR	PPV	NPV	ROC AUC
1	**training "O"/CTRL I vs. FGR I** (CTRL I, *n* = 14; FGR I, *n* = 14) [b]	13	1	13	1	0.93	0.93	0.07	0.07	0.93	0.93	0.95
2	**"development" test/CTRL I + II vs. FGR I + II** (CTRL, I + II, *n* = 28; FGR I + II, *n* = 29) [c]	26	6	22	3	0.90	0.79	0.21	0.10	0.81	0.88	0.88
3	**"valid" test/CTRL I + II and SGA I vs. FGR I + II** (CTRL I + II, *n* = 28; SGA I, *n* = 14; FGR I + II, *n* = 29) [c]	26	9	33	3	0.90	0.79	0.21	0.10	0.74	0.92	0.88

(a) cumulative score separator: > 1 = FGR; ≤ 1 = CTRL; (b) no. of mass spectra; Jmax determined cut-off values; c) no. of patients; combined cut-off values; TP: true positive; FP: false positive; TN: true negative; FN: false negative; sens: sensitivity; spec: specificity; FPR: false positive rate; FNR: false negative rate; PPV: positive predictive value; NPV: negative predictive value; ROC: receiver operating characteristic; AUC: area under the curve.

3.3. Combination of "Best Cut-Off" Values and Weighting of Cumulative Scores for Separating FGR from CTRL

Since the "best cut-off" values of 4.2, 5.0, and 4.0 for quotients A, B, and C, respectively, which were obtained in this study with training set "O", were somewhat different from those "best cut-off" values of 3.4, 7.0, and 5.1 for quotients A, B, and C, respectively, from our previous study (training set "W") [7], we decided to apply both sets of "best cut-off" values in combination when analyzing the test sets. The "development" test set (Supplemental Scheme S1) contained mass spectra from CTRL I (series MS2) and from FGR I (series MS2) as well as spectra from CTRL II (series MS3 and MS4) and from FGR II (series MS3 and MS4), summing up to 42 mass spectra for CTRL (28 women) and 44 mass spectra for FGR (29 patients). The quotient value distributions were found to be distinctive, such that the values for quotients A, B, and C were generally higher in the FGR group as compared to those of the CTRL group (Figure 3).
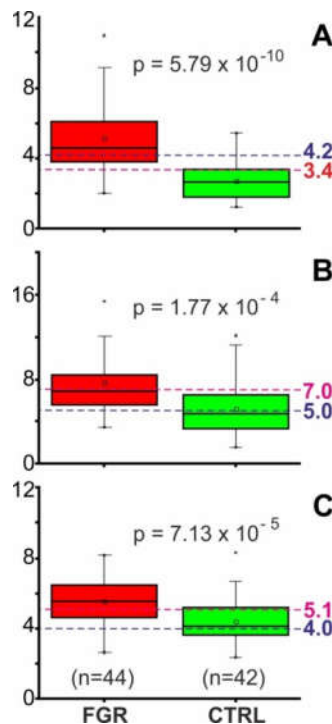
Figure 3. Distribution of quotient values for selected ion intensity differences of the "development" test set. Quotient values distributions are shown as box and whisker plots (second measurement series, MS2, of CTRL I and FGR I plus third and fourth measurement series, MS3 and MS4, of CTRL II and FGR II serum samples, $n = 86$). (**A**) Signal area of the ion at m/z 8916 over the signal area of the ion at m/z 8205. (**B**) Signal area of the ion at m/z 8766 over the sum of the signal areas of ions at m/z 9422 plus m/z 9713. (**C**) Signal area of the ion at m/z 8916 over the sum of signal areas of ions at m/z 8766 plus m/z 9422 plus m/z 9713. The boxes represent the 25th–75th percentiles. The horizontal lines within the boxes represent the medians; the small squares indicate the means. The whiskers specify the 5th and 95th percentiles and the crosses indicate the 1st and 99th percentiles. Dashed lines mark selected cut-off values. Cut-off values for the quotients are (**A**) 3.4 and 4.2, (**B**) 5.0 and 7.0, (**C**) 4.0 and 5.1. FGR, fetal growth restriction; CTRL, control individuals.

Since the application of two "best cut-off" values per quotient generated three value regimes (below—in between—above), the score of a mass spectrum was assigned "0.0" when falling into the regime "below", "0.5" when "in between", and "1.0" when "above". Accordingly, the cumulative score values of each spectrum, summed up from all three ion signal ratios, ranged between "0.0" and "3.0" with steps of 0.5. Keeping the cumulative score discriminator at 1.0, as was done above and in our previous studies, decided whether a given mass spectrum was assigned to the CTRL group or to the FGR group.

Using quotient values A, B, and C from the "development" test set separated the FGR group (n = 44) from the CTRL group (n = 42) quite satisfactorily by hierarchical clustering (Figure 4), confirming that the ion signal abundances of five proteins were carrying the requested information for differentiating FGR from CTRL with good confidence. Duplicate measurements from FGR samples are clearly sorted to the FGR group (right) and control samples to the CTRL group (left), except for FGR samples 302, 304, 310, 312, and 364 (one measurement each), which are allocated to the CTRL group, and CTRL samples 151 (both measurements) and 164 (one measurement) are grouped to the FGR group.
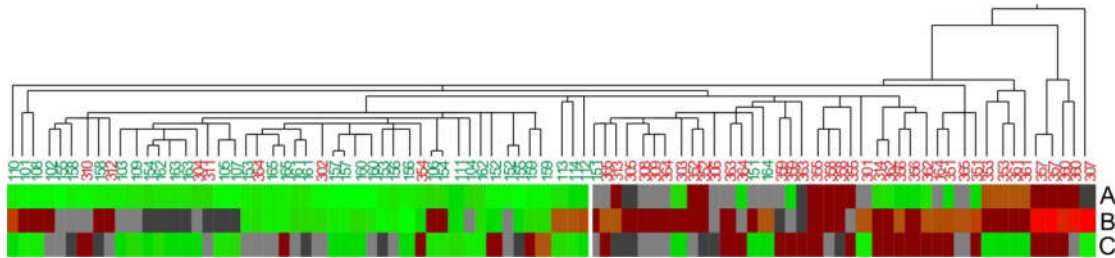
Figure 4. Hierarchical clustering analysis with quotient values A, B, and C of protein ion signal areas of the "development" test set. This set contains the second measurement series, MS2, of CTRL I and FGR I plus the third and fourth measurement series, MS3 and MS4, of CTRL II and FGR II serum samples (*n* = 86). Quotients A to C are arranged from top to bottom. Color code for the quotient values; red: high values; brown: medium high; grey: medium low; green: low. Patient numbering is as in Supplemental Tables S1 and S2.

Bio-statistic evaluation of the "development" test set performance revealed a false positive rate of 0.21 and a false negative rate of 0.10. Hence, an area under curve (AUC) in the receiver-operator characteristics (ROC) analysis of 0.88 was reached (Table 2). The cumulative score distribution was applied for power analysis investigations, which showed that the required minimal sample size was 9 FGR and 9 CTRL mass spectra to reach a statistically meaningful separation of the two groups (Supplemental Table S6).

3.4. Application of "Weighted Cumulative Scores" for Separating FGR from CTRL and from SGA

Encouraged by the separation power with which pregnant women whose fetuses suffered from FGR could be distinguished from CTRL individuals whose pregnancies were unaffected, solely based on ion signal abundances of serum proteins as recorded in MALDI mass spectra, we generated a "validation" test set (Scheme 1 and Supplemental Scheme S1) which contained 118 mass spectra from three different patient/donor groups (73 individuals). Because of indeterminate results, 4 mass spectra (patients 155 and 213) were excluded, leaving 114 mass spectra (71 individuals) for the biostatistics analysis. The FGR group contained 44 mass spectra (29 patients), 14 from cohort FGR I (series MS2) and 30 from cohort FGR II (series MS3 and MS4). The CTRL group contained 42 mass spectra (28 individuals), 14 from cohort CTRL I (series MS2) and 28 from cohort CTRL II (series MS3 and MS4). The SGA group contained 28 mass spectra (series MS 1 and MS2) from cohort SGA I (14 patients). The analysis procedure followed what was described above for the "development" test set and started with determining the quotient values A, B, and C, respectively.

Subjecting the quotient values (in total, 342 values) to Principal Component Analysis (PCA) afforded two well separated clusters. The first and second centered PCs of the quotient data yielded 48.6% (PC1) and 27.5% (PC2) of the total variances, respectively. The decision boundary, which was obtained from the SVM classifier, separated both clusters with the exceptions of FGR samples 301 and 302, which were placed on the CTRL side. Likewise, CTRL sample 164 was placed on the FGR side. It should be mentioned that SGA individuals clustered with the CTRL donors and, hence, were separated from FGR patients with good confidence (Figure 5).
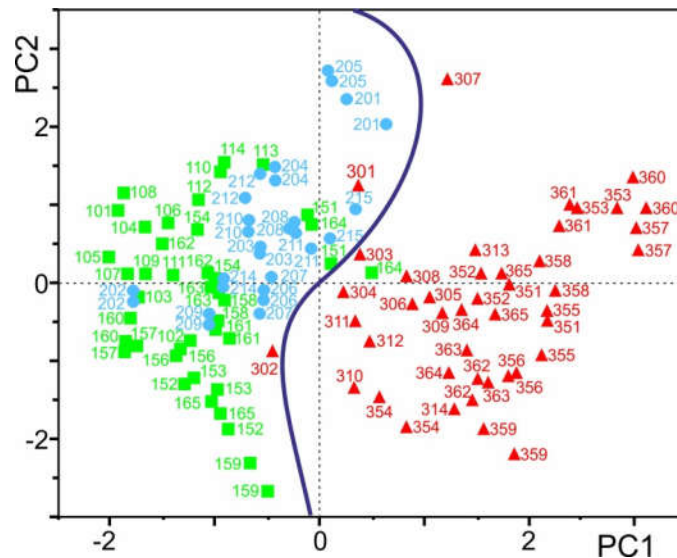
Figure 5. Principle component analysis with quotient values A, B, and C of protein ion signal areas of the "validation" test set. This set contains measurement series MS2 of cohorts CTRL I and FGR I plus measurement series MS3 and MS4 of cohorts CTRL II and FGR II, in addition to measurement series MS1 and MS2 of cohort SGA I serum samples (*n* = 114) which represent 71 individuals. Locations of mass spectra derived positioning from FGR samples are shown as red triangles, locations of CTRL samples as green squares, and SGA patients as blue circles (filled symbols). The curved line indicates the decision boundary obtained from the support vector machine (SVM) algorithm classifier.

In agreement with the obtained PCA results, good separation was achieved with the cumulative score discriminator of 1.0 as well. From the 71 individuals (114 mass spectra) of the "validation" test set, 59 were assigned correctly (26 TP and 33 TN), i.e., their grouping stood in agreement with the clinical assignment which served as the "gold standard". The positive predictive value was 0.74 and the negative predictive value 0.92, hence an area under curve (AUC) in the receiver-operator characteristics (ROC) analysis of 0.88 was reached (Table 2). The cumulative score distribution was applied for power analysis investigations, which showed that the required minimal sample size was 5 FGR and 5 CTRL/SGA mass spectra to reach a statistically meaningful separation of the two groups (Supplemental Table S6).

4. Discussion

The aim of the present study was to establish a blood-based biomarker test to detect FGR and to distinguish from constitutional SGA that is robust, simple, and easily available and may be added to current clinical practice to improve detection rates. The study took advantage of an existing biobank in which patients with suspected SGA/FGR and CTRL were included and well characterized by antenatal ultrasound inspection. Maternal serum proteins were analyzed by affinity mass spectrometry at the time point of admission to hospital. Our test discriminated between FGR and SGA as well as pregnancies unaffected by FGR, i.e., CTRL, with good confidence. The use of two cut-off values for each quotient of ion signal areas opened three value regimes: below—in between—above cut-offs. Despite differing from rather routinely used two value regimes (below—above cut-offs) for separation of samples/individuals, separation of FGR from CTRL/SGA was successfully employed. Examples of other clinical studies in which it was found that a three value regime was suitable for fulfilling the task to separate two conditions are "early risk prognosis of free-flap transplant failure", "MGMT promoter methylation for selecting glioblastoma patients into trials omitting Temozolomide", and "diagnostic criteria for high-dimensional metabolic data in newborn screening for medium-chain acyl-CoA dehydrogenase deficiency" [22,32,33], but also with sFlt-1/PlGF ratio (<38 and >85) [34,35] and PlGF measurements alone to predict still-birth FGR (<12 and >100) [36].

Our study is limited by the small sample size. Moreover, a selection bias of samples taken from the biobank cannot be excluded. Selection of suitable control groups for "case-control" clinical studies is very important and sometimes critical for the distinguishing ability of the assay [37,38]. Since it is known that maternal blood protein compositions change in complexity and abundance with advancing gestational age [39–41], such reasoning becomes critical with any blood protein-based assay that shall find application in pregnant women. Adaptation of cut-off values depending on gestational age has already found application in point-of-care diagnostics, which is based on abundance ratios of molecular markers found in maternal blood [42].

Strengths of our study are the well characterized patient cohorts and the application of multiparametric mass spectrometry measurements. A combination of marker proteins, i.e., angionenic factors and acute-phase proteins in serum samples, was found to yield in good discrimination of HELLP and preeclampsia from control [43]. The need for accumulating markers for screening purposes sooner or later may request to move away from immunoanalytical assays, such as ELISAs, and orient towards screening systems with inherent multiplexing capabilities. Affinity—mass spectrometry, as performed here, enables parallel analysis of dozens of proteins and accurate determination of relative protein abundances as well as ratios of, for example, differently modified protein species, which allow to differentiate varying glycosylation and other post-translational modifications simply by mass, but which may be difficult to detect and/or to differentiate by conventional antibody assays [18].

Current state of the art FGR detection is based on ultrasound assessment. However, even in high-income countries, like Germany, in which antenatal ultrasound is offered most frequently and usually routinely more than 3 times during pregnancy, FGR detection rate ranges between about 20–50% [8,9]. A high percentage of undetected cases lead to sub-standard care, stillbirth, and increased risk of perinatal mortality and morbidity. Moreover, diagnosis is often delayed because estimating fetal growth velocity needs to be performed at two different time points during pregnancy, which take place at least 14 days apart [44]. Diagnosis requires both availability of ultrasound equipment and ultrasound trained specialists [1,2,45]. Although stillbirth remains an important clinical issue for high-income countries, the majority of cases occur in low- and middle-income countries where ultrasound inspection is hardly available. Currently used clinical tests in these countries, such as measurement of symphysis-fundal height, may have even lower sensitivity and specificity for the identification of SGA infants—the primary step in diagnosing FGR—than ultrasound assessments [46]. Since ultrasound-based investigations obviously lack power, effort has been given to improve diagnosis, for example, by adding single marker proteins, such as PlGF-measurements, to standard care. The PELICAN trial aimed at evaluating the diagnostic accuracy of PlGF in women with suspected preeclampsia. They also challenged PlGF measurements for detecting SGA with birth weight below the 1st percentile. Using a PlGF cut-off below the 5th percentile for gestational age sensitivity ranged between 0.91 to 0.93, and specificity between 0.51 and 0.53 (before or after 35 weeks of gestation, respectively), resulting in a high degree of false positive classified patients [47]. Similarly, Benton et al. challenged PlGF measurements in 219 patients with antenatally suspected FGR defined as a fetal abdominal circumference (AC) <10th percentile for gestational age on ultrasound. In their cohorts from Canada, New Zealand, and the United Kingdom, which also included samples of the PELICAN trial, they found a sensitivity of 0.98 and a specificity of 0.75 for the antenatal identification of FGR using the 5th percentile of PlGF as a cut-off. They also highlighted that PlGF levels correlate with the degree of placental pathology in these patients [48]. Likewise, the addition of sFlt-1 to PlGF measurement has been suggested for the detection of high-risk pregnancies. An sFlt-1/PlGF ratio below 38 has been proven to be capable for ruling out pathologic pregnancies like preeclampsia [34,35]. In FGR pregnancies, sFlt-1/PlGF ratios are increased [34] and in a recent observational trial, Quezada et al. reported sFlt-1/PlGF ratios above 85 in 75% of patients with diagnosed FGR [49]. In the study of Visan et al., the combination of sFLT1/PlGF ratio at a cut-off of 38 to ultrasound-based estimation of fetal weight <10th percentile led to an increase in sensitivity for the detection of FGR from 44.4% to 84.2%, with a change in specificity from 89% to 84.3%, with a false-positive rate of 10% [10].

Similar to others, with our assay, we found a relatively higher rate (9 out of 71) of false positive classified patients with respect to ultrasound data ("gold standard"). A high false positive rate causes unnecessary anxiety of pregnant women and increases rates of intervention. Yet, time of uncertainty can be considered rather short (approximately 3–4 days) as in true positive cases, delivery is expected to take place rather soon after testing. Hence, if pregnancy continues for more than 5 days after testing, a repeated test may be scheduled to confirm or falsify the primary test result.

Obviously, earlier confirmation of placental dysfunction in suspected fetal growth restriction has the potential to improve risk stratification and earlier access to targeted surveillance. More studies combining ultrasound and blood-borne biomarkers are needed to determine whether this approach improves diagnostic accuracy over the use of ultrasound estimation of fetal size or biochemical markers of placental dysfunction alone [50]. Our multiparametric affinity—mass spectrometry test may aid in screening and in decision-making processes, e.g., to refer patients to ultrasound specialists, especially in rural areas with sub-standard care.

5. Conclusions

In conclusion, we have developed an affinity—mass spectrometry-based biomarker test for the detection of FGR in pregnant women, which was challenged against the actual gold standard of antenatal ultrasound-based diagnosis. Our approach allows for a multi-marker-based screening in a single blood test, which has been proven to be robust and easy to perform and allows FGR risk assessment with high confidence. The combination of this blood test with clinical examination offers a promising means for better antenatal care, which shall be further evaluated in follow-up multi-centric studies.

Supplementary Materials: The following are available online at www.mdpi.com/2077-0383/9/5/1374/s1, Scheme S1: Disease groups and patient cohorts; Table S1: Demographic Data, Clinical and Laboratory Parameters for all Patients and Control Individuals; Table S2: Areas of ion signals selected for scoring; Table S3: Determination of Youden Index (Jmax) for Quotient A; Table S4: Determination of Youden Index (Jmax) for Quotient B; Table S5: Determination of Youden Index (Jmax) for Quotient C; Table S6: Power analysis of mass spectrometric ion signal-derived proteome profile series.

Author Contributions: Conceptualization, W.R., U.P., and M.O.G.; methodology, C.A.O., M.R., M.W., and M.O.G.; validation, C.A.O., M.R., U.P., and M.O.G.; formal analysis, C.A.O., M.R., U.P., and M.O.G.; investigation, C.A.O., M.R., U.P., and M.O.G.; resources, W.R., U.P., and M.O.G.; data curation, C.A.O., M.W., U.P., and M.R.; writing—original draft preparation, C.A.O., U.P., K.A., and M.O.G.; visualization, U.P. and M.O.G.; supervision, U.P., W.R., and M.O.G.; project administration, K.A., U.P., and M.O.G.; funding acquisition, U.P., W.R., and M.O.G. All authors have read and agreed to the published version of the manuscript.

Conflicts of Interest: The authors declare no conflict of interest.

Abbreviations

ACOG: American College of Obstetricians and Gynecologists
MALDI ToF MS: Matrix-Assisted Laser Desorption/Ionization Time of Flight Mass Spectrometry
m/z: mass to charge ratio

References

1. American College of Obstetricians and Gynecologists. ACOG Practice Bulletin No. 204: Fetal Growth Restriction. *Obstet. Gynecol.* **2019**, *133*, e97–e109, doi:10.1097/AOG.0000000000003070.

2. Figueras, F.; Gratacos, E. Update on the diagnosis and classification of fetal growth restriction and proposal of a stage-based management protocol. *Fetal Diagn. Ther.* **2014**, *36*, 86–98, doi:10.1159/000357592.

3. Kehl, S.; Dotsch, J.; Hecher, K.; Schlembach, D.; Schmitz, D.; Stepan, H.; Gembruch, U. Intrauterine Growth Restriction. Guideline of the German Society of Gynecology and Obstetrics (S2k-Level, AWMF Registry No. 015/080, October 2016). *Geburtshilfe Und Frauenheilkd.* **2017**, *77*, 1157–1173, doi:10.1055/s-0043-118908.

4. Mazarico, E.; Martinez-Cumplido, R.; Diaz, M.; Sebastiani, G.; Ibanez, L.; Gomez-Roig, M.D. Postnatal Anthropometric and Body Composition Profiles in Infants with Intrauterine Growth Restriction Identified by Prenatal Doppler. *PLoS ONE* **2016**, *11*, e0150152, doi:10.1371/journal.pone.0150152.

5. Figueras, F.; Gardosi, J. Intrauterine growth restriction: New concepts in antenatal surveillance, diagnosis, and management. *Am. J. Obstet. Gynecol.* **2011**, *204*, 288–300, doi:10.1016/j.ajog.2010.08.055.

6. Gardosi, J. Customized charts and their role in identifying pregnancies at risk because of fetal growth restriction. *J. Obstet. Gynaecol. Can. JOGC J. D'Obstet. Gynecol. Du Can. JOGC* **2014**, *36*, 408–415, doi:10.1016/S1701-2163(15)30587-9.

7. Wölter, M.; Röwer, C.; Koy, C.; Rath, W.; Pecks, U.; Glocker, M.O. Proteoform profiling of peripheral blood serum proteins from pregnant women provides a molecular IUGR signature. *J. Proteom.* **2016**, *149*, 44–52, doi:10.1016/j.jprot.2016.04.027.

8. Jayawardena, L.; Sheehan, P. Introduction of a customised growth chart protocol increased detection of small for gestational age pregnancies in a tertiary Melbourne hospital. *Aust. N. Z. J. Obstet. Gynaecol.* **2019**, *59*, 493–500, doi:10.1111/ajo.12902.

9. Ernst, S.A.; Brand, T.; Reeske, A.; Spallek, J.; Petersen, K.; Zeeb, H. Care-Related and Maternal Risk Factors Associated with the Antenatal Nondetection of Intrauterine Growth Restriction: A Case-Control Study from Bremen, Germany. *Biomed Res. Int.* **2017**, *2017*, 1746146, doi:10.1155/2017/1746146.

10. Visan, V.; Scripcariu, I.S.; Socolov, D.; Costescu, A.; Rusu, D.; Socolov, R.; Avasiloaiei, A.; Boiculese, L.; Dimitriu, C. Better prediction for FGR (fetal growth restriction) with the sFlt-1/PlGF ratio: A case-control study. *Medicine* **2019**, *98*, e16069, doi:10.1097/MD.0000000000016069.

11. Wölter, M.; Russ, M.; Okai, C.A.; Rath, W.; Pecks, U.; Glocker, M.O. Comparison of blood serum protein analysis by MALDI-MS from either conventional frozen samples or storage disc-deposited samples: A study with human serum from pregnant donors and from patients with intrauterine growth restriction. *Eur. J. Mass Spectrom.* **2019**, *25*, 381–390, doi:10.1177/1469066718820991.

12. Pecks, U.; Kirschner, I.; Wölter, M.; Schlembach, D.; Koy, C.; Rath, W.; Glocker, M.O. Mass spectrometric profiling of cord blood serum proteomes to distinguish infants with intrauterine growth restriction from those who are small for gestational age and from control individuals. *Transl. Res. J. Lab. Clin. Med.* **2014**, *164*, 57–69, doi:10.1016/j.trsl.2013.12.003.

13. Wölter, M.; Röwer, C.; Koy, C.; Reimer, T.; Rath, W.; Pecks, U.; Glocker, M.O. A proteome signature for intrauterine growth restriction derived from multifactorial analysis of mass spectrometry-based cord blood serum profiling. *Electrophoresis* **2012**, *33*, 1881–1893, doi:10.1002/elps.201200001.

14. Pecks, U.; Seidenspinner, F.; Röwer, C.; Reimer, T.; Rath, W.; Glocker, M.O. Multifactorial analysis of affinity-mass spectrometry data from serum protein samples: A strategy to distinguish patients with preeclampsia from matching control individuals. *J. Am. Soc. Mass Spectrom.* **2010**, *21*, 1699–1711, doi:10.1016/j.jasms.2009.12.013.

15. Hadlock, F.P.; Harrist, R.B.; Sharman, R.S.; Deter, R.L.; Park, S.K. Estimation of fetal weight with the use of head, body, and femur measurements—A prospective study. *Am. J. Obstet. Gynecol.* **1985**, *151*, 333–337, doi:10.1016/0002-9378(85)90298-4.

16. Pecks, U.; Brieger, M.; Schiessl, B.; Bauerschlag, D.O.; Piroth, D.; Bruno, B.; Fitzner, C.; Orlikowsky, T.; Maass, N.; Rath, W. Maternal and fetal cord blood lipids in intrauterine growth restriction. *J. Perinat. Med.* **2012**, *40*, 287–296, doi:10.1515/jpm.2011.135.

17. Wölter, M.; Okai, C.A.; Smith, D.S.; Russ, M.; Rath, W.; Pecks, U.; Borchers, C.H.; Glocker, M.O. Maternal Apolipoprotein B100 Serum Levels are Diminished in Pregnancies with Intrauterine Growth Restriction and Differentiate from Controls. *Proteom. Clin. Appl.* **2018**, *12*, e1800017, doi:10.1002/prca.201800017.

18. Glocker, M.O.; Röwer, C.; Wölter, M.; Koy, C.; Reimer, T.; Pecks, U. Multiparametric Analysis of Mass Spectrometry-Based Proteome Profiling in Gestation-Related Diseases. In *Handbook of Spectroscopy*, 2nd ed.; Gauglitz, G., Moore, D.S., Eds.; Wiley-VCH Verlag GmbH & Co. KGaA, Weinheim, Germany: 2014; pp. 407–428, doi:10.1002/9783527654703.ch12.

19. Kiernan, U.A.; Tubbs, K.A.; Nedelkov, D.; Niederkofler, E.E.; Nelson, R.W. Detection of novel truncated forms of human serum amyloid A protein in human plasma. *FEBS Lett.* **2003**, *537*, 166–170, doi:10.1016/s0014-5793(03)00097-8.

20. Koy, C.; Heitner, J.C.; Woisch, R.; Kreutzer, M.; Serrano-Fernandez, P.; Gohlke, R.; Reimer, T.; Glocker, M.O. Cryodetector mass spectrometry profiling of plasma samples for HELLP diagnosis: An exploratory study. *Proteomics* **2005**, *5*, 3079–3087, doi:10.1002/pmic.200402098.

21. Nelsestuen, G.L.; Zhang, Y.; Martinez, M.B.; Key, N.S.; Jilma, B.; Verneris, M.; Sinaiko, A.; Kasthuri, R.S. Plasma protein profiling: Unique and stable features of individuals. *Proteomics* **2005**, *5*, 4012–4024, doi:10.1002/pmic.200401234.

22. Yang, J.; Finke, J.C.; Yang, J.; Percy, A.J.; von Fritschen, U.; Borchers, C.H.; Glocker, M.O. Early risk prognosis of free-flap transplant failure by quantitation of the macrophage colony-stimulating factor in patient plasma using 2-dimensional liquid-chromatography multiple reaction monitoring-mass spectrometry. *Medicine* **2016**, *95*, e4808, doi:10.1097/MD.0000000000004808.

23. Youden, W.J. Index for rating diagnostic tests. *Cancer* **1950**, *3*, 32–35.

24. Davis, P.J. *Interpolation and Approximation*; Courier Corporation, Chelmsford, Massachusetts, USA: 1975.

25. Metz, C.E. Basic principles of ROC analysis. *Semin. Nucl. Med.* **1978**, *8*, 283–298.

26. Benjamini, Y. Opening the box of a boxplot. *Am. Stat.* **1988**, *42*, 257–262.

27. Faraggi, D.; Reiser, B. Estimation of the area under the ROC curve. *Stat. Med.* **2002**, *21*, 3093–3106, doi:10.1002/sim.1228.

28. Greiner, M.; Pfeiffer, D.; Smith, R.D. Principles and practical application of the receiver-operating characteristic analysis for diagnostic tests. *Prev. Vet. Med.* **2000**, *45*, 23–41.

29. Röwer, C.; Koy, C.; Hecker, M.; Reimer, T.; Gerber, B.; Thiesen, H.J.; Glocker, M.O. Mass spectrometric characterization of protein structure details refines the proteome signature for invasive ductal breast carcinoma. *J. Am. Soc. Mass Spectrom.* **2011**, *22*, 440–456, doi:10.1007/s13361-010-0031-6.

30. Röwer, C.; Vissers, J.P.; Koy, C.; Kipping, M.; Hecker, M.; Reimer, T.; Gerber, B.; Thiesen, H.J.; Glocker, M.O. Towards a proteome signature for invasive ductal breast carcinoma derived from label-free nanoscale LC-MS protein expression profiling of tumorous and glandular tissue. *Anal. Bioanal. Chem.* **2009**, *395*, 2443–2456, doi:10.1007/s00216-009-3187-9.

31. Faul, F.; Erdfelder, E.; Lang, A.G.; Buchner, A. G*Power 3: A flexible statistical power analysis program for the social, behavioral, and biomedical sciences. *Behav. Res. Methods* **2007**, *39*, 175–191.

32. Hegi, M.E.; Genbrugge, E.; Gorlia, T.; Stupp, R.; Gilbert, M.R.; Chinot, O.L.; Nabors, L.B.; Jones, G.; Van Criekinge, W.; Straub, J.; et al. MGMT Promoter Methylation Cutoff with Safety Margin for Selecting Glioblastoma Patients into Trials Omitting Temozolomide: A Pooled Analysis of Four Clinical Trials. *Clin. Cancer Res. Off. J. Am. Assoc. Cancer Res.* **2019**, *25*, 1809–1816, doi:10.1158/1078-0432.CCR-18-3181.

33. Ho, S.; Lukacs, Z.; Hoffmann, G.F.; Lindner, M.; Wetter, T. Feature construction can improve diagnostic criteria for high-dimensional metabolic data in newborn screening for medium-chain acyl-CoA dehydrogenase deficiency. *Clin. Chem.* **2007**, *53*, 1330–1337, doi:10.1373/clinchem.2006.081802.

34. Rana, S.; Powe, C.E.; Salahuddin, S.; Verlohren, S.; Perschel, F.H.; Levine, R.J.; Lim, K.H.; Wenger, J.B.; Thadhani, R.; Karumanchi, S.A. Angiogenic factors and the risk of adverse outcomes in women with suspected preeclampsia. *Circulation* **2012**, *125*, 911–919, doi:10.1161/CIRCULATIONAHA.111.054361.

35. Zeisler, H.; Llurba, E.; Chantraine, F.; Vatish, M.; Staff, A.C.; Sennstrom, M.; Olovsson, M.; Brennecke, S.P.; Stepan, H.; Allegranza, D.; et al. Predictive Value of the sFlt-1:PlGF Ratio in Women with Suspected Preeclampsia. *N. Engl. J. Med.* **2016**, *374*, 13–22, doi:10.1056/NEJMoa1414838.

36. Sharp, A.; Chappell, L.C.; Dekker, G.; Pelletier, S.; Garnier, Y.; Zeren, O.; Hillerer, K.M.; Fischer, T.; Seed, P.T.; Turner, M.; et al. Placental Growth Factor informed management of suspected pre-eclampsia or fetal growth restriction: The MAPPLE cohort study. *Pregnancy Hypertens.* **2018**, *14*, 228–233, doi:10.1016/j.preghy.2018.03.013.

37. Grimes, D.A.; Schulz, K.F. Compared to what? Finding controls for case-control studies. *Lancet* **2005**, *365*, 1429–1433, doi:10.1016/S0140-6736(05)66379-9.

38.   Miettinen, O.S. The "case-control" study: Valid selection of subjects. *J. Chronic Dis.* **1985**, *38*, 543–548, doi:10.1016/0021-9681(85)90039-6.

39.   Abbassi-Ghanavati, M.; Greer, L.G.; Cunningham, F.G. Pregnancy and laboratory studies: A reference table for clinicians. *Obstet. Gynecol.* **2009**, *114*, 1326–1331, doi:10.1097/AOG.0b013e3181c2bde8.

40.   Flood-Nichols, S.K.; Tinnemore, D.; Wingerd, M.A.; Abu-Alya, A.I.; Napolitano, P.G.; Stallings, J.D.; Ippolito, D.L. Longitudinal analysis of maternal plasma apolipoproteins in pregnancy: A targeted proteomics approach. *Mol. Cell. Proteom. MCP* **2013**, *12*, 55–64, doi:10.1074/mcp.M112.018192.

41.   Winkler, K.; Wetzka, B.; Hoffmann, M.M.; Friedrich, I.; Kinner, M.; Baumstark, M.W.; Wieland, H.; Marz, W.; Zahradnik, H.P. Low density lipoprotein (LDL) subfractions during pregnancy: Accumulation of buoyant LDL with advancing gestation. *J. Clin. Endocrinol. Metab.* **2000**, *85*, 4543–4550, doi:10.1210/jcem.85.12.7027.

42.   Verlohren, S.; Herraiz, I.; Lapaire, O.; Schlembach, D.; Zeisler, H.; Calda, P.; Sabria, J.; Markfeld-Erol, F.; Galindo, A.; Schoofs, K.; et al. New gestational phase-specific cutoff values for the use of the soluble fms-like tyrosine kinase-1/placental growth factor ratio as a diagnostic test for preeclampsia. *Hypertension* **2014**, *63*, 346–352, doi:10.1161/HYPERTENSIONAHA.113.01787.

43.   Reimer, T.; Rohrmann, H.; Stubert, J.; Pecks, U.; Glocker, M.O.; Richter, D.U.; Gerber, B. Angiogenic factors and acute-phase proteins in serum samples of preeclampsia and HELLP patients: A matched-pair analysis. *J. Matern.-Fetal Neonatal Med. Off. J. Eur. Assoc. Perinat. Med. Fed. Asia Ocean. Perinat. Soc. Int. Soc. Perinat. Obs.* **2013**, *26*, 263–269, doi:10.3109/14767058.2012.733747.

44.   Mongelli, M.; Ek, S.; Tambyrajia, R. Screening for fetal growth restriction: A mathematical model of the effect of time interval and ultrasound error. *Obstet. Gynecol.* **1998**, *92*, 908–912, doi:10.1016/s0029-7844(98)00349-4.

45.   Lee, P.A.; Chernausek, S.D.; Hokken-Koelega, A.C.; Czernichow, P. International Small for Gestational Age Advisory Board consensus development conference statement: Management of short children born small for gestational age, April 24–October 1, 2001. *Pediatrics* **2003**, *111*, 1253–1261, doi:10.1542/peds.111.6.1253.

46.   Morse, K.; Williams, A.; Gardosi, J. Fetal growth screening by fundal height measurement. *Best Pract. Res. Clin. Obstet. Gynaecol.* **2009**, *23*, 809–818, doi:10.1016/j.bpobgyn.2009.09.004.

47.   Chappell, L.C.; Duckworth, S.; Seed, P.T.; Griffin, M.; Myers, J.; Mackillop, L.; Simpson, N.; Waugh, J.; Anumba, D.; Kenny, L.C.; et al. Diagnostic accuracy of placental growth factor in women with suspected preeclampsia: A prospective multicenter study. *Circulation* **2013**, *128*, 2121–2131, doi:10.1161/CIRCULATIONAHA.113.003215.

48.   Benton, S.J.; McCowan, L.M.; Heazell, A.E.; Grynspan, D.; Hutcheon, J.A.; Senger, C.; Burke, O.; Chan, Y.; Harding, J.E.; Yockell-Lelievre, J.; et al. Placental growth factor as a marker of fetal growth restriction caused by placental dysfunction. *Placenta* **2016**, *42*, 1–8, doi:10.1016/j.placenta.2016.03.010.

49.   Quezada, M.S.; Rodriguez-Calvo, J.; Villalain, C.; Gomez-Arriaga, P.I.; Galindo, A.; Herraiz, I. sFlt-1/PlGF ratio and timing of delivery in early-onset fetal growth restriction with antegrade umbilical artery flow. *Ultrasound Obstet. Gynecol. Off. J. Int. Soc. Ultrasound Obstet. Gynecol.* **2019**, doi:10.1002/uog.21949, doi:10.1002/uog.21949.

50.   Heazell, A.E.; Hayes, D.J.; Whitworth, M.; Takwoingi, Y.; Bayliss, S.E.; Davenport, C. Biochemical tests of placental function versus ultrasound assessment of fetal size for stillbirth and small-for-gestational-age infants. *Cochrane Database Syst. Rev.* **2019**, *5*, CD012245, doi:10.1002/14651858.CD012245.pub2.

Supplemental data
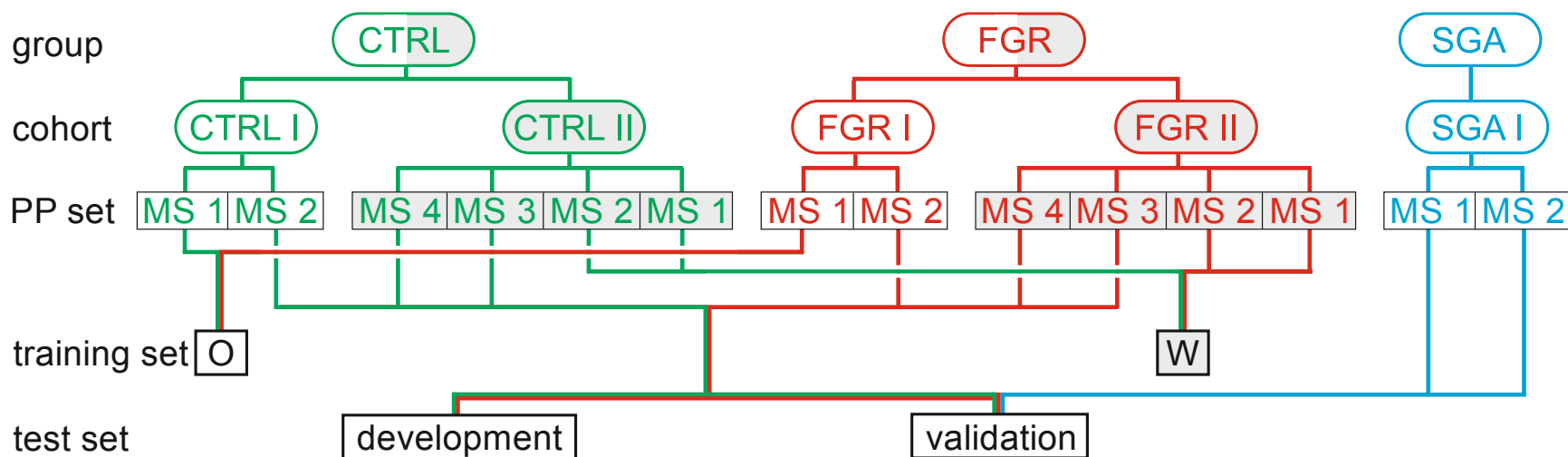
Supplemental Scheme 1: The three disease / control groups are represented by five patient cohorts. Individuals for cohorts CTRL I, FGR I, and SGA I have been recruited for this study, whereas cohorts CTRL II and FGR II consisted of individuals which were included in a previous study as well . The training sets "O" (this study) and "W" (from) were both used for determining cut-off values and the "development" test set for estimating assay performance. With the "validation" test set was investigated the assay´s capability to separate SGA from FGR in the presence of CTRL samples.

Supplemental Table 1: Demographic Data, Clinical and Laboratory Parameters for all Patients and Control Individuals

	patient / individual	age [a]	BMI [kg/m²]	parity [a]	median blood pressure [a.b] [mmHg]	proteinuria [mg/l] [a.c.d]	smoking status [e]	co-morb. [f]	gestational age at collection of blood [w+d] [g]	gestational age at delivery [w+d] [g]	Δd [h]	mode of delivery [i]	birth weight [g]	birth weight percentile	sex
CTRL I	101	35.0	20.4	0	108 / 60	0	0	/	29 + 4	39 + 2	68	s.c.	3210	40	f
	102	23.6	22.0	0	102 / 54	0	0	/	30 + 6	41 + 2	73	vaginal	3765	50	m
	103	28.9	20.3	0	120 / 60	0	0	/	32 + 4	41 + 4	63	vaginal	3580	50	f
	104	21.5	23.9	1	115 / 60	0	20	/	30 + 4	37 + 6	51	s.c.	3200	43	m
	105	31.7	23.9	1	110 / 70	0	0	/	28 + 5	40 + 0	79	vaginal	3690	60	m
	106	28.9	22.2	0	122 / 68	0	0	/	31 + 6	39 + 0	50	vaginal	3420	60	f
	107	39.2	21.1	1	127 / 61	0	0	/	31 + 3	39 + 0	53	vaginal	3440	60	f
	108	32.0	24.1	0	130 / 80	0	0	/	30 + 4	39 + 3	62	vaginal	3050	20	f
	109	25.1	26.9	0	99 / 87	0	0	/	27 + 6	37 + 3	67	vaginal	2960	30	m
	110	29.3	23.5	0	135 / 70	0	0	/	28 + 4	39 + 1	74	s.c.	3450	50	m
	111	31.2	23.2	1	116 / 81	0	0	/	28 + 0	41 + 0	91	vaginal	3750	70	f
	112	26.6	19.5	0	100 / 80	0	0	/	30 + 2	39 + 4	65	vaginal	3660	60	m
	113	24.5	22.4	1	115 / 59	0	2	/	26 + 2	38 + 2	84	vaginal	2970	30	f
	114	38.2	25.5	1	130 / 80	0	0	/	25 + 5	40 + 5	105	vaginal	3765	70	f
	115 [j]	25.7	23.1	1	105 / 63	0	25	/	28 + 4	40 + 4	84	vaginal	3070	14	f
CTRL II	151	24.9	20.3	2	109 / 53	0[f]	20	/	27+0	27+4	4	s.c.	1355	85	m
	152	37.9	23.1	2	108 / 65	0[f]	0	/	27+1	27+4	3	s.c.	1095	40	m
	153	30.5	22.1	0	114 / 61	0[f]	0	/	25+0	25+0	0	vaginal	740	30	m
	154	30.3	20.8	1	124 / 69	0[f]	0	/	31+2	33+6	18	s.c.	1960	25	f
	155	29.9	21.4	0	114 / 71	150	0	/	32+0	32+1	1	s.c.	1920	50	m
	156	24.2	35.7	0	129 /73	0[f]	10	/	31+6	31+6	0	vaginal	1750	50	f
	157	32.1	22.4	0	126 / 63	0[f]	0	/	37+4	37+4	0	s.c.	3130	50	f
	158	31.8	25.8	1	121 / 75	0[f]	0	/	37+5	37+5	0	s.c.	3465	70	m
	159	35.7	21.8	1	122 / 58	0[f]	0	/	33+6	34+6	7	s.c.	2420	40	f
	160	37.1	19.1	1	120 / 60	0[f]	0	/	38+6	39+0	1	s.c.	3150	30	f
	161	40.0	20.8	1	110 / 60	0[f]	0	/	36+0	36+0	0	s.c.	2920	60	m
	162	32.7	25.1	2	110 / 70	0[f]	0	/	32+3	32+3	0	s.c.	1850	50	f
	163	29.6	24.1	1	106 / 61	0[f]	0	/	27+5	28+4	6	s.c.	1250	60	f
	164	24.6	17.6	1	110 / 54	0[f]	5	/	28+0	28+0	0	s.c.	1030	40	f
	165	24.7	35.4	1	120 / 81	0[f]	0	/	39+2	39+2	0	s.c.	3895	80	m

Supplemental Table 1 (continued)

	patient / individual	age [a]	BMI [kg/m²]	parity [a]	median blood pressure [a,b] [mmHg]	proteinuria [mg/l] [a,c,d]	smoking status [e]	co-morb. [f]	gestational age at collection of blood [w+d] [g]	gestational age at delivery [w+d] [g]	Δd [h]	mode of delivery [i]	birth weight [g]	birth weight percentile	sex
IUGR I	301	41.8	23.7	3	134 / 78	0	0	/	33 + 6	34 + 1	2	s.c.	1525	3	m
	302	34.9	19.9	0	130 / 82	0	0	/	29 + 3	30 + 0	4	s.c.	755	2	m
	303	31.9	22.5	0	129 / 76	90	0	/	31 + 0	32 + 1	8	s.c.	1255	9	f
	304	24.5	19.7	0	122 / 53	0	40	/	26 + 1	26 + 4	3	s.c.	590	3	m
	305	28.8	26.0	1	120 / 80	0	15	/	30 + 5	31 + 5	7	s.c.	1190	6	m
	306	27.5	22.1	0	130 / 68	0	0	/	32 + 6	33 + 2	3	s.c.	1405	6	f
	307	30.7	24.0	0	120 / 75	0	10	/	28 + 1	28 + 5	4	s.c.	730	4	f
	308	29.4	20.1	0	103 / 59	0	0	/	29 + 6	31 + 4	12	s.c.	1240	9	m
	309	23.6	23.7	0	125 / 71	101	10	/	30 + 5	30 + 5	0	s.c.	940	4	f
	310	27.8	18.0	1	111 / 64	0	3	/	27 + 1	28 + 6	12	s.c.	900	8	m
	311	22.0	19.4	0	110 / 60	0	0	/	25 + 3	25 + 6	3	s.c.	495	3	m
	312	28.7	19.2	0	128 / 76	0	0	/	28 + 4	33 + 0	31	s.c.	1245	4	f
	313	23.4	23.5	0	96 / 52	0	5	/	29 + 3	29 + 5	2	s.c.	855	4	m
	314	23.1	29.0	0	109 / 77	0	5	/	29 + 4	29 + 6	2	s.c.	860	4	f
	315 [j]	23.4	22.7	1	139 / 65	0	0	/	31 + 2	31 + 4	2	s.c.	1240	9	m
IUGR II	351	31.9	22.5	0	129 / 76	90	0	/	31+0	32+1	8	s.c.	1255	9	f
	352	23.6	23.7	0	125 / 71	101	10	/	30+5	30+5	0	s.c.	940	4	f
	353	33.1	31.9	0	155 / 100	2324	10	PE	24+0	26+5	19	s.c.	650	4	m
	354	25.6	26.2	0	83 / 52	0[f]	0	/	37+3	37+5	2	s.c.	2550	5	m
	355	39.6	27.1	0	148 / 92	300	0	PE	28+2	28+2	0	s.c.	850	8	m
	356	34.3	19.9	0	136 / 71	0[f]	0	/	32+0	32+1	1	s.c.	1310	8	m
	357	23.8	21.5	0	162 / 100	500	0	PE	35+5	35+5	0	s.c.	1330	1	f
	358	27.5	22.1	0	130 / 68	150	0	/	32+6	33+2	3	s.c.	1405	6	f
	359	19.1	23.5	0	116 / 64	0[f]	10	/	35+5	36+1	3	s.c.	1870	2	m
	360	27.8	28.3	3	112 / 55	0[f]	0	/	27+0	27+0	0	s.c.	580	3	f
	361	31.7	20.2	1	100 / 60	0[f]	0	/	38+6	39+0	1	s.c.	1970	1	f
	362	34.0	23.8	2	140 / 90	1725	0	PE	26+4	26+6	2	s.c.	490	1	m
	363	25.1	22.6	0	122 / 79	0[f]	3	/	33+6	36+4	19	s.c.	1905	3	f
	364	37.9	22.1	0	150 / 80	0[f]	0	/	40+3	40+3	0	s.c.	2665	2	m
	365	41.5	28.0	0	155/101	200	0	PE	30+2	32+0	12	s.c.	975	3	f

mothers | infants

Supplemental Table 1 (continued)

	patient / individual	age [a)]	BMI [kg/m²]	parity [a)]	median blood pressure [a.b)] [mmHg]	proteinuria [mg/l] [a.c.d)]	smoking status [e)]	co-morb. [f)]	gestational age at collection of blood [w+d] [g)]	gestational age at delivery [w+d] [g)]	Δd[h)]	mode of delivery [i)]	birth weight [g]	birth weight percentile	sex
									mothers					**infants**	
	201	17.7	21.8	0	109 / 64	69	0	/	34 + 4	37 + 5	22	vaginal	2300	3	m
	202	31.8	20.0	2	120 / 80	84	0	/	32 + 3	38 + 3	42	s.c.	2545	4	f
	203	27.2	28.1	0	114 / 60	0	0	/	29 + 5	36 + 1	45	s.c.	2000	3	m
	204	25.6	16.2	0	138 / 48	0	0	/	32 + 3	38 + 4	43	s.c.	2740	6	m
	205	31.0	25.8	0	146 / 84	0	15	/	31 + 4	37 + 5	43	s.c.	2455	5	f
SGA I	206	30.5	24.5	1	132 / 62	0	0	/	29 + 5	36 + 1	45	s.c.	2040	4	f
	207	21.4	25.0	0	104 / 59	70	5	/	32 + 1	40 + 5	60	vaginal	2780	3	f
	208	40.2	26.0	1	120 / 75	0	0	/	32 + 2	38 + 2	42	s.c.	2590	7	f
	209	36.6	21.9	1	84 / 45	0	0	/	33 + 6	37 + 3	25	s.c.	1950	1	m
	210	19.7	18.4	0	104 / 73	0	30	/	31 + 4	38 + 1	46	vaginal	2750	8	m
	211	36.1	25.5	5	121 / 73	0	0	/	32 + 6	38 + 3	39	vaginal	2560	3	m
	212	40.2	20.6	1	117 / 70	0	0	/	30 + 1	37 + 2	50	s.c.	2560	9	m
	213	27.0	21.1	0	110 / 70	0	0	/	22 + 6	37 + 6	105	s.c.	2170	2	f
	214	22.9	18.2	0	110 / 60	0	15	/	33 + 0	39 + 0	42	vaginal	2780	5	m
	215	25.0	23.6	0	134 / 71	0	0	/	25 + 6	40 + 1	100	s.c.	2750	4	f

a)	determined at begining of hospitalization (time point of blood collection)
b)	systolic/diastolic pressure
c)	immunoturbidimetric assay (Tina-quant albumin; Roche Diagnostics. Mannheim, Germany); proteinuria is defined as urinary protein excretion >300 mg/L
d)	dip stick assay; significant protein is present with readings of more than +1 (max: +3)
e)	amount of cigarettes per day
f)	preeclampsia
g)	w: week, d: day
h)	Δd: time difference between blood sample collection and delivery in days
i)	s.c.: sectio caesarea
j)	spectra not used for biostatistical analyses

Supplemental Table 2: Areas of ion signals selected for scoring.

clinical diagnosis	patient ID	measurement [a,b]	areas of ion signals (m/z)				
			apo CII [c] 8205 [d]	apo CIII$_0$ [c] 8766 [d]	pro-apo CII [c] 8916 [d]	apo CIII$_1$ [c] 9422 [d]	apoCIII$_2$ [c] 9713 [d]
CTRL	101	MS1	414.30	200.24	883.56	2074.71	539.74
CTRL	101	MS2	400.35	206.89	841.79	2383.00	622.14
CTRL	102	MS1	698.00	150.34	1247.64	1569.02	681.66
CTRL	102	MS2	705.71	133.29	1264.78	1534.71	652.39
CTRL	103	MS1	421.90	107.80	921.31	1840.63	402.83
CTRL	103	MS2	457.38	105.68	1019.10	1990.28	489.84
CTRL	104	MS1	264.59	116.04	961.72	2034.77	467.03
CTRL	104	MS2	178.14	106.47	658.71	1933.72	420.97
CTRL	105	MS1	500.00	156.60	977.96	2285.33	593.77
CTRL	105	MS2	464.62	141.43	920.55	2197.40	587.02
CTRL	106	MS1	222.37	126.91	791.88	1778.87	394.30
CTRL	106	MS2	213.55	143.11	763.30	1885.79	430.03
CTRL	107	MS1	438.96	159.81	970.72	2400.46	409.66
CTRL	107	MS2	475.35	127.37	939.19	2109.18	364.65
CTRL	108	MS1	377.30	232.00	727.85	2564.50	554.57
CTRL	108	MS2	383.90	203.30	684.85	2141.79	398.44
CTRL	109	MS1	329.15	106.16	911.18	1942.23	492.75
CTRL	109	MS2	325.66	108.23	917.82	1948.87	509.50
CTRL	110	MS1	390.37	281.28	982.85	1860.78	523.74
CTRL	110	MS2	380.13	265.66	907.92	1739.45	446.88
CTRL	111	MS1	238.20	102.48	886.59	1953.43	479.76
CTRL	111	MS2	251.44	101.71	936.77	2040.18	482.76
CTRL	112	MS1	312.80	238.63	967.43	2128.26	439.25
CTRL	112	MS2	324.25	234.88	974.10	2150.88	464.01
CTRL	113	MS1	254.58	278.50	1027.06	2026.04	427.75
CTRL	113	MS2	281.71	292.17	1106.54	2132.15	461.05
CTRL	114	MS1	144.47	182.59	589.61	1461.07	320.83
CTRL	114	MS2	152.05	178.65	584.65	1455.51	327.33
CTRL	115 [e]	MS1	281.34	14.20	1167.01	1110.15	413.78
CTRL	115 [e]	MS2	231.69	18.74	937.52	977.23	402.52
SGA	201	MS1	215.62	270.94	789.79	1330.84	339.23
SGA	201	MS2	263.98	460.72	1037.82	2435.07	655.13
SGA	202	MS1	732.59	93.49	876.16	2469.79	564.72
SGA	202	MS2	654.59	91.84	769.69	2215.84	510.94
SGA	203	MS1	233.77	141.40	1082.29	2776.67	526.12
SGA	203	MS2	233.77	141.40	1082.29	2776.67	526.12
SGA	204	MS1	306.25	262.94	937.48	2267.95	442.92
SGA	204	MS2	273.12	283.39	844.56	2332.37	435.84
SGA	205	MS1	292.18	456.29	907.95	2217.01	629.64
SGA	205	MS2	217.11	399.58	691.47	1921.16	582.48
SGA	206	MS1	411.65	128.55	977.60	1703.53	552.24
SGA	206	MS2	433.39	131.13	1017.58	1770.33	649.78
SGA	207	MS1	520.37	184.78	1227.13	2247.78	404.80
SGA	207	MS2	523.52	165.27	1260.87	2034.50	375.76
SGA	208	MS1	120.34	99.83	679.65	1608.17	595.25
SGA	208	MS2	118.43	99.81	704.81	1762.08	614.28
SGA	209	MS1	483.31	80.24	908.62	1778.71	437.86
SGA	209	MS2	504.72	76.05	897.84	1826.20	476.90

clinical diagnosis	patient ID	measurement [a,b]	areas of ion signals (m/z)				
			apo CII [c]	apo CIII$_0$ [c]	pro-apo CII [c]	apo CIII$_1$ [c]	apoCIII$_2$ [c]
			8205 [d]	8766 [d]	8916 d)	9422 [d]	9713 [d]
SGA	210	MS1	197.06	132.67	787.89	2419.87	418.73
SGA	210	MS2	168.81	124.32	679.19	2021.89	317.82
SGA	211	MS1	201.32	157.10	892.48	1903.22	420.12
SGA	211	MS2	170.87	130.35	781.20	1517.58	330.60
SGA	212	MS1	239.09	225.91	637.04	1840.71	497.30
SGA	212	MS2	293.11	217.61	766.70	1913.29	524.41
SGA	213	MS1	319.36	281.63	1057.62	2544.11	496.54
SGA	213	MS2	243.79	227.11	829.42	2215.08	422.14
SGA	214	MS1	464.05	152.31	979.33	2000.95	519.80
SGA	214	MS2	540.68	150.61	1129.53	2173.92	608.80
SGA	215	MS1	107.24	122.08	636.23	1336.81	363.48
SGA	215	MS2	157.04	130.62	883.08	1777.3	520.11
IUGR	301	MS1	192.37	235.80	825.99	2279.91	404.18
IUGR	301	MS2	194.27	245.49	853.32	2481.24	441.21
IUGR	302	MS1	567.62	81.83	1174.89	2088.35	639.09
IUGR	302	MS2	659.08	102.29	1320.98	2364.86	635.10
IUGR	303	MS1	364.36	220.96	1245.24	2128.28	554.69
IUGR	303	MS2	352.85	225.31	1252.01	2323.04	618.43
IUGR	304	MS1	304.41	132.04	1112.63	1861.06	375.89
IUGR	304	MS2	263.48	123.54	940.25	1765.63	404.76
IUGR	305	MS1	217.45	163.06	1083.87	1687.21	452.45
IUGR	305	MS2	236.67	147.27	1180.20	1695.96	457.25
IUGR	306	MS1	220.31	122.83	1070.73	1806.31	430.47
IUGR	306	MS2	232.44	126.49	1215.18	1946.77	444.06
IUGR	307	MS1	213.23	399.97	1071.57	2112.83	424.41
IUGR	307	MS2	139.88	343.33	671.93	1850.29	389.32
IUGR	308	MS1	212.31	130.90	929.72	1175.19	592.87
IUGR	308	MS2	201.66	129.91	856.22	1109.21	598.61
IUGR	309	MS1	239.50	166.24	1135.39	1948.42	395.73
IUGR	309	MS2	233.65	134.17	1094.62	1505.65	308.34
IUGR	310	MS1	418.20	97.19	934.46	1417.34	383.97
IUGR	310	MS2	484.28	88.89	1051.94	1347.04	307.99
IUGR	311	MS1	262.66	99.87	937.06	1606.35	339.85
IUGR	311	MS2	263.28	99.37	958.19	1638.39	353.77
IUGR	312	MS1	477.13	145.12	1254.09	1709.73	469.29
IUGR	312	MS2	480.48	142.78	1233.48	1666.21	433.14
IUGR	313	MS1	180.27	183.17	1029.00	1663.82	331.00
IUGR	313	MS2	191.68	186.87	1156.24	1830.70	396.27
IUGR	314	MS1	293.84	105.08	924.29	1241.76	235.34
IUGR	314	MS2	434.38	124.61	1449.40	1512.45	269.20
IUGR	315 [e]	MS1	n.d.	n.d.	n.d.	n.d.	n.d.
IUGR	315 [e]	MS2	n.d.	n.d.	n.d.	n.d.	n.d.

a) MS1: first measurement of ClinProt work-up, ("training set").
b) MS2: second measurement of ClinProt work-up, ("test set").
c) abbreviated protein name
d) m/z value in MALDI mass spectrum
e) n.d.: ion signal areas not determined

Supplemental Table 3: Determination of Youden Index (Jmax) for Quotient A.

patient ID	clinical diagnosis	quotient A [a]	test cut-off	below cut-off	above cut-off	TP [b]	FP [b]	TN [b]	FN [b]	sensitivity	specificity	J [c]
	min	0.8										
102	CTRL	1.8	1.3	0	28	14	14	0	0	1.00	0.00	0.00
108	CTRL	1.9	1.9	1	27	14	13	1	0	1.00	0.07	0.07
105	CTRL	2.0	1.9	2	26	14	12	2	0	1.00	0.14	0.14
302	IUGR	2.1	2.0	3	25	14	11	3	0	1.00	0.21	0.21
101	CTRL	2.1	2.1	4	24	13	11	3	1	0.93	0.21	0.14
103	CTRL	2.2	2.2	5	23	13	10	4	1	0.93	0.29	0.21
107	CTRL	2.2	2.2	6	22	13	9	5	1	0.93	0.36	0.29
310	IUGR	2.2	2.2	7	21	13	8	6	1	0.93	0.43	0.36
110	CTRL	2.5	2.4	8	20	12	8	6	2	0.86	0.43	0.29
312	IUGR	2.6	2.6	9	19	12	7	7	2	0.86	0.50	0.36
109	CTRL	2.8	2.7	10	18	11	7	7	3	0.79	0.50	0.29
112	CTRL	3.1	2.9	11	17	11	6	8	3	0.79	0.57	0.36
314	IUGR	3.1	3.1	12	16	11	5	9	3	0.79	0.64	0.43
303	IUGR	3.4	3.3	13	15	10	5	9	4	0.71	0.64	0.36
106	CTRL	3.6	3.5	14	14	9	5	9	5	0.64	0.64	0.29
311	IUGR	3.6	3.6	15	13	9	4	10	5	0.64	0.71	0.36
104	CTRL	3.6	3.6	16	12	8	4	10	6	0.57	0.71	0.29
304	IUGR	3.7	3.6	17	11	8	3	11	6	0.57	0.79	0.36
111	CTRL	3.7	3.7	18	10	7	3	11	7	0.50	0.79	0.29
113	CTRL	4.0	3.9	19	9	7	2	12	7	0.50	0.86	0.36
114	CTRL	4.1	4.1	20	8	7	1	13	7	0.50	0.93	0.43
301	IUGR	4.3	**4.2**	**21**	**7**	**7**	**0**	**14**	**7**	**0.50**	**1.00**	**0.50**
308	IUGR	4.4	4.3	22	6	6	0	14	8	0.43	1.00	0.43
309	IUGR	4.7	4.6	23	5	5	0	14	9	0.36	1.00	0.36
306	IUGR	4.9	4.8	24	4	4	0	14	10	0.29	1.00	0.29
305	IUGR	5.0	4.9	25	3	3	0	14	11	0.21	1.00	0.21
307	IUGR	5.0	5.0	26	2	2	0	14	12	0.14	1.00	0.14
313	IUGR	5.7	5.4	27	1	1	0	14	13	0.07	1.00	0.07
	max	6.7	6.2	28	0	0	0	14	14	0.00	1.00	0.00

a) ranking according to the values of quotients A after adjoining theoretical minimum and maximum values
b) FN = false negative, FP = false positive, TN = true negative, TP = true positive.
c) J=Youden index; bold print: J_{max}

Supplemental Table 4: Determination of Youden Index (Jmax) for Quotient B.

patient ID	clinical diagnosis	quotient B [a]	test cut-off	below cut-off	above cut-off	TP [b]	FP [b]	TN [b]	FN [b]	sensitivity	specificity	J [c]
	min	2.0										
302	IUGR	3.0	2.5	0	28	14	14	0	0	1.00	0.00	0.00
111	CTRL	4.2	3.6	1	27	13	14	0	1	0.93	0.00	-0.07
109	CTRL	4.4	4.3	2	26	13	13	1	1	0.93	0.07	0.00
104	CTRL	4.6	4.5	3	25	13	12	2	1	0.93	0.14	0.07
103	CTRL	4.8	4.7	4	24	13	11	3	1	0.93	0.21	0.14
311	IUGR	5.1	**5.0**	**5**	**23**	**13**	**10**	**4**	**1**	**0.93**	**0.29**	**0.21**
310	IUGR	5.4	5.3	6	22	12	10	4	2	0.86	0.29	0.14
105	CTRL	5.4	5.4	7	21	11	10	4	3	0.79	0.29	0.07
306	IUGR	5.5	5.5	8	20	11	9	5	3	0.79	0.36	0.14
107	CTRL	5.7	5.6	9	19	10	9	5	4	0.71	0.36	0.07
106	CTRL	5.8	5.8	10	18	10	8	6	4	0.71	0.43	0.14
304	IUGR	5.9	5.9	11	17	10	7	7	4	0.71	0.50	0.21
312	IUGR	6.7	6.3	12	16	9	7	7	5	0.64	0.50	0.14
102	CTRL	6.7	6.7	13	15	8	7	7	6	0.57	0.50	0.07
309	IUGR	7.1	6.9	14	14	8	6	8	6	0.57	0.57	0.14
314	IUGR	7.1	7.1	15	13	7	6	8	7	0.50	0.57	0.07
308	IUGR	7.4	7.3	16	12	6	6	8	8	0.43	0.57	0.00
108	CTRL	7.4	7.4	17	11	5	6	8	9	0.36	0.57	-0.07
305	IUGR	7.6	7.5	18	10	5	5	9	9	0.36	0.64	0.00
101	CTRL	7.7	7.6	19	9	4	5	9	10	0.29	0.64	-0.07
303	IUGR	8.2	7.9	20	8	4	4	10	10	0.29	0.71	0.00
301	IUGR	8.8	8.5	21	7	3	4	10	11	0.21	0.71	-0.07
313	IUGR	9.2	9.0	22	6	2	4	10	12	0.14	0.71	-0.14
112	CTRL	9.3	9.2	23	5	1	4	10	13	0.07	0.71	-0.21
114	CTRL	10.2	9.8	24	4	1	3	11	13	0.07	0.79	-0.14
113	CTRL	11.3	10.8	25	3	1	2	12	13	0.07	0.86	-0.07
110	CTRL	11.8	11.6	26	2	1	1	13	13	0.07	0.93	0.00
307	IUGR	15.8	13.8	27	1	1	0	14	13	0.07	1.00	0.07
	max	16.8	16.3	28	0	0	0	14	14	0.00	1.00	0.00

a) ranking according to the values of quotients A after adjoining theoretical minimum and maximum values
b) FN = false negative, FP = false positive, TN = true negative, TP = true positive.
c) J=Youden index; bold print: J_{max}

Supplemental Table 5: Determination of Youden Index (Jmax) for Quotient C.

patient ID	clinical diagnosis	quotient C [a]	test cut-off	below cut-off	above cut-off	TP [b]	FP [b]	TN [b]	FN [b]	sensitivity	specificity	J [c]
		min	1.2									
108	CTRL	2.2	1.7	0	28	14	14	0	0	1.00	0.00	0.00
301	IUGR	2.8	2.5	1	27	14	13	1	0	1.00	0.07	0.07
114	CTRL	3.0	2.9	2	26	13	13	1	1	0.93	0.07	0.00
101	CTRL	3.1	3.1	3	25	13	12	2	1	0.93	0.14	0.07
105	CTRL	3.2	3.2	4	24	13	11	3	1	0.93	0.21	0.14
107	CTRL	3.3	3.3	5	23	13	10	4	1	0.93	0.29	0.21
106	CTRL	3.4	3.4	6	22	13	9	5	1	0.93	0.36	0.29
112	CTRL	3.4	3.5	7	21	13	8	6	1	0.93	0.43	0.36
111	CTRL	3.5	3.5	8	20	13	7	7	1	0.93	0.50	0.43
109	CTRL	3.6	3.5	9	19	13	6	8	1	0.93	0.57	0.50
307	IUGR	3.6	3.6	10	18	13	5	9	1	0.93	0.64	0.57
104	CTRL	3.7	3.7	11	17	12	5	9	2	0.86	0.64	0.50
110	CTRL	3.7	3.7	12	16	12	4	10	2	0.86	0.71	0.57
113	CTRL	3.8	3.7	13	15	12	3	11	2	0.86	0.79	0.64
103	CTRL	3.9	3.8	14	14	12	2	12	2	0.86	0.86	0.71
302	IUGR	4.2	**4.0**	**15**	**13**	**12**	**1**	**13**	**2**	**0.86**	**0.93**	**0.79**
303	IUGR	4.3	4.2	16	12	11	1	13	3	0.79	0.93	0.71
309	IUGR	4.5	4.4	17	11	10	1	13	4	0.71	0.93	0.64
306	IUGR	4.5	4.5	18	10	9	1	13	5	0.64	0.93	0.57
311	IUGR	4.6	4.6	19	9	8	1	13	6	0.57	0.93	0.50
304	IUGR	4.7	4.6	20	8	7	1	13	7	0.50	0.93	0.43
305	IUGR	4.7	4.7	21	7	6	1	13	8	0.43	0.93	0.36
313	IUGR	4.7	4.7	22	6	5	1	13	9	0.36	0.93	0.29
308	IUGR	4.9	4.8	23	5	4	1	13	10	0.29	0.93	0.21
310	IUGR	4.9	4.9	24	4	3	1	13	11	0.21	0.93	0.14
102	CTRL	5.2	5.1	25	3	2	1	13	12	0.14	0.93	0.07
312	IUGR	5.4	5.3	26	2	2	0	14	12	0.14	1.00	0.14
314	IUGR	5.8	5.6	27	1	1	0	14	13	0.07	1.00	0.07
		max	6.8	6.3	28	0	0	0	14	14	0.00	1.00	0.00

a) ranking according to the values of quotients A after adjoining theoretical minimum and maximum values
b) FN = false negative, FP = false positive, TN = true negative, TP = true positive.
c) J=Youden index; bold print: J_{max}

Supplemental Table 6: Power analysis of mass spectrometric ion signal-derived proteome profile series [a].

no.	type of data set	group	mean	std dev.	required sample size	used sample size [b]	type I error (α)	type II error (β)	actual power
1	**training "O": CTRL I vs FGR I** (CTRL I, n=14; FGR I, n=14) [b]	CTRL	0.79	0.58	3	14	0.05	0.20	0.81
		FGR	2.29	0.61	3	14			
2	**"development" test: CTRL I+II vs FGR I+II** (CTRL I+II, n=28; FGR I+II, n=29) [c]	CTRL	0.91	0.75	9	28	0.05	0.20	0.83
		FGR	1.82	0.67	9	44			
3	**"validation" test: CTRL I+II and SGA I vs FGR I+II** (CTRL I+II, n=28; SGA I, n=14; FGR I+II, n=29) [c]	CTRL+SGA	0.93	0.65	5	42	0.05	0.20	0.81
		FGR	2.15	0.63	5	29			

a) cumulative score separator: >1 = FGR; ≤ 1 = CTRL.
b) number of individuals
c) only via Jmax determined cut-off values: quotient A = 4.2; quotient B = 5.0; quotient C = 4.0.
d) combined cut-off values: quotient A = 4.2 and 3.4; quotient B = 5.0 and 7.0; quotient C = 4.0 and 5.1.

2.3 Comparison of blood serum protein analysis by MALDI-MS from either conventional frozen samples or storage disc-deposited samples: A study with human serum from pregnant donors and from patients with intrauterine growth restriction

Comparison of blood serum protein analysis by MALDI-MS from either conventional frozen samples or storage disc-deposited samples: A study with human serum from pregnant donors and from patients with intrauterine growth restriction

Manja Wölter[1], Manuela Russ[1], Charles A Okai[1], Werner Rath[2], Ulrich Pecks[2] and Michael O Glocker[1] (iD)

Abstract

Mass spectrometric profiling of intact serum proteins, i.e. determination of relative protein abundance differences, was performed using two different serum sample preparation methods: one with frozen and thawed serum, the other with at room temperature deposited and dried serum. Since in a typical clinical setting freezing of serum is difficult to achieve, sampling at room temperature is preferred and can be met when using the Noviplex™ card system. Once deposited and dried, serum proteins can be stored and shipped at room temperature. After resolubilization of serum proteins from ''dried serum spots'', mass spectra of high quality have been recorded comparable to those that were obtained using fresh-frozen and subsequently thawed serum samples. Differentiation between patients with intrauterine growth restriction and control individuals was achievable, independent from the sample work-up procedure. Having at hand a reliable and robust method for serum storage and shipment which works at room temperature bridges the gap between the clinics and the protein analysis laboratory. Our novel serum handling protocol reduces costs for both, storage and shipping, and ultimately enables clinical risk assessment based on mass spectrometric determination of intact protein abundance profiles.

Keywords

Introduction

Intrauterine growth restriction (IUGR) is a pathological pregnancy condition in which the fetus does not reach its genetically given growth potential and, in addition, is a risk factor for cardiovascular and metabolic diseases later in life.[1–3] About 3–8% of all pregnancies are affected.[4,5] Of note, other preterm babies, categorized as ''small for gestational age (SGA)'', are not associated with developmental risks. The majority of SGA neonates is born small by genetic constitution and grows in utero in accordance with their percentiles.[6,7] Differentiating these two pregnancy conditions is important to (i) improve pregnancy management and (ii) to start close surveillance and treatment during early weeks of infancy.[8] As even at time of birth, SGA is difficult to distinguish from IUGR by clinical means, a robust molecular assay with only minimal invasive procedures prior to or at time of delivery was highly desired.

Mass spectrometry-based proteome profiling provides a powerful approach to diagnose polygenic diseases like IUGR due to its ability to characterize individual serum samples based on complex proteome signatures from both, newborns and pregnant women.[9,10] However, one of the remaining challenges for making a mass spectrometry-based profiling assay of delicate samples attractive for clinical use is to bridge the distance between the delivery room and the mass spectrometry

[1]Proteome Center Rostock, Medical Faculty and Natural Science Faculty, University of Rostock, Rostock, Germany
[2]Department of Obstetrics and Gynecology, University of Schleswig-Holstein, Kiel, Germany

Corresponding author:
Michael O Glocker, Proteome Center Rostock, University of Rostock, Schillingallee 69, D-18057 Rostock, Germany.
Email: michael.glocker@med.uni-rostock.de

laboratory. Both, cord blood serum and maternal peripheral blood serum have to be prepared directly in the clinics immediately after blood withdrawal. Current state-of-the-art preparation of serum requests centrifugation followed by freezing, i.e. placing freshly prepared serum in a freezer or keep it on dry ice.[7,9–11] However, storing serum at freezing temperatures is in many cases too demanding for regular birth clinics and can only be guaranteed by specialized obstetric care centers. In addition, serum shipment on dry ice is costly and requires access to advanced mail carriers. In the serum-receiving laboratory, samples have to be kept frozen until time of analysis, which typically is initiated by thawing.[12]

As of yet, most hospitals are not prepared to store and ship frozen serum. Instead, keeping blood and other specimen and transporting such samples at room temperature is preferred routine.[13] Dried blood spots have been prepared on filter paper cards which provide a suitable storage and shipment device for clinical samples[13] and analysis of small molecules, such as phospholipids, creatinine, and drug metabolites by mass spectrometry has been successful upon resolubilization.[14–16] While quantitation of blood proteins from dried blood spots can be done by multiple reaction monitoring mass spectrometry (MRM MS) analysis of enzymatically generated partial peptides,[17–19] elution of intact proteins and subsequent analysis by mass spectrometry to generate a proteome profile has not yet been reported. A suitable means to avoid demanding and costly serum freezing was storing and shipping of serum as so-called "dried serum spots".[20] Dried blood spots have found wide-spread application for sampling of specimen in the clinics[21] and analysis of small molecules by mass spectrometry from these sources has become routine even for screening of larger populations.[14–16] Dried blood spot sampling as well as dried serum spot sampling was preferred, particularly because freeze/thaw cycles[22] can be avoided.

In this study, we are comparing the linear mode MALDI-ToF mass spectra obtained from intact blood serum proteins either stored on a membrane disc which functions as serum storage device and onto which serum can be deposited and kept at room temperature with mass spectra obtained from fresh frozen serum after conventional work-up.[9,10,23] Key step for successful relative abundance analysis of intact serum proteins derived from dried serum spots by mass spectrometry is the resolubilization procedure by which deposited proteins can be prepared and analyzed in a reliable and robust fashion.

Patients, materials and methods

Patient stratification

Blood samples were from eight pregnant Caucasian women who attended the Department of Obstetrics and Gynecology, University Hospital of the RWTH Aachen (Supplemental Table 1). The study was approved by the Ethics Committee of the RWTH Aachen (EK 119/08). Written informed consent was obtained from all participating women. Gestational age was established on the basis of the last menstrual period and was confirmed by ultrasonic examination between the 10th and the 14th week of gestation. Sonographic examinations were done antenatally on Logiq 5® and Voluson 730 Expert® Ultrasound Systems (GE Healthcare Systems, Solingen, Germany). The regression equation including biparietal diameter, femur length, and head and abdominal circumferences,[24] was used to estimate fetal weight. Neonatal birth weight centile was determined according to the population-based newborn weight charts.[25] IUGR was defined in accordance to the ACOG guidelines[26] as described.[27]

Blood sample collection and generation of serum aliquots

In the clinic, blood samples (up to 9 ml, each) were taken from each individual antenatally from the right or left cubital vein using monovette syringes (Serum Z/9 mL; Monovette®, Sarstedt, Germany). After incubation at room temperature for 15–30 minutes, samples were subjected to sedimentation of blood cells by centrifugation (Labofuge 400R; Fa. Heraeus Instruments, Waltham, USA) at $2000 \times g$ at room temperature for 15 minutes. Serum was aspirated and divided into aliquots (100 µl each).

Serum storage and transport

Conventional blood serum sample treatment was applied, i.e. serum was shock frozen and stored at −80°C.[9,10,23] Altogether, time between blood sample collection and storage of frozen serum aliquots averaged around less than 1 hour. Frozen serum aliquots were shipped on dry ice to the Proteome Center Rostock to maintain the cold-chain.

For developing an alternative serum sample storage and shipment procedure, a tiny volume of just 2 µl of serum was deposited on the "serum storage disc" that is mounted on the base sheet of a Noviplex™ card (Shimadzu Europe, Duisburg, Germany).[28] Serum deposits were let to dry at ambient temperature in a clean box and deposited serum proteins were stored dry at room temperature for up to three days. Dried serum spots were shipped to the Proteome Center Rostock by courier at room temperature.

Re-solubilization of serum proteins

A serum protein-containing serum storage disc was put with tweezers into the cap of a 1.5 ml Eppendorf tube (Eppendorf, Hamburg, Germany). To each serum storage disc were added 10 µl of 0.1% RapiGest solution (dissolved in 50 mM NH_4HCO_3) and the cavity was covered with fabric (Gaze, Holzhaus Medical Remscheid, Germany). Tubes were closed and kept upside-down during shaking for 1 hour at room temperature.

Afterwards, tubes were turned upright, placed into a centrifuge (Hettich, Tuttlingen, Germany) and samples were centrifuged at 10,000 r/min at room temperature for 5 minutes to collect the solvent at the bottom of the tube while the "emptied" serum storage disc was kept behind on the fabric. Fabric and serum storage disc were removed and protein solutions were immediately subjected to further work-up.

For double-extraction of serum storage discs, one serum storage disc (from patient 8), from which proteins had been eluted with 0.1% RapiGest solution (see above), was transferred into an 1.5 ml Eppendorf tube. After adding 200 μl of extraction buffer (1% sodium deoxycholate (SDC), 20 mM dithiothreitol (DTT) in 50 mM NH_4HCO_3), shaking was maintained for 1 hour at room temperature. Thereafter, 200 μl of 50 mM NH_4HCO_3 were added (end concentration: 0.5% SDC, 10 mM DTT in 50 mM NH_4HCO_3) and incubated for 5 minutes at 95°C. Next, tubes were placed into an ultrasonic bath (Bandelin, Berlin, Germany) for 15–30 seconds and then shaken for 10 minutes. This procedure was repeated three times. Finally, centrifugation for 10 minutes at 20°C and at $16,000 \times g$ sedimented the serum storage disc. The supernatant (400 μl) with re-solubilized serum proteins was transferred into a new tube for further use.

Preparation of compatible protein extracts for MALDI-MS analysis

To prepare MALDI-MS compatible serum protein solutions from frozen serum, serum aliquots were thawed and 5 μl were incubated with 10 μl MB-HIC8 "binding buffer" and 5 μl of MB-HIC8 bead slurry for 1 min (Profiling Kit 100 MB-HIC8; Bruker Daltonik, Bremen, Germany). After washing the beads three times with 100 μl of "wash buffer", each, proteins were eluted with 10 μl of "elution buffer", consisting of a 50% ACN solution; according to established protocols.[7,9–11] Protein-containing solutions were immediately subjected to mass spectrometric analysis in duplicate.

To record protein profiles by MALDI-MS from serum proteins that had been stored and re-solubilized from serum storage discs, 2 μl of each protein resolubilization solution was incubated with 5 μl MB-HIC8 "binding buffer" and 2 μl of MB-HIC8 bead slurry for 1 min. After washing the beads three times (40 μl of "wash buffer", each), proteins were eluted with 4 μl of "elution buffer". Protein-containing solutions were immediately subjected to mass spectrometric analysis in duplicate.

MALDI-MS analysis of serum proteins

After extraction from beads, serum protein-containing solutions (0.5 μl each) were spotted in duplicate directly onto a stainless steel MTP 384 target plate (Bruker Daltonik, Bremen, Germany) together with 0.5 μl ferulic acid solution (10 mg ferulic acid, Sigma-Aldrich, München, Germany) dissolved in ACN/0.1% aqueous

TFA (33/67, v/v) as matrix. After drying, 0.5 μl ferulic acid solution was added to each sample spot again. Since protein samples were prepared in duplicate for each patient/donor was recorded a first and a second measurement (MS1 and MS2).[7,9,10]

Matrix-embedded protein mixtures were analyzed with a Reflex III MALDI TOF mass spectrometer (Bruker Daltonik, Bremen, Germany) which was equipped with a SCOUT source for delayed extraction and was operated in linear positive ion mode using an acceleration voltage of 20 kV. Spectra were recorded in a mass range from 4 to 20 kDa, respectively, accumulating 900 shots per spectrum. Spectra were externally calibrated using a commercially available Protein Calibration Standard (Bruker Daltonik, Bremen, Germany). All mass spectra were internally recalibrated using average masses of ion signals at m/z 13762.4 (singly charged and unmodified transthyretin); uniprot accession number P02766; at m/z 14040.2 (doubly charged and unmodified Apo A-I, uniprot P02647); and at m/z 6631.6 (singly charged and unmodified apolipoprotein C, uniprot P02654). Ion signal areas were determined with the ClinProTools 2.2 software (Bruker Daltronik, Bremen, Germany) as described previously.[23,29]

Raw data processing and bio-statistical analysis

Our recently established multiparametric analysis[9,10,23] in which the signal areas of five ion signals within each spectrum were brought into context to each other by forming quotients of ion signal areas was applied. First, the signal area of the ion at m/z 8916 was divided by the signal area of the ion at m/z 8205 from one and the same spectrum to produce a value for spectra assessment (quotient A). Second was calculated the value of the signal area of the ion at m/z 8766 over the sum of the signal areas of the ions at m/z 9422 plus m/z 9713 (quotient B). Third, the signal area of the ion at m/z 8916 over the sum of the signal areas of the ions at m/z 8766 plus m/z 9422 plus m/z 9713 were determined (quotient C) as third assessment value. This data processing was applied for each of the spectra. Cutoff values for the quotients had been defined at 3.4 (quotient A), 7.0 (quotient B), and 5.1 (quotient C), respectively.[10] When the value of the quotient of the specific spectrum was higher than the respective cut-off value, a score of "1" was given to this respective spectrum. In the contrary case, the score for this spectrum was set to "0". Next, it was determined that a cumulative score of above "1" sorted the respective spectrum into the IUGR group. Sensitivity and specificity as well as receiver operating characteristic (ROC) curve[30,31] were calculated using the Origin statistics software (version 8.1 G; Originlab Corporation, Northampton, MA, USA).

In-solution digestion of re-solubilized serum proteins

To 400 μl of the protein mixture that was obtained after double-extraction of a serum storage disc (see above),

5 μl of trypsin solution (0.1 μg/μl; dissolved in 50 mM NH$_4$HCO$_3$) was added and the mixture was incubated for 16 hours at 37°C. First, 350 μl of digested solution were removed. Then, 350 μl ethyl acetate and 7 μl tri-fluoroacetic (TFA) were added and mixed immediately. After removing the aqueous phase (lower phase, about 300 μl) with a gel loader tip, the peptide solution was concentrated by using the SpeedVac (SpeedVac RVC 2-25CDplus, Martin Christ GmbH, Osterode am Harz, Germany). End volume of the peptide mixture was about 10 μl.

Desalination of peptides

Following previously published protocols,[32] two layers of C18 filter paper (Empore C18 Extraction Disc, Model 2215 3 M, Singapore) were placed into a 200 μl pipette tip (Greiner, Frickenhausen, Germany). The C18 filter was conditioned first with 50 μl methanol and then with 50 μl 80% acetonitrile (ACN), 0.5% acetic acid by centrifugation (1200 r/min; Eppendorf, Hamburg, Germany) for a few seconds, respectively. Solvents were discarded after each step. Then, 10 μl of peptide-containing solution and 40 μl of 0.5% acetic acid were added and tips were again centrifuged (1200 r/min; Eppendorf, Hamburg, Germany) for about 30 seconds. After washing the C18 filters with 50 μl 0.5% acetic acid, solvent was removed. Then, peptides were eluted with 20 μl 80% ACN, 0.5% acetic acid. Subsequently, solvent was removed by lyophilization (SpeedVac RVC 2-25CDplus, Martin Christ GmbH, Osterode am Harz, Germany). Thereafter, lyophilized peptides were dissolved in 20 μl of aqueous 0.1% formic acid (FA) that contained ACN (2%, v/v). Peptide concentration was determined using the Qubit assay kit (Invitrogen, Carlsbad, CA).[33]

NanoLC-ESI-MS configuration

Nanoscale LC separation of tryptic peptides was performed with a nanoACQUITY UPLC system (Waters Corporation, Manchester, UK), equipped with a C18 nanoACQUITY trap column: 100 Å 5 μm, 180 μm × 20 mm (Waters Corporation) and a nano ACQUITY UPLC HSS T3, 10 K lbf/in^2, 100 Å, 1.8 μm, 75 μm × 200 mm analytical reversed phase column (Waters Corporation), following previously published procedures.[34,35] The tryptic peptide solution was diluted to 5 ng/μl with solvent mixture A (H$_2$O/0.1% FA) plus 2% B (ACN/0.1% FA). The peptide mixture, 2 μl partial loop injection, was initially transferred with an aqueous 0.1% FA/0.1% ACN solution to the pre-column at a flow rate of 10 μl/min for 6 min. Mobile phase A was 0.1% FA in water whereas mobile phase B was 0.1% FA in ACN. After desalting and preconcentration, the peptides were eluted from the pre-column to the analytical column and separated with a gradient of 3–40% mobile phase B within 90 min at a flow rate of 0.3 μl/min, followed by a 9 minute rinse

with 85% of mobile phase B. The column was re-equilibrated for 31 min to achieve initial conditions. The column temperature was maintained at 35°C. The lock mass compound, [Glu1]-fibrinopeptide B, was delivered by the auxiliary pump of the LC system at 0.5 μl/min at a concentration of 100 fmol/μl to the reference sprayer of the NanoLockSpray source of the mass spectrometer. The precursor ion masses and associated fragment ion spectra of the tryptic peptides were measured with a SYNAPT G2S HDMS mass spectrometer (Waters Corporation, Manchester, UK) directly coupled to the chromatographic system and operated in positive ion mode. The time-of-flight analyzer of the mass spectrometer was externally calibrated with fragment ions of [Glu1]-fibrinopeptide B from m/z 50 to 2000, with the data post-acquisition lock mass corrected using the monoisotopic mass of the doubly charged precursor of [Glu1]-fibrinopeptide B. The reference sprayer was sampled every 30 s. Accurate mass data were collected in data independent mode of acquisition by alternating the energy applied to the collision cell between a low energy and elevated energy state as described previously.[36,37] The spectral acquisition time in each mode was 0.5 s.

NanoLC-ESI-MS data processing and protein identification

LC–MS data were processed according to published protocols,[34] using ProteinLynx GlobalSERVER version 3.0 (Waters Corporation, Manchester, UK). Protein identifications were obtained by comparing the mass spectrometric peptide ion data with the human protein-derived in-silico digested entries of a UniProt/Swiss-Prot database (UniProt release 1 November 2013). Search criteria used for protein identification included automatic peptide and fragment ion tolerance settings, one allowed missed cleavage, and variable methionine oxidation. Details on the principle of the search algorithm for data independently acquired LC–MS data have been previously presented.[38] Protein identifications were accepted if at least three fragment ions per peptide, seven fragment ions per protein and two peptides per protein were matched.

Results

Comparison of work-up procedures and resulting MALDI-MS profiles

The newly developed work-flow (Figure 1) replaced freezing and thawing of serum by depositing serum (2 μl) onto the "serum storage disc" on the Noviplex™ card at room temperature. After drying, serum proteins were stored, also at room temperature, for several days. Then, loaded "serum storage discs" on the Noviplex™ cards were shipped to the laboratory in a clean dry envelope. Here, serum proteins were re-solubilized using RapiGest™ as detergent.
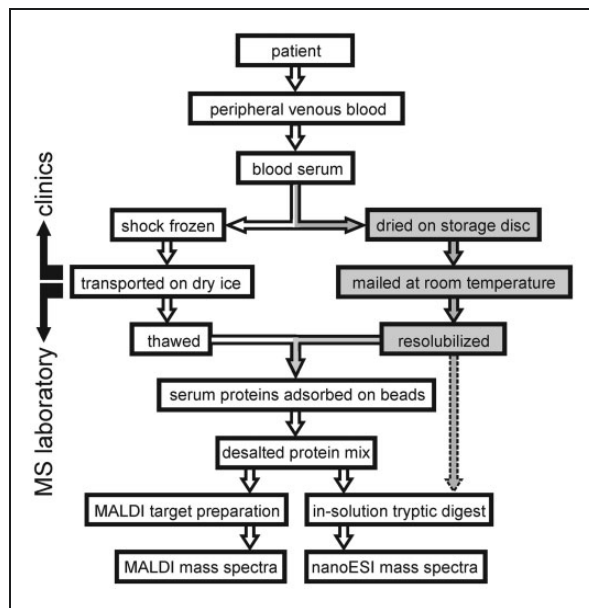
Figure 1. Work-flow for conventional (left fork) and novel (right fork) work-up protocol that is suitable for generating MALDI-ToF-MS proteome profiles of intact proteins and for recording nanoESI MS^E spectra of peptides after tryptic digestion of blood serum proteins. Serum is prepared in the clinics (top) and protein analysis in the mass spectrometry laboratory (bottom).

Figure 2. Linear MALDI-ToF mass spectra of intact proteins from patient 6 upon conventional (a) and novel (b) work-up of maternal peripheral venous blood. Ion signals which were selected for multiparametric analysis are labeled with "#". Ion signals which were used for internal re-calibration are marked with *. Ferulic acid was used as matrix.

The re-solubilized serum protein solutions were then worked-up for MALDI-MS analysis by desalting, target preparation, and matrix addition.

To investigate whether the sample work-up protocol had had an impact on the mass spectrometrically determined serum protein signature, eight previously analyzed and grouped blood serum samples were investigated. Four were from control individuals (CTRL), i.e. from pregnant women who delivered healthy infants adequate for gestational age, all being born preterm for various reasons. And four blood samples were from patients which belonged to the IUGR group, i.e. from pregnant women who delivered infants that suffered from IUGR, three of them needed mandatory preterm delivery (Supplemental Table 1).

The conventional procedure for preparing serum proteins followed established protocols which included freezing of serum, shipping of samples in the frozen state, and thawing of serum in the laboratory (Figure 1). Thawed sera were subjected to subsequent work-up steps in duplicate. Each serum sample was worked-up in parallel, including desalting, target preparation, and addition of matrix. MALDI MS analysis of protein profiles was done in linear mode (Figure 2(A)).

The resulting MALDI MS profiles upon preparing serum proteins from a "serum storage disc" (Figure 2(B)) were almost identical to the ones that were obtained from the same blood serum when using conventional work-up procedures. Again, the mass spectra from all work-ups from all eight blood samples

that were done with the novel serum depositing and resolubilization protocol looked nearly identical (Supplemental Figures 1 to 8).

Typically, MALDI mass spectra of conventionally prepared and/or of alternatively prepared serum protein samples showed ca. 50–70 strong ion signals in the mass range between m/z 4000 and m/z 20,000 (Figure 2), reflecting serum proteins of moderate abundance. High abundant serum proteins, such as serum albumin and immunoglobulins, were depleted during work-up, most likely during the desalting step. In all spectra, the two most prominent ion signals were found at m/z 8916 and at m/z 9422. Since mass spectra for all serum protein mixtures from all four patients and from all four control individuals looked very similar to each other (Supplemental Figures 1 to 8), they were subjected to biostatistical analysis.

Biostatistical data analysis of MALDI MS protein profiles

From all MALDI mass spectra (cf. Supplemental Figures 1 to 8) were extracted the areas under the ion signals of the pre-defined signature ion signals (Table 1); at m/z 8205 (apolipoprotein C2), m/z 8766 (apolipoprotein C3$_0$), m/z 8916 (pro-apolipoprotein C2), m/z

Table 1. Areas of profile ion signals selected for IUGR scoring.

Mother (no.)[a]	MALDI spectrum	Serum storage disc	Areas of ion signals (m/z)[b]				
			8205	8766	8916	9422	9713
1	1	No	912.63	88.57	1654.79	1753.41	244.10
1	2	No	692.45	50.04	1248.52	1270.10	148.99
2	1	No	280.39	97.90	771.32	1731.44	409.70
2	2	No	228.99	83.87	636.99	1185.37	235.78
3	1	No	442.47	68.32	1005.80	1605.37	267.76
3	2	No	519.65	62.73	1130.90	1633.43	273.89
4	1	No	263.78	140.97	976.65	2165.50	400.03
4	2	No	189.89	117.18	816.82	2201.06	354.85
5	1	No	295.67	158.35	1100.91	1091.85	176.76
5	2	No	279.03	172.91	1055.31	1186.35	237.48
6	1	No	130.21	193.54	931.66	1198.36	201.42
6	2	No	137.98	195.25	942.13	1172.94	202.48
7	1	No	144.88	152.06	712.42	1397.50	183.95
7	2	No	171.77	161.66	845.94	1686.70	275.35
8	1	No	212.85	112.33	1087.08	1997.76	232.32
8	2	No	330.53	162.66	1295.84	1949.12	253.85
1	3	Yes	333.19	70.68	549.64	761.98	76.03
1	4	Yes	506.10	81.92	871.49	1476.36	192.45
2	3	Yes	187.11	69.60	514.49	1230.78	222.15
2	4	Yes	217.04	64.49	555.39	1450.04	353.32
3	3	Yes	265.96	65.37	599.87	811.38	118.34
3	4	Yes	290.02	59.52	617.51	840.91	117.21
4	3	Yes	330.56	109.35	784.84	1267.69	247.46
4	4	Yes	239.03	92.97	553.09	1021.92	238.04
5	3	Yes	175.67	150.44	597.64	714.73	114.86
5	4	Yes	183.51	171.40	650.76	835.65	125.70
6	3	Yes	75.91	137.79	391.13	802.60	164.15
6	4	Yes	76.46	114.74	348.52	651.10	112.05
7	3	Yes	104.57	97.01	422.48	739.52	102.89
7	4	Yes	159.35	122.00	705.41	1474.42	241.08
8	3	Yes	335.00	108.85	894.12	1065.99	173.45
8	4	Yes	286.67	87.43	744.41	940.61	174.28

IUGR: intrauterine growth restriction.
[a]For numbering see Supplemental Table 1.
[b]Arbitrary units.

9422 (apolipoprotein $C3_1$), and m/z 9713 (apolipoprotein $C3_2$). As in our previous analyses, the lowest area values for an ion signal of interest were around 70 a.u. for ion signals at m/z 8766 and the highest values were about 2000 a.u. for ion signals at m/z 9422.

Areas under the ion signals of a given MALDI mass spectrum were then used to form ion signal ratios: quotients A, B, and C. The previously defined inclusion/exclusion criteria, i.e. cut-off values for quotient A (3.4), quotient B (7.0), and quotient C (5.1) were applied for each of the work-up series and showed that the quotient values were about the same in each case (Figure 3). The individual cumulative score for each mass spectrum characterized a mass spectrum, i.e. the respective serum sample, to belong either to the group of IUGR or to the group of control individuals, respectively.

The IUGR serum samples of both, the conventional work-up series and of the alternative work-up series with use of Noviplex™ cards, clearly differentiated from the control serum samples, such that cumulative score values were higher in the IUGR groups as compared to the control groups. Particularly, quotients A and B from the IUGR groups were in most cases above their respective threshold values and quotients from the control groups were below. Values for quotient C did not differentiate the two groups,

independent of the work-up protocol, but contributed to the cumulative score of each individual serum sample. Results from the duplicate measurements confirmed each other.

Statistical evaluation of the mass spectrometry signature and comparison with clinical data that were used as "gold standard" provided with both work-up procedures good results, i.e. the number of true positive assignments of spectra was 7 out of 8 when serum was conventionally worked-up and 8 out of 8 when serum was worked up using our novel protocol where no freeze/thaw cycles were necessary (Table 2).

Likewise, the number of true negative spectra assignments was 8 out of 8 when serum was conventionally worked-up and 6 out of 8 when serum was worked up with our novel protocol, i.e. without freezing serum for storage and during shipping (Table 2). As in both cases, the area under the curve (AUC) was greater than 0.9 in ROC curve analyses, high confidence was reached with the newly developed experimental approach.
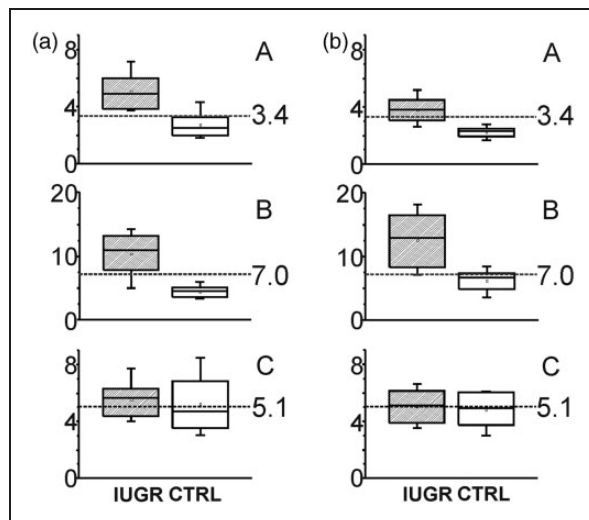
Figure 3. Distributions of quotient values derived from protein ion intensities in all MALDI mass spectra after conventional work-up (a) and after novel work-up (b) of maternal peripheral venous blood samples. Box and whisker plots show value distributions from the ion signal area quotients A, B, and C. The boxes represent the 25th to the 75th percentiles. The horizontal lines within the boxes represent the medians; the small squares indicate the means. The whiskers specify the 5th and 95th percentiles. Dashed horizontal lines mark cut-off values.
IUGR: intrauterine growth restriction; CTRL: control individuals.

Estimation of protein re-solubilization efficiency

To guarantee satisfactory mass spectrometric profiling data with our here developed protocol that included Noviplex[TM] cards, the proteins had to be present in the resolubilization solution in high enough protein amounts to saturate the beads which were requested for desalting. To test whether serum storage discs from the Noviplex[TM] cards that were applied for MALDI MS profiling contained more than enough protein material, we subjected an already eluted serum storage disc from patient 8 to an additional elution of residual proteins, using somewhat harsher conditions. Instead of using RapiGest[TM] as detergent, for this second elution an SDC-containing buffer was applied at elevated temperatures. The second eluted protein mixture was then tryptically digested in total and the resulting peptide mixture was analyzed by nanoLC-ESI-MS[E] (Figure 4).

NanoLC-ESI-MS[E] analysis of the resulting peptide mixture provided a total ion current chromatogram that contained 5997 ion signals from the low energy regime of which 764 peptide ion signals were matched to protein entries of the Uniprot database. Applying the chosen quality criteria for protein assignments resulted in the identification of 73 non-redundant proteins (Supplemental Table 2).

As an example, the doubly charged precursor ion signal at m/z 519.27 was recorded in the total ion current time segment of around 27.02 min together with about a dozen other peptide ion signals (Figure 4). Some of the 688,747 high energy ions of the total dataset were fragment ions from this precursor ion and could be assigned to Y″ ions of a peptide whose sequence was "TAAQNLYEK". This amino acid sequence represents the partial amino acid sequence 25–33 of apolipoprotein C2 and the partial amino acid sequence 31–39 of pro-apolipoprotein C2. Confidence of identification of the mentioned amino acid sequence was high and yielded a score of 1369.9 which, thus, proved the presence of the peptide and, therefore, the presence of at least one of the two originating proteins.

In sum, the fact that so many proteins were identified in the second elution of this serum storage disc convinced us that the first elution was already containing enough protein material to saturate the beads which were used for desalting during sample work-up. Elution

Table 2. Statistical evaluation of mass spectrometric profiling results.

Serum storage disc	True positive	False positive	True negative	False negative	Sensitivity	Specificity	False pos. rate	False neg. rate	Pos. pred. value	Neg. pred. value	ROC AUC[a]
No	7	0	8	1	0.88	1.00	0.11	0.00	1.00	0.89	0.95
Yes	8	2	6	0	1.00	0.75	0.00	0.20	0.80	1.00	0.91

[a]ROC: receiver operating characteristic; AUC: area under the curve of two measurement series.
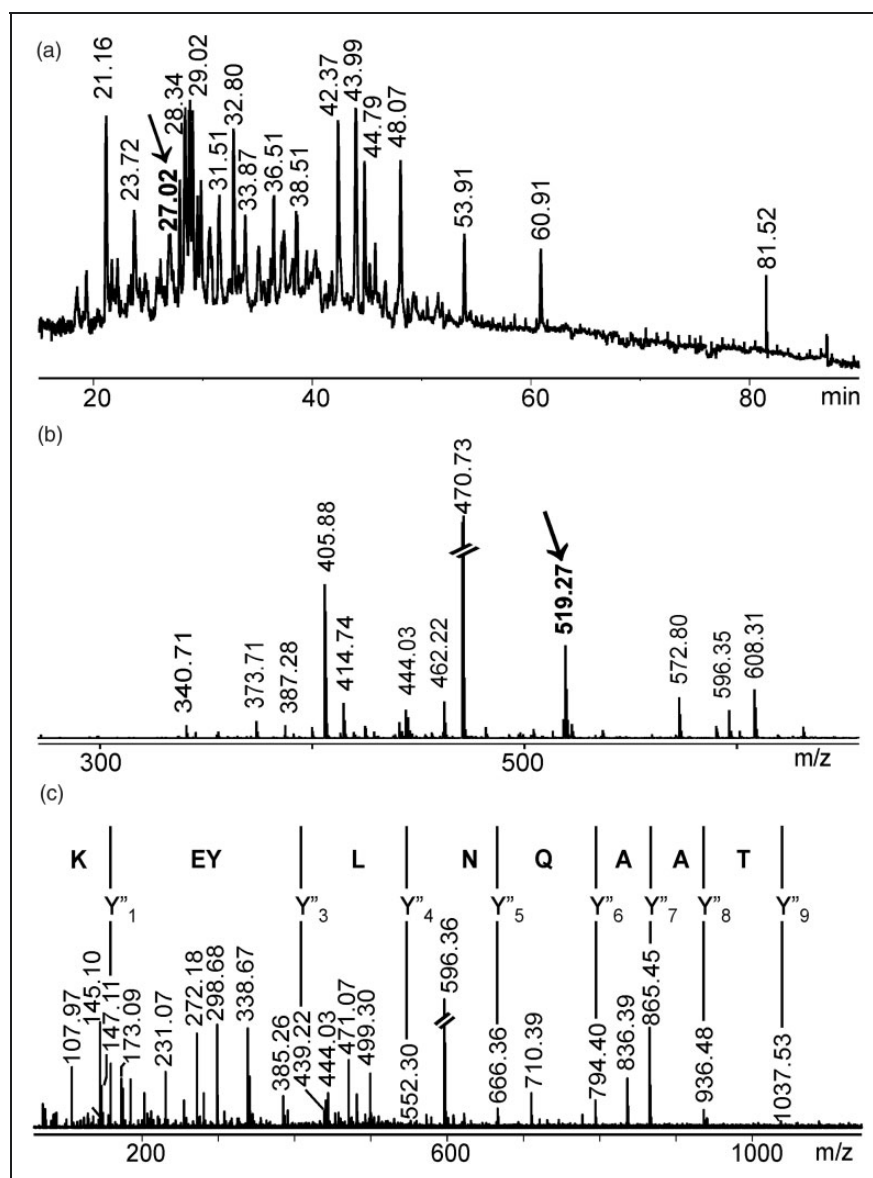
Figure 4. NanoLC-ESI-MS[E] analysis of re-solubilized and tryptically digested proteins from patient 8 using the novel work-up protocol of maternal peripheral venous blood. Total ion current chromatogram after in-solution digest and nanoLC separation (a). The arrow points to the time segment for which the mass spectrum is shown in (b). Precursor ion ESI mass spectrum of peptides eluting at 27.02 min (b). The arrow points to the doubly charged precursor ion for which the fragment mass spectrum is shown in (c). Fragment ion mass spectrum of doubly charged precursor ion at m/z 519.27 (c). Y″ fragment ions are marked and partial amino acid sequence is given in single letter code. Selected ion signals are labeled with m/z values.

of proteins from the beads and preparing of matrix enabled to generate MALDI-ToF-MS profiles of the patients' serum samples in a reliable fashion.

Discussion

Patient samples from dried blood spots and from dried serum spots have been subjected to global proteome analyses[39] and to targeted proteome analyses,[40] respectively. Strikingly, analysis of intact proteins either from dried blood spots or from dried serum spots has as of yet not been reported. The closest to analyzing intact proteins from filter paper sources possibly is "paper spray" of protein complexes.[41] Yet, because "paper spray" produces multiply charged ions supplied by wetted paper, the comparison may be skewed. Also, as multiply charged ions are produced, profiling of complex bio-fluids may perhaps not become the prime application of this method. Noviplex[TM] cards were developed for generating plasma out of full blood,[28] and hence, they provide a suitable storage disc, similar to filter paper, but with the potential to resolubilize proteins under fairly mild elution conditions. Rapigest[TM] was chosen by us to be added to the elution solution, because of its detergent properties which are desired for resolubilization of deposited serum proteins. But, because Rapigest[TM] can be destroyed by simple acidification,[42] this detergent enables to employ mass

spectrometry as detection assay of intact proteins. The desalting procedure of choice as part of our work-flow has turned out to be the ClinProt^{TM} bead system for mainly two reasons. First, the ClinProt^{TM} bead system provides a large surface onto which proteins may attach to after removal of detergent; thereby sample losses are minimized. Second, the ClinProt^{TM} bead system has already been found suitable to generate serum protein profiles that, when analyzed by linear MALDI-ToF-MS, have enabled us previously to distinguish between IUGR and control individuals.[7,9–11]

Despite the fact that the number of patient samples that were investigated in this study was too small for clinical and/or biostatistical disease evaluation, the point to be made was reached. Instead of demonstrating whether the analyzed mass spectra belonged to either the IUGR group or to the control group, the goal of this project was to prove that the serum protein profiles were of comparable quality independent of the chosen work-up protocol. The conclusion from our analyses is that our novel procedure that avoids freeze/thaw steps and prepares serum proteins at room temperature is well suitable for recording proteome profiles by MALDI-ToF-MS. The robustness of all involved steps makes this assay attractive to clinics world-wide, paving the way for future mass spectrometric assessments of other diseases.

ORCID iD
Michael O Glocker http://orcid.org/0000-0001-9190-482X

Supplemental material
Supplemental material is available for this article online.

References
1. Hales CN, Barker DJ, Clark PM, et al. Fetal and infant growth and impaired glucose tolerance at age 64. *BMJ (Clin Res Ed)* 1991; 303: 1019–1022.
2. Phipps K, Barker DJ, Hales CN, et al. Fetal growth and impaired glucose tolerance in men and women. *Diabetologia* 1993; 36: 225–228.
3. Barker DJ, Winter PD, Osmond C, et al. Weight in infancy and death from ischaemic heart disease. *Lancet* 1989; 2: 577–580.
4. Villar J, Carroli G, Wojdyla D, et al. Preeclampsia, gestational hypertension and intrauterine growth restriction, related or independent conditions? *Am J Obstet Gynecol* 2006; 194: 921–931.
5. Huppertz B. Placental origins of preeclampsia: challenging the current hypothesis. *Hypertension* 2008; 51: 970–975.
6. Lee PA, Chernausek SD, Hokken-Koelega ACS, et al. International small for gestational age advisory board consensus development conference statement: management of short children born small for gestational age, April 24–October 1, 2001. *Pediatrics* 2003; 111: 1253–1261.
7. Pecks U, Kirschner I, Wolter M, et al. Mass spectrometric profiling of cord blood serum proteomes to distinguish infants with intrauterine growth restriction from those who are small for gestational age and from control individuals. *Transl Res* 2014; 164: 57–69.
8. Wolter M, Okai CA, Smith DS, et al. Maternal apolipoprotein B100 serum levels are diminished in pregnancies with intrauterine growth restriction and differentiate from controls. *Proteomics Clin Appl* 2018; 12(6): e1800017. DOI: 10.1002/prca.201800017.
9. Wolter M, Rower C, Koy C, et al. A proteome signature for intrauterine growth restriction derived from multifactorial analysis of mass spectrometry-based cord blood serum profiling. *Electrophoresis* 2012; 33: 1881–1893.
10. Wolter M, Rower C, Koy C, et al. Proteoform profiling of peripheral blood serum proteins from pregnant women provides a molecular IUGR signature. *J Proteomics* 2016; 149: 44–52.
11. Pecks U, Seidenspinner F, Rower C, et al. Multifactorial analysis of affinity-mass spectrometry data from serum protein samples: a strategy to distinguish patients with preeclampsia from matching control individuals. *J Am Soc Mass Spectrom* 2010; 21: 1699–1711.
12. Glocker MO, Wölter M, Ruß M, et al. Protein profiling from dried serum spots. *GIT Lab J* 2016; 20: 2–4.
13. Wagner M, Tonoli D, Varesio E, et al. The use of mass spectrometry to analyze dried blood spots. *Mass Spectrom Rev* 2016; 35: 361–438.
14. Zakaria R, Allen KJ, Koplin JJ, et al. Advantages and challenges of dried blood spot analysis by mass spectrometry across the total testing process. *EJIFCC* 2016; 27: 288–317.
15. Nakano M, Uemura O, Honda M, et al. Development of tandem mass spectrometry-based creatinine measurement using dried blood spot for newborn mass screening. *Pediatr Res* 2017; 82: 237–243.
16. Perez JW, Pantazides BG, Watson CM, et al. Enhanced stability of blood matrices using a dried sample spot assay to measure human butyrylcholinesterase activity and nerve agent adducts. *Anal Chem* 2015; 87: 5723–5729.
17. Lehmann S, Picas A, Tiers L, et al. Clinical perspectives of dried blood spot protein quantification using mass spectrometry methods. *Crit Rev Clin Lab Sci* 2017; 54: 173–184.
18. Chambers AG, Percy AJ, Yang J, et al. Multiple reaction monitoring enables precise quantification of 97 proteins in dried blood spots. *Mol Cell Proteomics* 2015; 14: 3094–3104.

19. Ozcan S, Cooper JD, Lago SG, et al. Towards reproducible MRM based biomarker discovery using dried blood spots. *Sci Rep* 2017; 7: 45178.
20. Desbois D, Roque-Afonso AM, Lebraud P, et al. Use of dried serum spots for serological and molecular detection of hepatitis a virus. *J Clin Microbiol* 2009; 47: 1536–1542.
21. Lehmann S, Delaby C, Vialaret J, et al. Current and future use of "dried blood spot" analyses in clinical chemistry. *Clin Chem Lab Med* 2013; 51: 1897–1909.
22. Kluge JA, Li AB, Kahn BT, et al. Silk-based blood stabilization for diagnostics. *Proc Natl Acad Sci USA* 2016; 113: 5892–5897.
23. Glocker MO, Röwer C, Wölter M, et al. Multiparametric analysis of mass spectrometry-based proteome profiling in gestation-related diseases. In: Günter G and David SM (eds) *Handbook of spectroscopy*. Wiley-VCH Verlag GmbH & Co. KGaA, 2014, pp.407–428. DOI: 10.1002/9783527654703.ch12.
24. Hadlock FP, Harrist RB, Sharman RS, et al. Estimation of fetal weight with the use of head, body, and femur measurements—a prospective study. *Am J Obstet Gynecol* 1985; 151: 333–337.
25. Voigt M, Schneider KT and Jahrig K. Analysis of a 1992 birth sample in Germany. 1: new percentile values of the body weight of newborn infants. *Geburtshilfe Frauenheilkd* 1996; 56: 550–558.
26. Intrauterine growth restriction. Clinical management guidelines for obstetrician-gynecologists. American College of Obstetricians and Gynecologists. *Int J Gynaecol Obstetr* 2001; 72: 85–96.
27. Pecks U, Caspers R, Schiessl B, et al. The evaluation of the oxidative state of low-density lipoproteins in intrauterine growth restriction and preeclampsia. *Hypertens Pregnancy* 2012; 31: 156–165.
28. Kim JH, Woenker T, Adamec J, et al. Simple, miniaturized blood plasma extraction method. *Anal Chem* 2013; 85: 11501–11508.
29. Pecks U, Schutt A, Rower C, et al. A mass spectrometric multicenter study supports classification of preeclampsia as heterogeneous disorder. *Hypertens Pregnancy* 2012; 31: 278–291.
30. Greiner M, Pfeiffer D and Smith RD. Principles and practical application of the receiver-operating characteristic analysis for diagnostic tests. *Prev Vet Med* 2000; 45: 23–41.
31. Faraggi D and Reiser B. Estimation of the area under the ROC curve. *Stat Med* 2002; 21: 3093–3106.
32. Rappsilber J, Mann M and Ishihama Y. Protocol for micro-purification, enrichment, pre-fractionation and storage of peptides for proteomics using StageTips. *Nat Protoc* 2007; 2: 1896–1906.
33. Yefremova Y, Opuni KFM, Danquah BD, et al. Intact Transition Epitope Mapping (ITEM). *J Am Soc Mass Spectrom* 2017; 28: 1612–1622.
34. Rower C, George C, Reimer T, et al. Distinct ezrin truncations differentiate metastases in sentinel lymph nodes from unaffected lymph node tissues, from primary breast tumors, and from healthy glandular breast tissues. *Transl Oncol* 2018; 11: 1–10.
35. Kumar VV, James BL, Russ M, et al. Proteome analysis reveals that de novo regenerated mucosa over fibula flap-reconstructed mandibles resembles mature keratinized oral mucosa. *Oral Oncol* 2018; 78: 207–215.
36. Silva JC, Denny R, Dorschel CA, et al. Quantitative proteomic analysis by accurate mass retention time pairs. *Anal Chem* 2005; 77: 2187–2200.
37. Geromanos SJ, Vissers JP, Silva JC, et al. The detection, correlation, and comparison of peptide precursor and product ions from data independent LC–MS with data dependant LC–MS/MS. *Proteomics* 2009; 9: 1683–1695.
38. Li GZ, Vissers JP, Silva JC, et al. Database searching and accounting of multiplexed precursor and product ion spectra from the data independent analysis of simple and complex peptide mixtures. *Proteomics* 2009; 9: 1696–1719.
39. Martin NJ, Bunch J and Cooper HJ. Dried blood spot proteomics: surface extraction of endogenous proteins coupled with automated sample preparation and mass spectrometry analysis. *J Am Soc Mass Spectrom* 2013; 24: 1242–1249.
40. Ruhaak LR, Miyamoto S, Kelly K, et al. N-Glycan profiling of dried blood spots. *Anal Chem* 2012; 84: 396–402.
41. Zhang Y, Ju Y, Huang C, et al. Paper spray ionization of noncovalent protein complexes. *Anal Chem* 2014; 86: 1342–1346.
42. Yu YQ, Gilar M, Lee PJ, et al. Enzyme-friendly, mass spectrometry-compatible surfactant for in-solution enzymatic digestion of proteins. *Anal Chem* 2003; 75: 6023–6028.
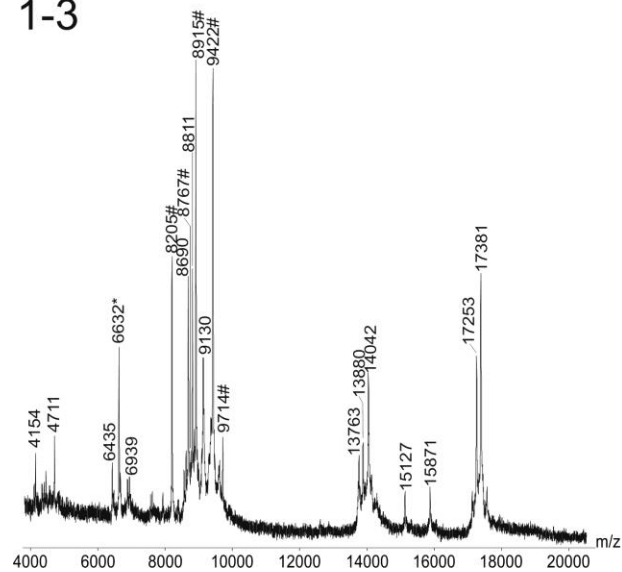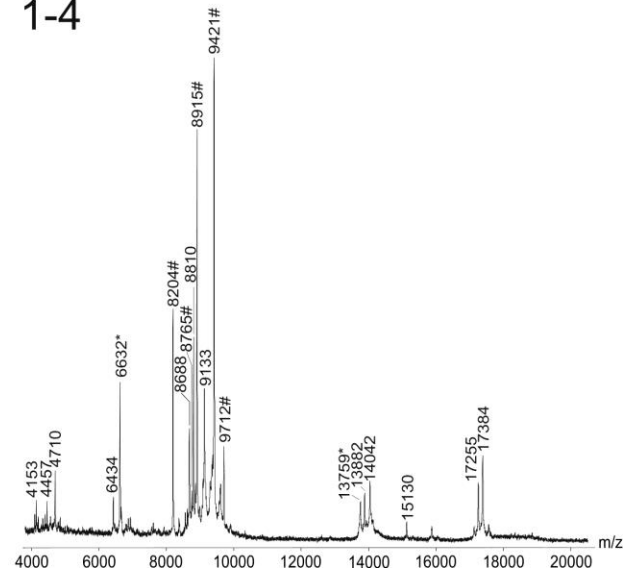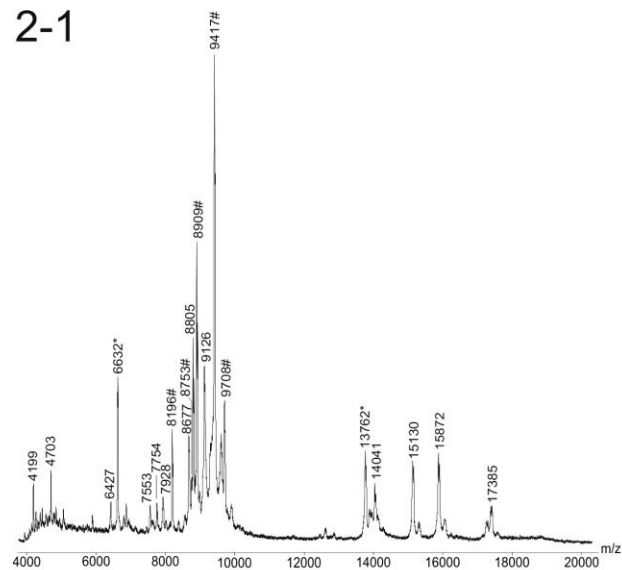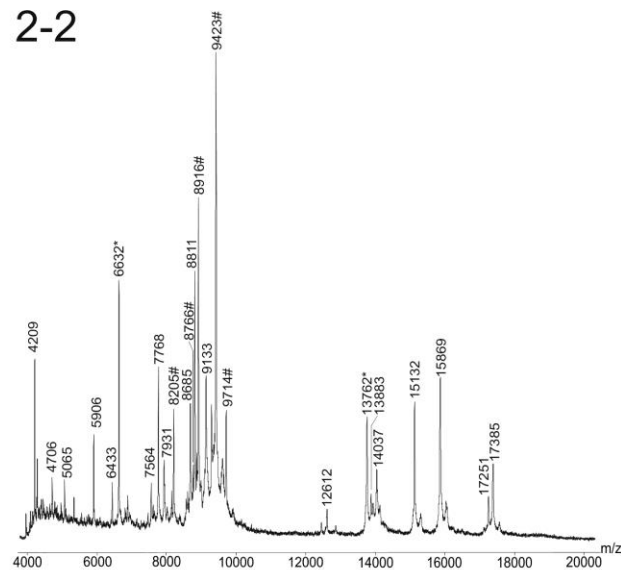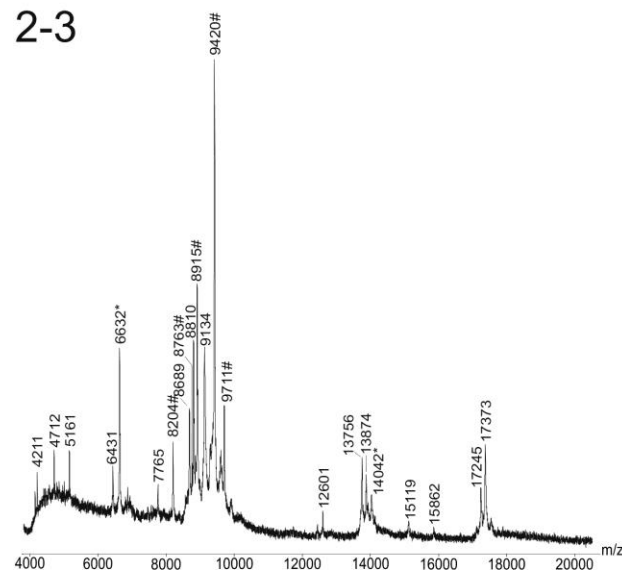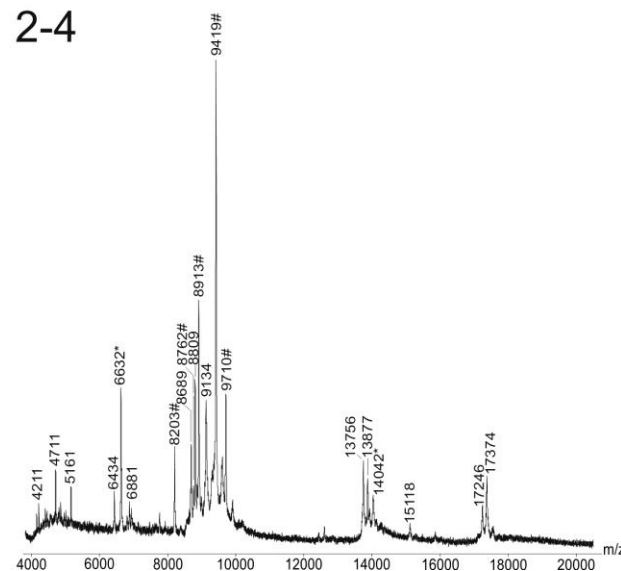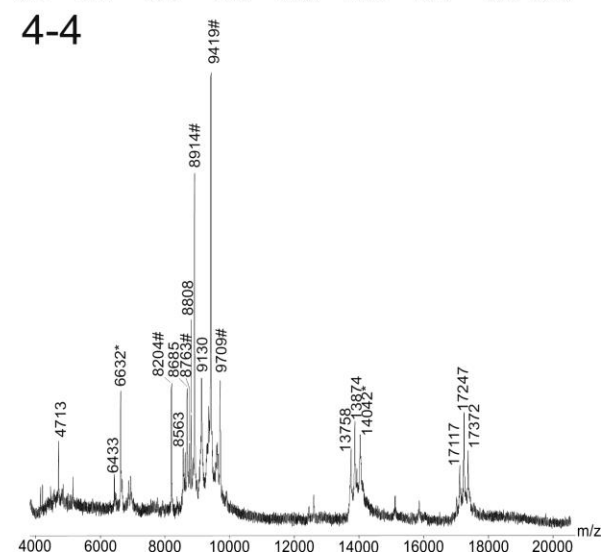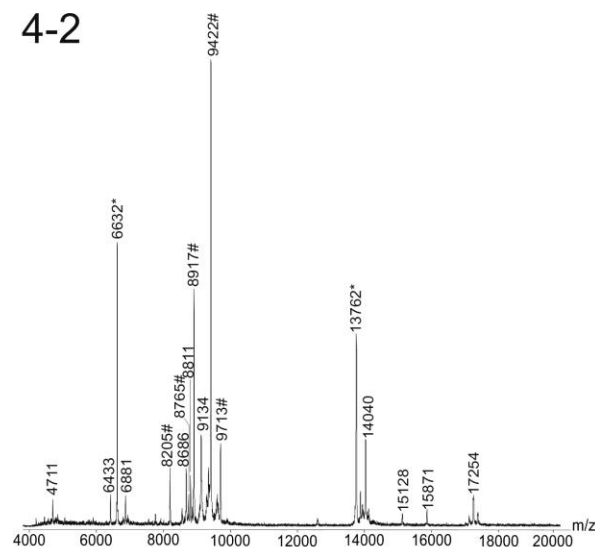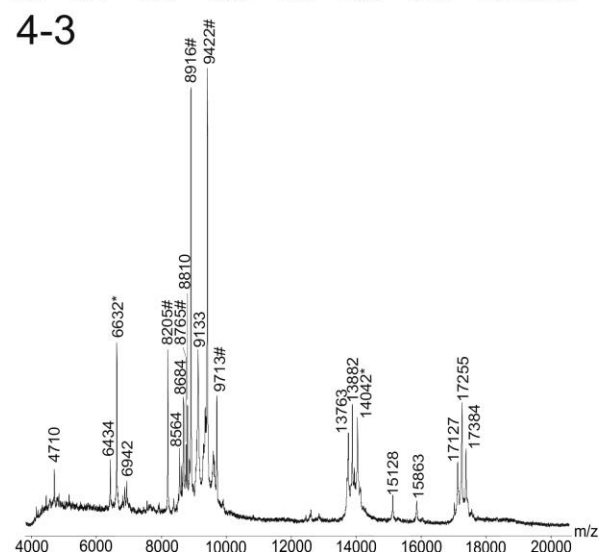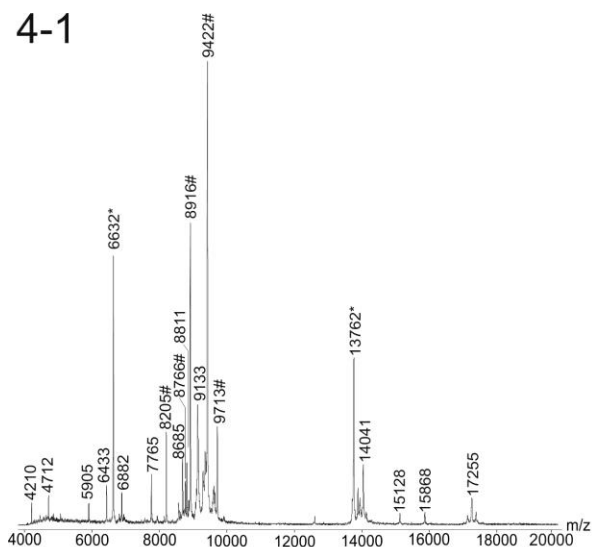
Supplemental data
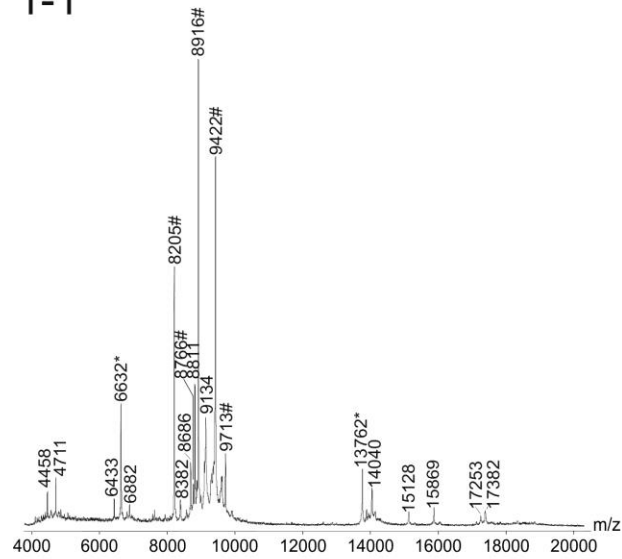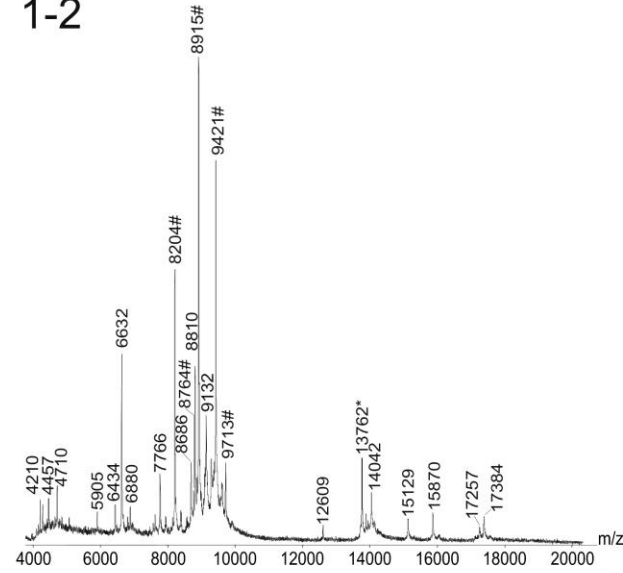
Supplemental Figure 1:

MALDI-ToF mass spectra of intact peripheral blood proteins from mother 1 upon conventional serum work-up including freeze / thaw steps (spectra 1-1 and 1-2), and following our novel work flow with depositing serum on serum storage discs at room temperature (spectra 1-3 and 1-4).

Ion signals labeled: „#" indicate mass peaks whose area under signals were used for multiparametric analysis; „*" indicates ion signals which were chosen for mass calibration. Mass range m/z 4000 – 20000. Ferulic acid was used as matrix.

Supplemental Figure 2:

MALDI-ToF mass spectra of intact peripheral blood proteins from mother 2 upon conventional serum work-up including freeze / thaw steps (spectra 2-1 and 2-2), and following our novel work flow with depositing serum on serum storage discs at room temperature (spectra 2-3 and 2-4).

Ion signals labeled: „#" indicate mass peaks whose area under signals were used for multiparametric analysis; „*" indicates ion signals which were chosen for mass calibration. Mass range m/z 4000 – 20000. Ferulic acid was used as matrix.
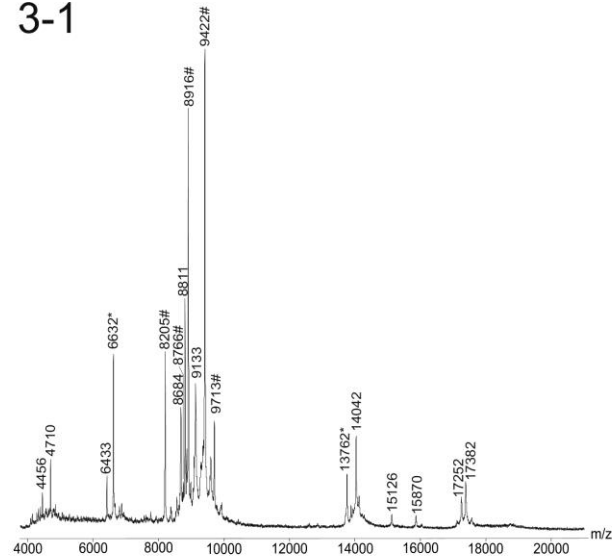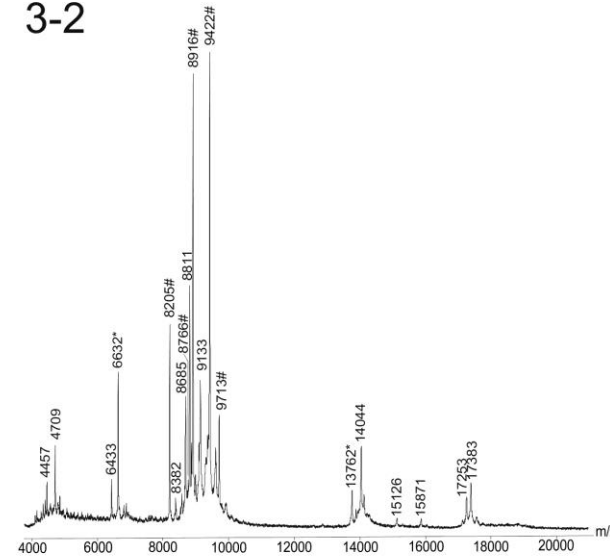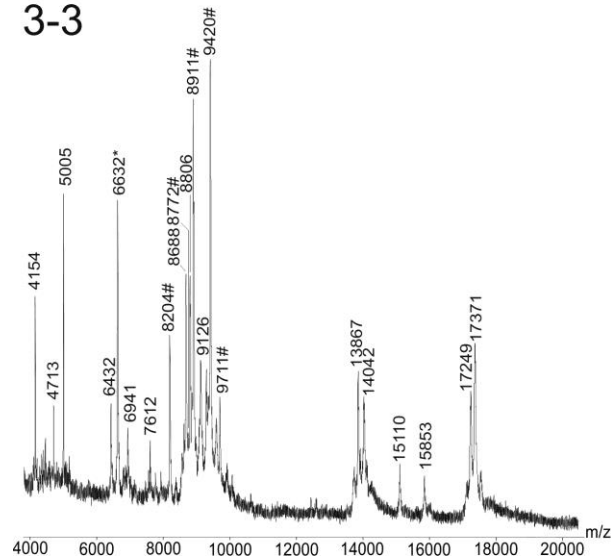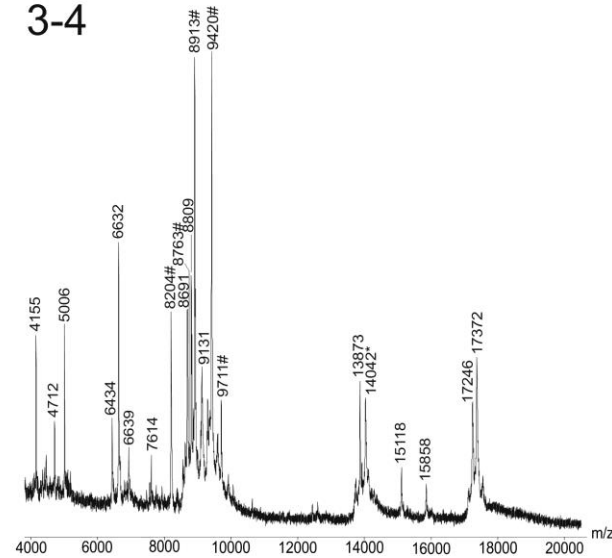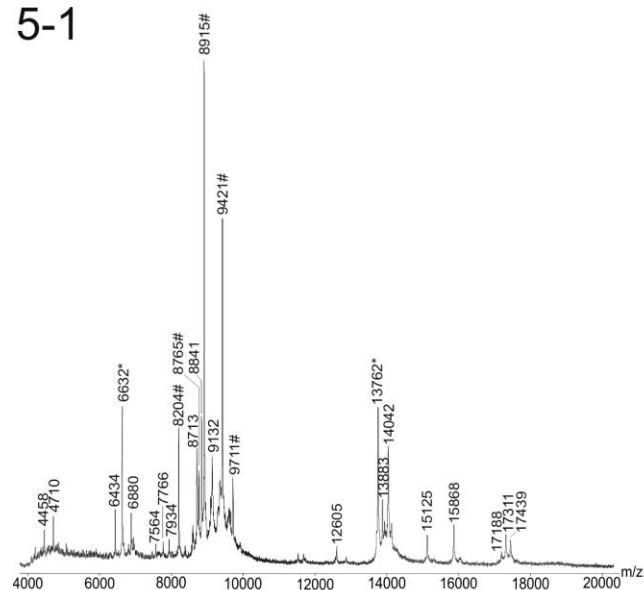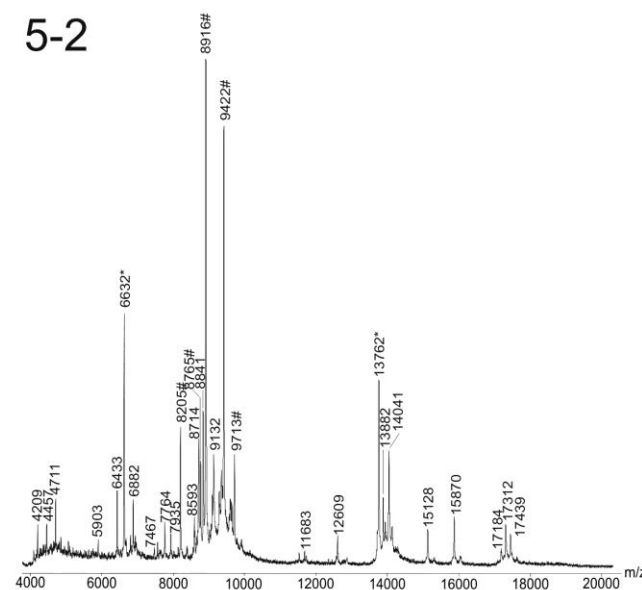
Supplemental Figure 3:

MALDI-ToF mass spectra of intact peripheral blood proteins from mother 3 upon conventional serum work-up including freeze / thaw steps (spectra 3-1 and 3-2), and following our novel work flow with depositing serum on serum storage discs at room temperature (spectra 3-3 and 3-4).

Ion signals labeled: „#" indicate mass peaks whose area under signals were used for multiparametric analysis; „*" indicates ion signals which were chosen for mass calibration. Mass range m/z 4000 – 20000. Ferulic acid was used as matrix.
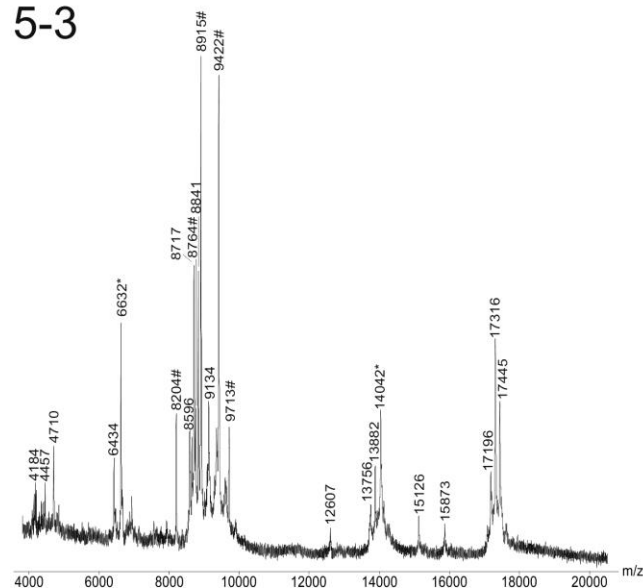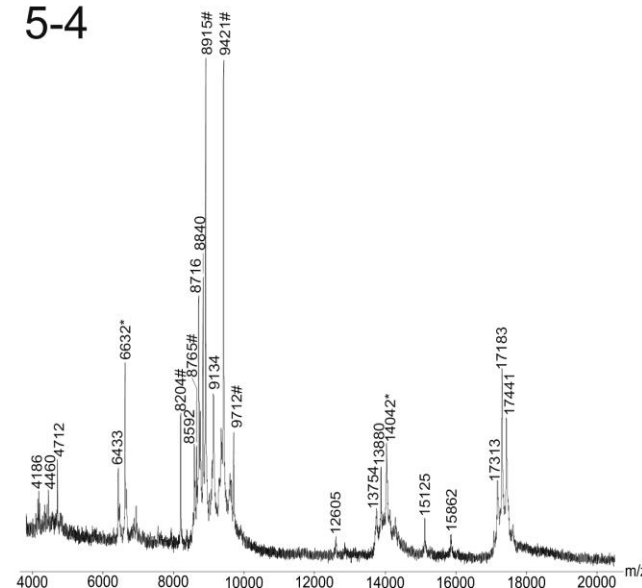
Supplemental Figure 4:

MALDI-ToF mass spectra of intact peripheral blood proteins from mother 4 upon conventional serum work-up including freeze / thaw steps (spectra 4-1 and 4-2), and following our novel work flow with depositing serum on serum storage discs at room temperature (spectra 4-3 and 4-4).

Ion signals labeled: „#" indicate mass peaks whose area under signals were used for multiparametric analysis; „*" indicates ion signals which were chosen for mass calibration. Mass range m/z 4000 – 20000. Ferulic acid was used as matrix.

Supplemental Figure 5:

MALDI-ToF mass spectra of intact peripheral blood proteins from mother 5 upon conventional serum work-up including freeze / thaw steps (spectra 5-1 and 5-2), and following our novel work flow with depositing serum on serum storage discs at room temperature (spectra 5-3 and 5-4).

Ion signals labeled: „#" indicate mass peaks whose area under signals were used for multiparametric analysis; „*" indicates ion signals which were chosen for mass calibration. Mass range m/z 4000 – 20000. Ferulic acid was used as matrix.
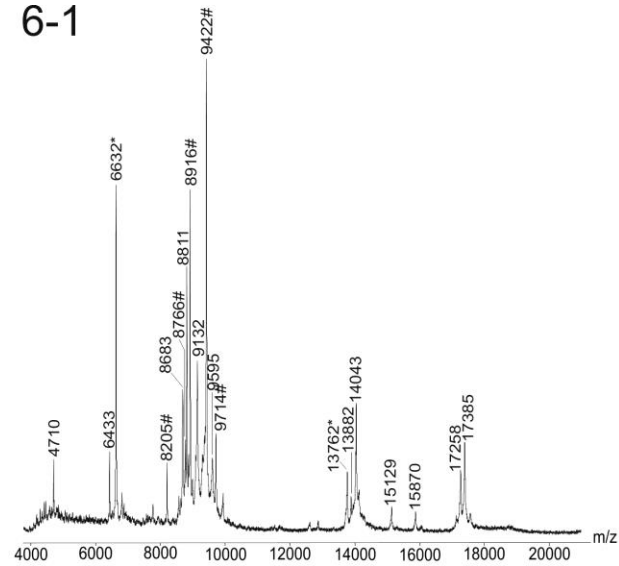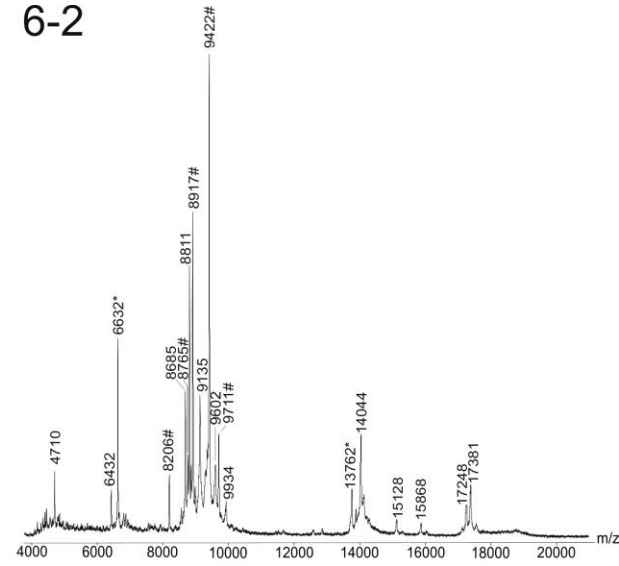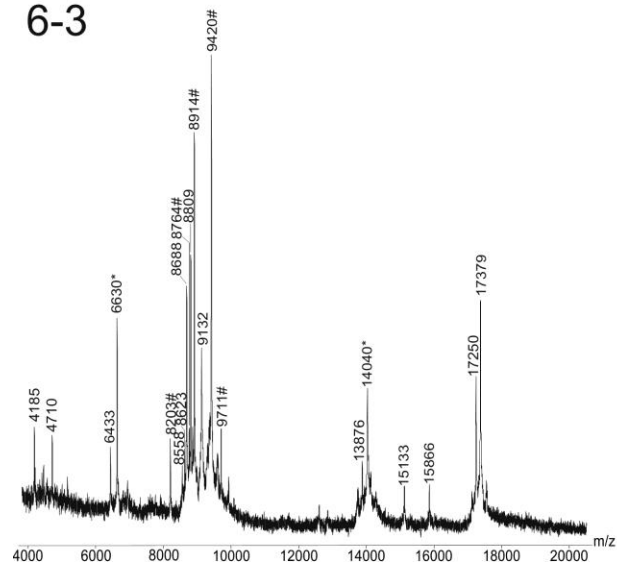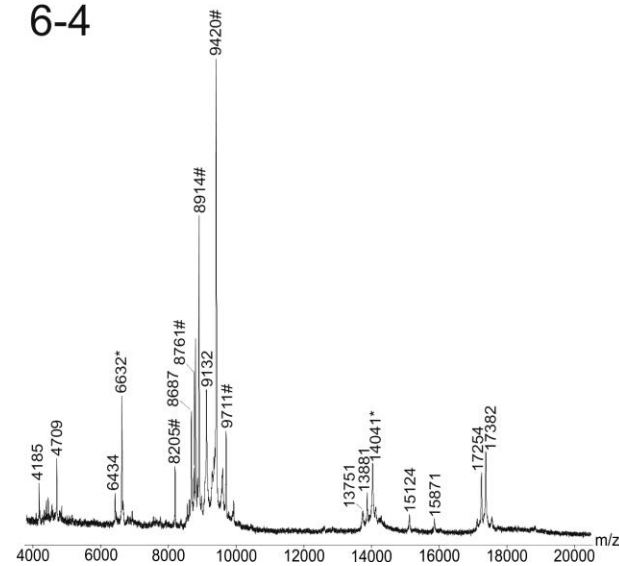
6-1

6-2

6-3

6-4

Supplemental Figure 6:

MALDI-ToF mass spectra of intact peripheral blood proteins from mother 6 upon conventional serum work-up including freeze / thaw steps (spectra 6-1 and 6-2), and following our novel work flow with depositing serum on serum storage discs at room temperature (spectra 6-3 and 6-4).

Ion signals labeled: „#" indicate mass peaks whose area under signals were used for multiparametric analysis; „*" indicates ion signals which were chosen for mass calibration. Mass range m/z 4000 – 20000. Ferulic acid was used as matrix.
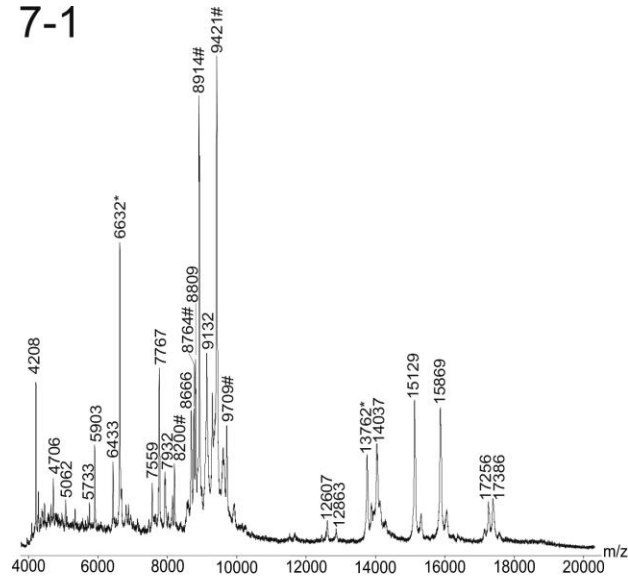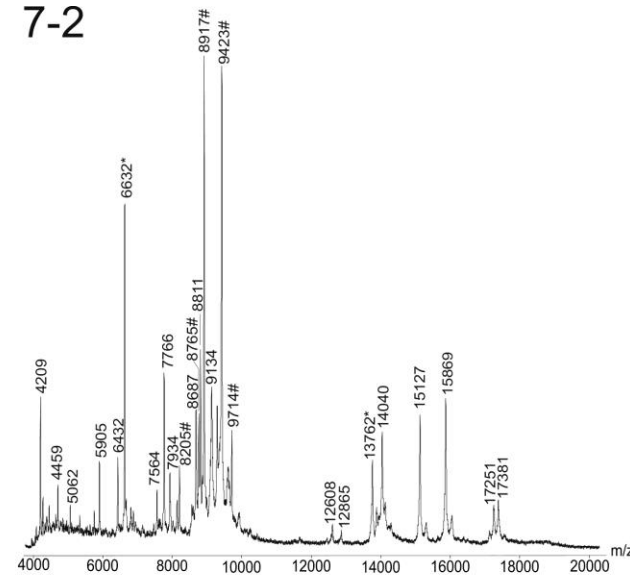
Supplemental Figure 7:

MALDI-ToF mass spectra of intact peripheral blood proteins from mother 7 upon conventional serum work-up including freeze / thaw steps (spectra 7-1 and 7-2), and following our novel work flow with depositing serum on serum storage discs at room temperature (spectra 7-3 and 7-4).

Ion signals labeled: „#" indicate mass peaks whose area under signals were used for multiparametric analysis; „*" indicates ion signals which were chosen for mass calibration. Mass range m/z 4000 – 20000. Ferulic acid was used as matrix.
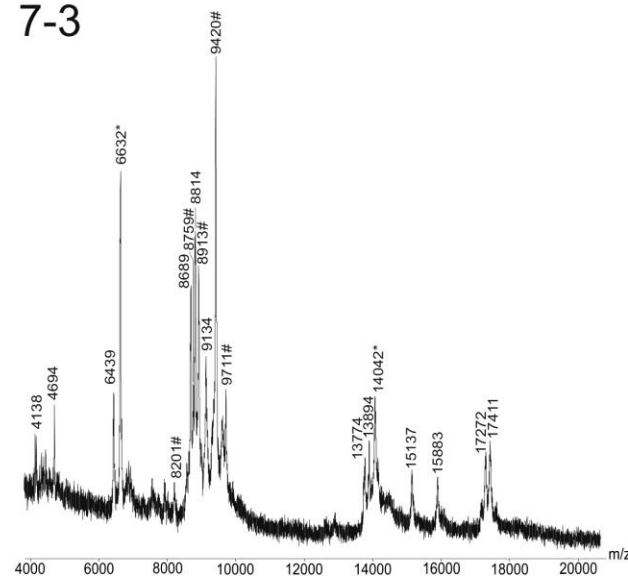
8-1

8-2

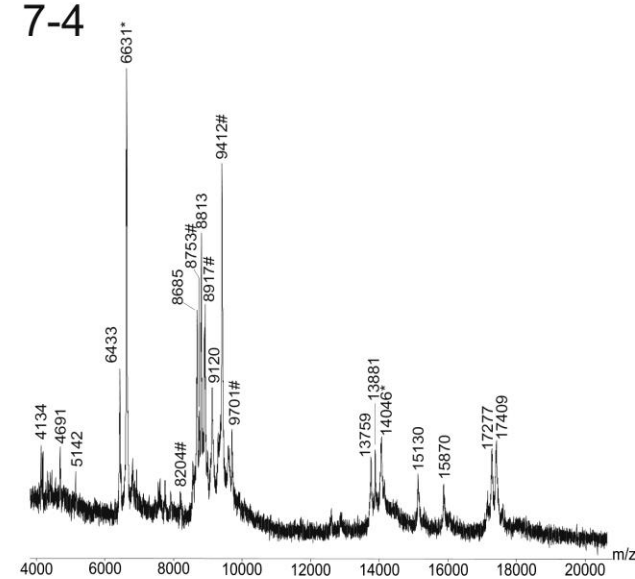**8-3**

8-4

Supplemental Figure 8:

MALDI-ToF mass spectra of intact peripheral blood proteins from mother 8 upon conventional serum work-up including freeze / thaw steps (spectra 8-1 and 8-2), and following our novel work flow with depositing serum on serum storage discs at room temperature (spectra 8-3 and 8-4).

Ion signals labeled: „#" indicate mass peaks whose area under signals were used for multiparametric analysis; „*" indicates ion signals which were chosen for mass calibration. Mass range m/z 4000 – 20000. Ferulic acid was used as matrix.
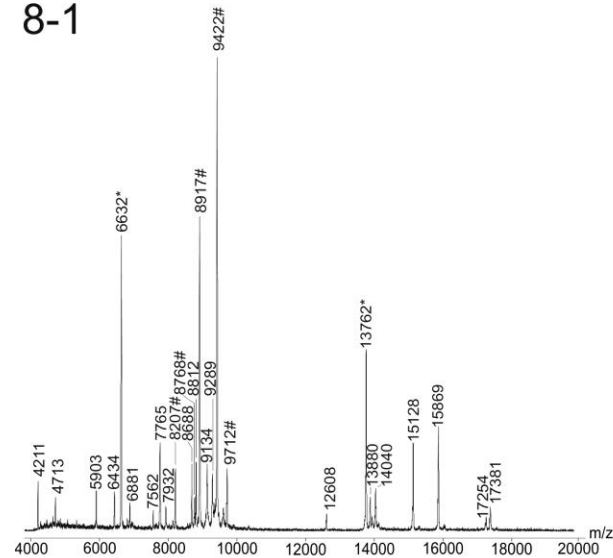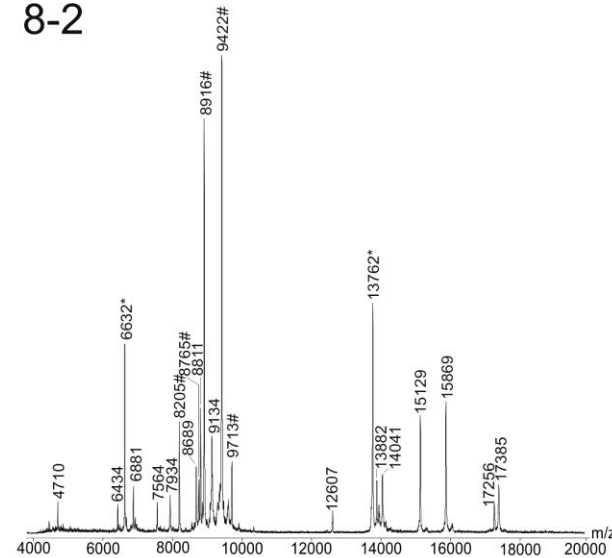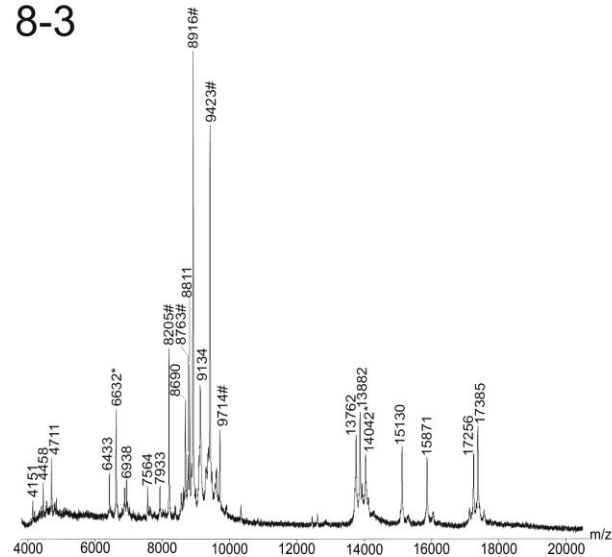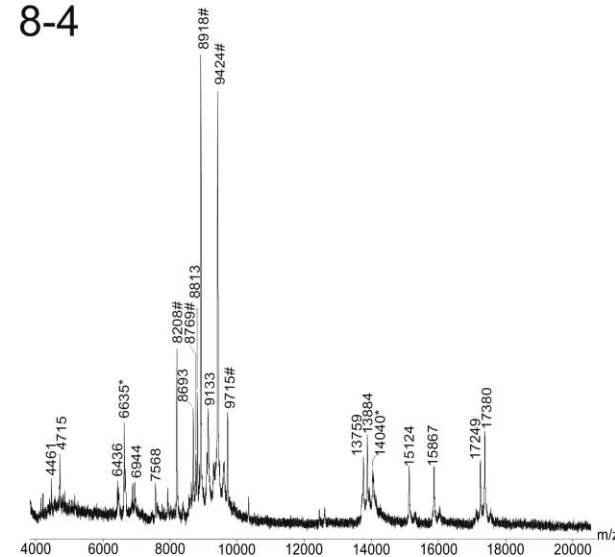
Supplemental Table 1: Demographic data, clinical and laboratory parameters for all patients and control individuals.

mother [no.]	age [a)] [y]	BMI [kg/m²]	parity	smoking status (cig/d) [a)]	systolic BP [a)] [mmHg]	diastolic BP [a)] [mmHg]	protein-uria [a,b,c)] [mg/d]	gestation weeks at delivery	mode of delivery	fetal gender	fetal weight	fetal weight centile [d)]
1	35.7	21.8	1	0	122	58	0 [c)]	34 6/7	c-section	f	2420	40
2	29.6	24.1	1	0	106	61	0 [c)]	28 4/7	c-section	f	1250	60
3	24.7	35.4	1	0	120	81	0 [c)]	39 2/7	c-section	m	3895	80
4	24.6	23.0	0	0	110	70	0 [c)]	34 3/7	c-section	m	2450	50
5	31.9	22.5	0	0	129	76	77 [b)]	32 1/7	c-section	f	1255	9
6	23.6	23.7	0	10	125	71	182 [b)]	30 5/7	c-section	f	940	4
7	27.8	28.3	3	0	112	55	0 [c)]	27 0/7	c-section	f	580	3
8	21.6	17.0	0	5	110	70	0 [c)]	29 6/7	c-section	m	1000	10

a) at beginning of hospitalization
b) immunoturbidimetric assay (Tina-quant albumin; Roche Diagnostics. Mannheim. Germany); proteinuria is defined as urinary protein excretion >300 mg/d.
c) dip stick assay; significant proteinuria is present with readings of more than + (max: +++).
d) standard deviations to the mean birth weight centiles according to the population based newborn weight charts.

Supplemental Table 2: List of identified proteins after resolubilization from serum storage disc.

Entry No.	Uniprot Code	Accession Number	Average Mass (Da)	Number of Matched Peptides	Sequence Coverage (%)
1	IGKC_HUMAN	P01834	11,780	3	41.51
2	ALBU_HUMAN	P02768	71,363	32	45.48
3	APOA1_HUMAN	P02647	30,778	15	42.32
4	HPT_HUMAN	P00738	45,890	11	24.88
5	IGHM_HUMAN	P01871	49,991	12	26.99
6	TRFE_HUMAN	P02787	79,345	18	25.70
7	IGHA1_HUMAN	P01876	38,510	7	19.55
8	APOC2_HUMAN	P02655	11,284	3	28.71
9	APOA2_HUMAN	P02652	11,289	5	26.00
10	IGLL5_HUMAN	B9A064	23,405	3	14.49
11	LAC3_HUMAN	P0CG06	11,409	2	21.70
12	LAC2_HUMAN	P0CG05	11,465	2	21.70
13	LAC1_HUMAN	P0CG04	11,519	2	21.70
14	APOA4_HUMAN	P06727	45,399	13	28.28
15	IGJ_HUMAN	P01591	18,555	4	28.30
16	IGHG3_HUMAN	P01860	42,313	5	13.53
17	IGHG1_HUMAN	P01857	36,619	5	15.45
18	IGHG2_HUMAN	P01859	36,528	5	15.64
19	HPTR_HUMAN	P00739	39,543	7	15.52
20	IGHG4_HUMAN	P01861	36,454	4	13.15
21	CLUS_HUMAN	P10909	53,065	6	13.36
22	A1AT_HUMAN	P01009	46,908	10	20.57
23	APOE_HUMAN	P02649	36,268	7	23.03
24	HBB_HUMAN	P68871	16,112	3	23.13
25	A2MG_HUMAN	P01023	164,717	17	11.26
26	CO3_HUMAN	P01024	188,688	35	18.46
27	MUCB_HUMAN	P04220	43,571	8	20.20
28	IGHA2_HUMAN	P01877	37,325	4	9.71
29	SAMP_HUMAN	P02743	25,501	6	26.91
30	AACT_HUMAN	P01011	47,822	5	10.41
31	FETUA_HUMAN	P02765	40,123	2	3.81
32	HEMO_HUMAN	P02790	52,418	7	13.64
33	CO4A_HUMAN	P0C0L4	194,383	24	11.81
34	CO4B_HUMAN	P0C0L5	194,291	23	11.35
35	CFAB_HUMAN	P00751	86,902	9	11.91
36	CXCL7_HUMAN	P02775	14,179	2	14.84
37	PZP_HUMAN	P20742	165,346	10	6.48
38	CERU_HUMAN	P00450	123,061	7	7.51
39	CFAH_HUMAN	P08603	143,773	11	8.20
40	APOL1_HUMAN	O14791	44,031	4	8.04

Entry No.	Uniprot Code	Accession Number	Average Mass (Da)	Number of Matched Peptides	Sequence Coverage (%)
41	HEP2_HUMAN	P05546	57,242	6	9.62
42	THRB_HUMAN	P00734	71,520	6	6.75
43	VTNC_HUMAN	P04004	55,104	5	8.16
44	ITIH4_HUMAN	Q14624	103,586	7	6.24
45	AMBP_HUMAN	P02760	39,912	4	7.39
46	APOH_HUMAN	P02749	39,610	2	5.22
47	CD5L_HUMAN	O43866	39,628	3	7.20
48	A1BG_HUMAN	P04217	54,824	4	8.08
49	VTDB_HUMAN	P02774	54,560	4	6.96
50	ITIH2_HUMAN	P19823	106,920	7	6.66
51	K2C1_HUMAN	P04264	66,210	6	8.54
52	K1C10_HUMAN	P13645	59,055	5	7.53
53	C1QC_HUMAN	P02747	26,002	2	12.24
54	PON1_HUMAN	P27169	39,902	3	8.73
55	ZA2G_HUMAN	P25311	34,487	2	7.38
56	ANGT_HUMAN	P01019	53,439	3	6.60
57	KNG1_HUMAN	P01042	73,041	5	6.06
58	AFAM_HUMAN	P43652	71,008	3	5.34
59	ITIH1_HUMAN	P19827	101,846	4	3.18
60	FHR1_HUMAN	Q03591	38,791	3	10.91
61	K22E_HUMAN	P35908	65,718	2	3.13
62	C1S_HUMAN	P09871	78,224	4	5.67
63	K1C16_HUMAN	P08779	51,610	3	3.38
64	K1C14_HUMAN	P02533	51,904	3	3.39
65	PLMN_HUMAN	P00747	93,306	4	4.32
66	PSG1_HUMAN	P11464	47,622	3	7.40
67	FIBA_HUMAN	P02671	95,715	2	2.42
68	K1C28_HUMAN	Q7Z3Y7	51,195	3	5.39
69	PEDF_HUMAN	P36955	46,483	2	5.02
70	C1R_HUMAN	P00736	81,658	3	3.26
71	PSG8_HUMAN	Q9UQ74	48,171	2	4.69
72	K1C27_HUMAN	Q7Z3Y8	50,450	2	3.92
73	K1C25_HUMAN	Q7Z3Z0	49,888	2	4.00

3. Curriculum Vitae

Personal data	
Name	Charles Ayensu Okai
Address	Erich-Schlesinger-Str. 37b, Zimmer 013
	18059 Rostock, Germany
Telephone	+4915214037931
E-mail	charles.okai@uni-rostock.de; charles.okai@outlook.com
Nationality	Ghana
Date of birth	15.09.1974
Gender	Male
Marital Status	Married, 2 children
Education	
Date	October 2016 to date
Title of qualification awarded	**PhD student**
Institution	Proteom-Zentrum Rostock, Institute of Immunology, University of Rostock, Schilligallee 69, 18057, Rostock, Germany
Date	June 2007
Title of qualification awarded	**MSc. Pharmaceutical Analysis & Quality Control**
Institution	Kwame Nkrumah University of Science & Technology,
	Faculty of Pharmacy & Pharmaceutical Sciences, Kumasi, Ghana.
Date	March 2003

Title of qualification awarded	**Bsc. Chemistry (Hons)**
Institution	Kwame Nkrumah University of Science & Technology, Faculty of Physical & Computational Sciences, Kumasi, Ghana.
Date	June, 1995
Title of qualification awarded	**G.C.E Advanced Level**
Institution	Akim Swedru Secondary School, Akim Swedru, Ghana
Date	June 1991
Title of qualification awarded	**G.C.E Ordinary Level**
Institution	Adisadel College, Cape Coast, Ghana
Work experience	
Dates	November 2011 to date
Position held	**Lecturer**
Employer	Kumasi Technical University, Faculty of Health Sciences, Kumasi, Ghana
Dates	November 2010 to October 2011
Position held	**Quality Assurance Manager**
Employer	SALOM Pharmacy Limited, Kumasi, Ghana
Dates	May 2006 to October 2010
Position held	**Quality Control Manager**
Employer	Tradewinds Chemist Limited, Kumasi, Ghana

Awards	
	University of Rostock Travel Stipend for Restoring Hope Scientific Conference 2019 in Accra, Ghana, 30th October to 1st November 2019
	University of Rostock Travel Stipend for 2nd Int. Summer School 2018 in Iasi, Romania, 9th to 13th July 2018
	ERASMUS grant for ERASMUS+ Praktikum Exchange Programme between University of Rostock and Alexander Ioan Cuza in Iasi, Romania, 1st July to 31st August 2018
	University of Rostock Travel Stipend for MS Pharma Network 2018 Conference in Rome, Italy, 19th to 21st February 2018
	DAAD Stipend for Doctoral studies, University of Rostock, Germany, October 2016 to June 2016
	DAAD Stipend for German language, Goethe Institute, Göttingen, Germany, June to September 2016
	DAAD Stipend for German language, Goethe Institute, Ghana, April to May 2016
Academic and Professional Membership	
	Member, DGMS, March 2017 to date
	Member, Graduate Academy, University of Rostock, October 2016 to date
	Member, MD/PhD Structured Curriculum, "Molecular Mechanisms of Regenerative Processes" (MMRP), University of Rostock, October 2016 to date
	Senior Member, Kumasi Technical University, Ghana, November 2011 to date

4. List of Publications and Presentations

Publications

Okai, C. A., Russ, M., Wölter, M., Andresen, K., Rath, W., Pecks, U. and Glocker, M. O., Precision Diagnostics by Affinity - Mass Spectrometry: A Novel Approach for Fetal Growth Restriction Screening During Pregnancy. *J. Clin. Med*. **2020**, 9(5), 1374

Wolter, M., **Okai, C. A.**, Smith, D. S., Ruß, M., Rath, W., Pecks, U., Borchers, C. H. and Glocker, M. O. Maternal Apolipoprotein B100 Serum Levels are Diminished in Pregnancies with Intrauterine Growth Restriction and Differentiate from Controls. *Proteomics. Clin. Appl*. **2018**, 12 (6), e1800017

Wölter, M., Russ, M., **Okai, C. A.**, Rath, W., Pecks, U. and Glocker, M. O. Comparison of blood serum protein analysis by MALDI-MS from either conventional frozen samples or storage disc-deposited samples: A study with human serum from pregnant donors and from patients with intrauterine growth restriction. *Eur. J. Mass Spectrom*. **2019**, 25(4), 381–390

Oral presentations

Charles A. Okai, Manja Wölter, Manuela Ruß, Werner Rath, Ulrich Pecks and Glocker, M.O. "Analysis of Maternal Peripheral Blood Serum Proteins by Affinity-Mass Spectrometry Distinguishes IUGR from Control and SGA" on 25th November, **2019**; Proteom-Zentrum Rostock/Institute of Immunology Group meeting WS 2019/20, Rostock.

Charles A. Okai, Manuela Ruß, Manja Wölter, Werner Rath, Ulrich Pecks and Michael O. Glocker. "Precision Diagnostics by Affinity - Mass Spectrometry with Maternal Peripheral Blood Serum Improves Screening for Pregnancy Complications" at "Restoring Hope Scientific Conference 2019" from 30th October - 1st November, **2019**, Accra, Ghana

Charles A. Okai, Manja Wölter, Manuela Ruß, Werner Rath, Ulrich Pecks and Michael O. Glocker. "Distinguishing IUGR from Controls During Early Pregnancy by Affinity-Mass Spectrometry Analysis of Maternal Blood Serum Proteins" 24th June, **2019**, Proteom-Zentrum Rostock/Institute of Immunology Group meeting SS 2019, Rostock, Germany

Charles A. Okai, Manja Wölter, Manuela Ruß, Raheem F. El-Kased, Alina B. Petre, and Michael O. Glocker. "Dried Serum Spots – An excellent means to bridge the divide between the clinics and the protein mass spectrometry laboratory" at the 52nd Annual German Society for Mass Spectrometry (DGMS) Conference from 10th - 13th March, **2019**, Rostock, Germany

Charles A. Okai, Manja Wölter, Manuela Ruß, Werner Rath, Ulrich Pecks and Michael O. Glocker. "MALDI Mass Spectrometric Profiling of Dried Serum Spots Distinguishes Healthy Pregnancies from Women whose Fetuses Suffer from Intra-Uterine Growth-Restriction" on 5th - 6th December, **2018**, Participants' Camp WS 2018/19, Rostock, Germany

Charles A. Okai, Manja Wölter, Derek Smith, Manuela Ruß, Werner Rath, Ulrich Pecks, Christoph H. Borchers and Michael O. Glocker. "IUGR risk prediction by LC-MRM/MS analysis of serum proteins from pregnant women" at "2nd Int. Summer School 2018" from 9th - 13th July, **2018**, Iasi, Romania

Charles A. Okai, Manja Wölter, Derek Smith, Manuela Ruß, Werner Rath, Ulrich Pecks, Christoph H. Borchers and Michael O. Glocker. "Maternal Apolipoprotein B100 Serum Levels are Diminished in Pregnancies with Intrauterine Growth Restriction and Differentiate from Controls" on 5th July, **2018**; Participants' Camp SS 2018, Rostock, Germany

Charles A. Okai, Manja Wölter, Derek Smith, Manuela Ruß, Werner Rath, Ulrich Pecks, Christoph H. Borchers and Michael O. Glocker. "Quantitative LC-MRM/MS analysis of maternal serum proteins during pregnancy is capable to predict the risk of IUGR in preterm babies" at "MS Pharma Network 2018" from 19th - 21st February, **2018**, Rome, Italy

Charles A. Okai, Manja Wölter, Manuela Ruß, Werner Rath, Ulrich Pecks and Michael O. Glocker. "Intrauterine-Growth-Restriction (IUGR) Scoring in Early Pregnancies by Affinity-Mass Spectrometry Profiling of Maternal Serum Proteins" on 15th January, **2018**; Proteom-Zentrum Rostock/Institute of Immunology Group meeting WS 2017/18, Rostock, Germany

Charles A. Okai, Manja Wölter, Manuela Ruß, Werner Rath, Ulrich Pecks, and Michael O. Glocker. "Intrauterine-Growth-Restriction (IUGR) Scoring in Early Pregnancies by Affinity-Mass Spectrometry Profiling of Maternal Serum Proteins" on 6th - 7th December, **2017**; 14th Proteome Forum and Participants' Camp WS 2017/18, Rostock, Germany

Charles A. Okai, Ulrich Pecks, Raheem F. El-Kased and Michael O. Glocker. "How to Cross the Distance from the Clinics to the Lab" from 28th - 29th June, **2017**; Participants' Camp SS 2017, Rostock, Germany

Charles A. Okai and Michael O. Glocker. "Affinity-Mass Spectrometric Analysis of Apolipoprotein CIII Isoforms from Human Serum" on 6th February, **2017**; Proteom-Zentrum Rostock/Institute of Immunology Group meeting WS 2016/17, Rostock, Germany

Charles A. Okai, Ulrich Pecks and Michael O. Glocker. "Diagnostics of Intrauterine Growth Restriction by Serum Profiling using Affinity-Mass Spectrometry" from 14th - 15th December, **2016**; Participants' Camp WS 2016/17, Rostock, Germany